THE HONG KONG
POLYTECHNIC UNIVERSITY
香港理工大學
Pao Yue-kong Library
包玉剛圖書館

Copyright Undertaking

This thesis is protected by copyright, with all rights reserved.

By reading and using the thesis, the reader understands and agrees to the following terms:

1. The reader will abide by the rules and legal ordinances governing copyright regarding the use of the thesis.
2. The reader will use the thesis for the purpose of research or private study only and not for distribution or further reproduction or any other purpose.
3. The reader agrees to indemnify and hold the University harmless from and against any loss, damage, cost, liability or expenses arising from copyright infringement or unauthorized usage.

IMPORTANT

If you have reasons to believe that any materials in this thesis are deemed not suitable to be distributed in this form, or a copyright owner having difficulty with the material being included in our database, please contact lbsys@polyu.edu.hk providing details. The Library will look into your claim and consider taking remedial action upon receipt of the written requests.

Pao Yue-kong Library, The Hong Kong Polytechnic University, Hung Hom, Kowloon, Hong Kong

http://www.lib.polyu.edu.hk

STRUCTURE-ACTIVITY RELATIONSHIP (SAR) OF SOME ISATIN-BASED GLYCOSYLTRANSFERASE INHIBITORS: MOLECULAR DESIGN, SYNTHESIS AND ANTIBACTERIAL ACTIVITIES

CHEONG WING LAM

Ph.D

THE HONG KONG POLYTECHNIC UNIVERSITY

2018

THE HONG KONG POLYTECHNIC UNIVERSITY

DEPARTMENT OF

APPLIED BIOLOGY & CHEMICAL TECHNOLOGY

STRUCTURE-ACTIVITY RELATIONSHIP (SAR) OF SOME ISATIN-BASED GLYCOSYLTRANSFERASE INHIBITORS: MOLECULAR DESIGN, SYNTHESIS AND ANTIBACTERIAL ACTIVITIES

CHEONG WING LAM

A thesis submitted

in

partial fulfillment of the requirements

for

the degree of Doctor of Philosophy

July 2017

Certificate of Originality

I hereby declare that this thesis is my own work and that, to the best of my knowledge and belief, it reproduces no material previously published or written, nor material that has been accepted for the award of any other degree or diploma, except where due acknowledgement has been made in the text.

Cheong Wing Lam

Abstract

Antibacterial Resistance (ABR) has been a global challenge. The abusive use of antibiotics stimulates natural selection of bacteria and results in loss of activity against their targets. Peptidoglycan glycosyltransferase (GT), an enzyme which is essential for cell wall biosynthesis, is a potential novel drug target. It offers several advantages as a drug target: (i) it is absent in human cells; (ii) its sequence is highly conserved among bacteria; (iii) it is easily accessible on the surface of the cell; and (iv) its ABR is not significant. However, research on GT is hindered by its membrane-bound nature, which increases the difficulty to obtain crystallographic structures. Moreover, the activity assay of GT is also limited by the extremely low yield in the production of its substrate, lipid II. These factors all limited the development of GT inhibitors.

With the aid of computational virtual screening on a library of 3,000,000 compounds, our research group previously discovered a potential isatin-based GT inhibitor, 2-(3-(2-Carbamimidoylhydrazone)-2-oxoindolin-1-yl)-*N*-(3-nitrophenyl) acetamide **(10b-27)**, which has moderate antibacterial activity. Competitive saturation-transfer difference (STD)-NMR suggested that it binds to GT and shares the same active-site pocket with the known inhibitor moenomycin A.

In this thesis, the structure-activity relationship (SAR) of the isatin-based inhibitors was studied by further modifying the structure of **10b-27** with reference to the binding pose revealed by the GT crystal structure (PDB ID 2OLV). To achieve this goal, 20 new isatin derivatives with the aminoguanidinyl group conserved were designed and synthesized. The antibacterial activity (in terms of *S. aureus* MIC) showed a 4-fold enhancement when the nitrophenyl substituent was replaced by a *m,p*-naphthyl group. The best derivative (**10-32**), with the methanediylamidyl linkage removed and the substituent replaced by butyl, showed an overall 8-fold enhancement compared to **10b-27**.

The interaction between **10-32** and GT was confirmed by competitive saturation-transfer difference (STD)-NMR experiments. STD-NMR is one of the excellent alternatives to activity assay since it detects small molecules binding to macromolecules and does not consume the lipid II substrate. Upon addition of **10-32** into GT (100:1 ratio), strong STD-NMR signals of **10-32** were detected, suggesting that **10-32** and GT were in close contact ($\leq$ 5 μM). Further addition of moenomycin A displaced the STD signal intensities, suggested that **10-32** shares the same active-site binding pocket of GT as moenomycin A.

Surprisingly, the clinically significant MRSA (ATCC® BAA-41™) did not show any detectable resistance to **10-32**, revealing its potential to be a promising antibiotic candidate. Taking into account that there are currently no GT inhibitors being used clinically, the studies of **10-32** opened up a new direction on novel antibiotic drug development.

Acknowledgements

I am deeply indebted to my chief supervisor Prof. K. Y. Wong for his invaluable encouragement, suggestions, supervision and discussions during the course of my study. I am also grateful to Prof. Thomas Y. C. Leung for his support. His professional guidance inspired my interest in biological science. Gratitude also goes to Dr. Kin-Fai Chan for his exceptional ideas in drug design and Dr. Y. W. Chen for his suggestions to my thesis writing.

I would like to thank Dr. Peter Y. Wang for his guidance in organic synthesis and Dr. Ann L. Y. So for her guidance in molecular biology. I would also like to thank Ms. Aya K. C. Cheung for demonstrating the MIC experiments. I deeply thank Dr. Kenneth S. C. Yan for his support in STD-NMR experiments, and Dr. P. K. So and Dr. Melody Y. M. Wong for their assistance in mass spectrometric studies.

I would also like to thank my colleagues in my research group for their support and encouragement in the course of my study. Furthermore, I would like to acknowledge the support from the Research Grants Council on this project, the Partner State Key Laboratory of Chirosciences and the Hong Kong Polytechnic

University for the studentship and conference grant.

Last but not least, I would like to express my deepest appreciation to my family for their support and care.

Table of Contents

Abbreviations

ABR	Antibacterial Resistance
AMR	Antimicrobial Resistance
GT	Bacterial Peptidoglycan Glycosyltransferase
TP	Bacterial Peptidoglycan Transpeptidase
DAP	Diaminopimelic Acid
ESI-MS	Electrospray Ionization Mass Spectrometry
σ	Hammett Substituent Constant
HSQC	Heteronuclear Single-quantum Correlation
MIC	Minimum Inhibitory Concentration
NDM-1	New Delhi metallo-beta-lactamase 1
NOE	Nuclear Overhauser Effect
PBP(s)	Penicillin-binding Protein(s)
STD	Saturation-transfer Difference
SDS-PAGE	Sodium Dodecyl Sulfate Polyacrylamide Gel Electrophoresis
SAR	Structure-activity Relationship
π	Substituent Hydrophobicity Constant
SPR	Surface Plasma Resonance

UDP-GlcNAc	Uridine diphosphate-*N*-acetylglucosamine
UDP-MurNAc	Uridine diphosphate-*N*-acetylmuramic acid

Chapter 1

Introduction

1.1 The emergence of antibacterial resistance (ABR)

Antibacterial resistance (ABR) is a challenging and alarming problem worldwide. Antibiotics that have been effective in treating infections become less effective because of the development of ABR [1]. Antibacterial resistance is in general much more severe than the resistance developed against the antifungals and antivirals [2]. Bacteria with multi-drug resistance are termed "superbugs". The development of ABR is a natural selection process for bacteria to overcome environmental pressure, and it has been accelerated due to the overuse of antibiotics in medical treatments and farming of food-producing animals [1].

According to the "Antimicrobial Resistance Global Report on Surveillance 2014" by World Health Organization, around 23,000 people per year died of ABR in the United States, with an overall annual societal cost of $35 billion US dollars [1]. The figure was just the tip of an iceberg as the problem can be more serious in other countries. Besides the conventional β-lactams such as penicillin, resistance has also been developed against the less popular non-β-lactam antibiotics such as vancomycin [3] and colistin [4].

Table 1.1 Bacteria with detectable ABR and its associated diseases (Adopted from reference [1]).

Bacterium	Drug(s) with reduced susceptibility	Corresponding disease(s) (excerpt)
Escherichia coli	3rd generation cephalosporins, fluoroquinolones, colistin	Peritonitis, meningitis in neonates, urinary tract infections
Klebsiella pneumoniae	3rd generation cephalosporins, carbapenems, colistin	Urinary and respiratory tract infections, bloodstream infections
Staphylococcus aureus	Methicillin, vancomycin	Skin, soft tissue, bone and bloodstream infections, postoperative wound infections
Streptococcus pneumoniae	Penicillin	Acuteotitis media, meningitis
Nontyphoidal Salmonella (Nontyphoidal)	Fluoroquinolones	Gastroenteritis, enteric fever
Shigella species	Fluoroquinolones	Diarrhoea, dysentery
Neisseria gonorrhoeae	3rd generation cephalosporins	Gonorrhoea

1.2 Mechanisms of antibacterial agents

Antibacterials (or antibiotics) are substances which kill or inhibit the growth of bacteria. They are commonly used to treat bacterial infections. The concept of "antibacterials" can be traced back to the visualization of bacteria by Anton van Leeuwenhoek in the 1670's [5] and the experimental proof of the "germ theory of disease" by Louis Pasteur in 1880 [6], when people realized that bacteria are the causes of many infections. After the introduction of penicillins in 1942 [5], the successful story of this "magic bullet" continued and many new antibacterial agents were discovered, including bacitracin in 1945 [7], chloramphenicol in 1947 [8], chlortetracycline in 1948 [9], and colistin in 1950 [10].

The mechanisms of antibacterial agents can be broadly classified into five major categories : (i) inhibition of cell-wall biosynthesis; (ii) inhibition of DNA precursor (folate) biosynthesis; (iii) inhibition of DNA/RNA biosynthesis; (iv) inhibition of protein biosynthesis; and (v) obstruction of cell membrane scaffold (Fig. 1.1) [11-12].

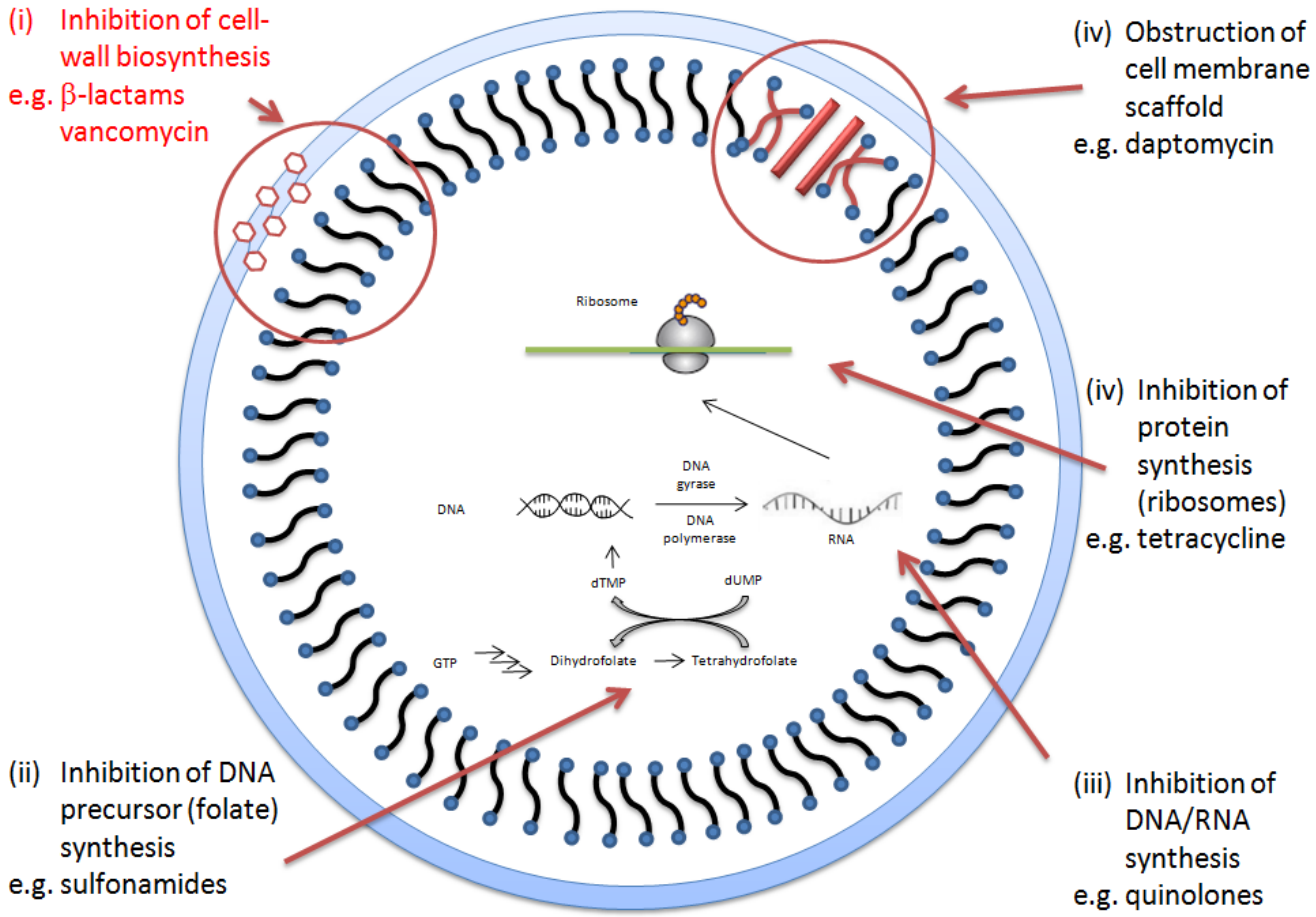

Fig. 1.1 Mechanisms of antibacterial agents.

1.3 Mechanism of antibacterial resistance (ABR)

ABR may exist naturally in some bacteria, such as the expression of penicillinase, to allow their survival under the natural antibiotic environment produced by other micro-organisms, or even by the bacteria themselves (so called producer immunity) [12-13]. The extensive therapeutic use of antibiotics not only encourages the spread of producer immunity, but also induces the development of acquired resistance: random mutation (which happens once per 10^7 bases) of one or a few bacteria can confer resistance to certain antibiotics. Because the bacteria population is controlled by factors such as nutrients and space, those resistant bacteria that survive under a harsh environment replenish the dead (or dormant) sensitive population, resulting in the acquisition of ABR to the entire population [12]. Some bacteria can also share ABR by transferring their resistance gene(s) via plasmids, bacteriophages or free DNA released during cell lysis [11]. The clinically important *S. aureus* with both methicillin and vancomycin-resistant phenotypes are typical examples of bacterial gene transfer. ABR can be classified into 4 major mechanisms, individual bacterium may reveal one or more at any one time [12]. Details of the mechanisms of antibacterial resistance are given below.

1.3.1 Modifications or inactivation of the antibiotics

Most antibiotics bind to a specific target and interfere with the corresponding biochemical reaction essential for the survival of the bacteria. For example, the β-lactam antibiotics bind to the penicillin-binding proteins (PBPs) and the aminoglycoside antibiotics bind to the 16S ribosomal RNA on the 30S ribosome. Bacterial modification of the chemical structure of these antibiotics lead to a reduced affinity toward the corresponding drug targets, resulting in the weakening of the antibacterial activities. For example, the functional azetidinyl group of β-lactam antibiotics can be hydrolyzed into PBPs-inactive carboxylic acids by the clinically significant enzyme β-lactamase while the nucleophilic groups (e.g. hydroxyl and amino groups) of aminoglycosides can be modified into bulky, less nucleophilic derivatives either by acetylation, adenylation or phosphorylation. These derivatives can no longer bind to their corresponding drug targets, hence the antibiotics are inactivated [12].

1.3.2 Efflux pumps

Some transmembrane proteins may actively efflux toxic substances out of the

cytoplasm, including antibiotics. Bacteria can survive when the apparent drug concentration inside the cell is lower than the lethal dosage. For the 4 transmembrane protein efflux pump families, 3 of them (the major facilitator subfamily, the small multidrug regulator family and the resistance / nodulation / cell division family) efflux foreign substances by proton motive force while the fourth one (the ATP-binding cassette family) consumes energy from ATP hydrolysis for the active transport of foreign compounds. For example, the tetracycline pump TetA has a high affinity to the Mg^{2+}-tetracycline complex and the complex within the inner cell membrane is being exchanged against protons outside the cell membrane [12].

1.3.3 Modifications of the antibacterial targets

For antibiotics which bind to a specific drug target, bacteria can reduce the binding affinity by modifying or replacing the target. The altered target resumes the biological cell functions and thus diminishes the antibacterial activity. For example, the methicillin-resistant *S. aureus* (MRSA) has a modified penicillin-binding protein (PBP2a) which possesses a non-penicillin binding domain, modifying the scaffold of the transpeptidase domain resulting in a lower affinity towards methicillin [14]. *S. aureus* may also exhibit vancomycin resistance by modifying the $_{D}$-Ala-$_{D}$-Ala group

of the bacteria murein precursor lipid II into $_{D}$-Ala-$_{D}$-lactate, resulting in poor binding affinity towards vancomycin but conserved cross-linking capability [12].

1.3.4 Reduction of membrane permeability

Small molecules diffuse into bacterial cells through porins located in the outer membrane, the rate of permeation is determined by its particle size and charge. Gram-negative bacteria can actively restrict the inward diffusion of small-molecule antibiotics by controlling the expression of porins. Examples include the carbapenem-resistant *P. aeruginosa* showing loss of outer membrane porin (OprD) [15] and the deletion of outer membrane proteins (OmpF) in multi-drug resistant *E. coli* [16].

1.4 The β-lactam antibiotics and its resistance

Before the discovery of penicillin G, the first clinically used β-lactam antibiotic, antibacterial chemotherapy was not prevalent, and people relied on serotherapy with little efficacy [17]. After treatment of the first patient with penicillin in 1941, more β-lactam antibiotics were discovered, either by isolation or chemical synthesis, with conservation of the core azetidinyl ring. Currently, β-lactam antibiotics are still the most effective antibacterial agents for many infections [17]. The exceptional performance largely relies on the unique antibacterial mechanism - the inhibition of bacterial cell wall (peptidoglycan) biosynthesis.

1.4.1 The bacterial peptidoglycan biosynthesis

Peptidoglycan (also known as murein) is the fundamental structural material of bacterial cell wall responsible for maintaining the architecture of the cells. The rigid structure allows bacteria to keep a stable scaffold under different osmotic pressures. Since the cell wall is highly conserved in most bacteria, yet absent in eukaryotic cells, inhibition of murein synthesis becomes extremely important for the development of antibiotics as it will lead to least side effects in mammals. Peptidoglycan synthesis

involves a series of biological reactions with more than ten enzymes [18-19]. The initial reactions of peptidoglycan synthesis occur within the cytoplasm, while the latter reactions occur in the plasma membrane.

In the beginning, the simple molecule uridine diphosphate-*N*-acetylglucosamine (UDP-GlcNAc) in the cytoplasm is converted to uridine diphosphate-*N*-acetylmuramic acid (UDP-MurNAc) by enzymes MurA and MurB (Fig. 1.2). Amino acids $_{L}$-alanine, γ-$_{D}$-glutamic acid, $_{L}$-lysine (or *m*-diaminopimelic acid) and $_{D}$-alanine-$_{D}$-alanine are attached to UDP-MurNAc by the enzymes MurC-F, giving a water-soluble product UDP-MurNAc pentapeptide. The lipid II of *S. aureus* has five extra glycines attached to the $_{L}$-lysine residue [18-19].

The UDP-MurNAc pentapeptide then diffuses to the internal surface of plasma membrane and reacts with undecaprenyl phosphate (anchored in the membrane) catalyzed by a membrane-bound enzyme MraY, forming the lipid-soluble compound lipid I. Lipid II is further produced when an extra *N*-acetylglucosamine is coupled to the *N*-acetylmuramic part of lipid I. This reaction is catalyzed by another membrane-bound enzyme MurG (Fig. 1.3) [18-19].

After lipid II is transferred from the internal surface of plasma membrane to the external surface by an unknown flippase (hypothetically FtszW [20] or MurJ [21]), it is polymerized into the final murein scaffold by the penicillin-binding protein (PBP). Some PBPs are membrane proteins containing 2 catalytic domains: glycosyltransferase domain (GT) and transpeptidase domain (TP). GT first polymerizes lipid II into a single-chain polysaccharide of repeating units of the GlcNAc-MurNAc pentapeptide, the polysaccharides further cross-link between each other by elimination of a $_{D}$-Ala group within the peptide portion of the murein chain catalyzed by the TP domain (Fig. 1.3) [22].

1.4.2 The β-lactam antibiotics inhibit bacterial transpeptidation

β-Lactam antibiotics are antibacterial agents which can effectively inactivate the final step of bacterial peptidoglycan synthesis (i.e. transpeptidation) leading to the death of the bacteria. β-Lactam contains a closed-loop azetidinyl group capable to bind to the transpeptidase domain of PBPs, forming a stable acyl-enzyme complex, thus inhibiting the transpeptidase activity as suicide substrate. The high binding affinity is largely due to its structural similarity to its substrate, the acyl-$_{D}$-Ala-$_{D}$-Ala portion of the peptidoglycan strand [22-23].

1.4.3 Overdependence and resistance to β-lactam antibiotics

Because of its incomparable effectiveness, broad-spectrum activity, low production cost and minimal side effects, β-lactam antibiotics are the preferred clinical prescription in the treatment of infections. The overdependence of β-lactam antibiotics, however, has already caused an imbalance in the bacterial ecosystem [24]. They are pressed to develop resistant mechanisms. Structure-based modifications of β-lactams help at the early stage, but bacteria soon become resistant to the modifications. The recently discovered resistance mechanism, the expression of New Delhi metallo-beta-lactamase 1 (NDM-1) carbapenemase [25] which can hydrolyze most of the new-generation β-lactam antibiotics, allows the bacteria to be susceptible only to some non-β-lactam antibiotics [26]. Table 1.2 summarizes some typical β-lactam antibiotics and their corresponding resistance mechanisms.

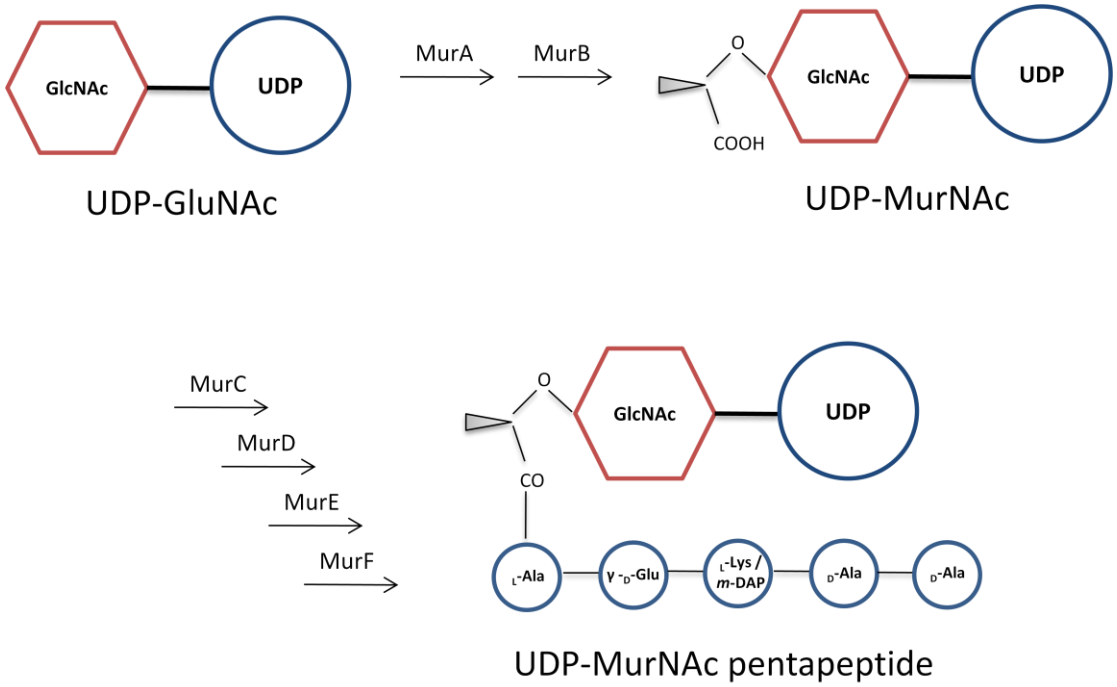

Fig. 1.2 Bacterial biosynthesis of UDP-MurNAc pentapeptide. The 5 blue small circles in UDP-MurNAc pentapeptide represent amino acids (from left to right) $_{L}$-alanine, γ-$_{D}$-glutamic acid, $_{L}$-lysine (or *m*-diaminopimelic acid), $_{D}$-alanine and $_{D}$-alanine. The lipid II of *S. aureus* has 5 extra glycines attached to the $_{L}$-lysine residue.

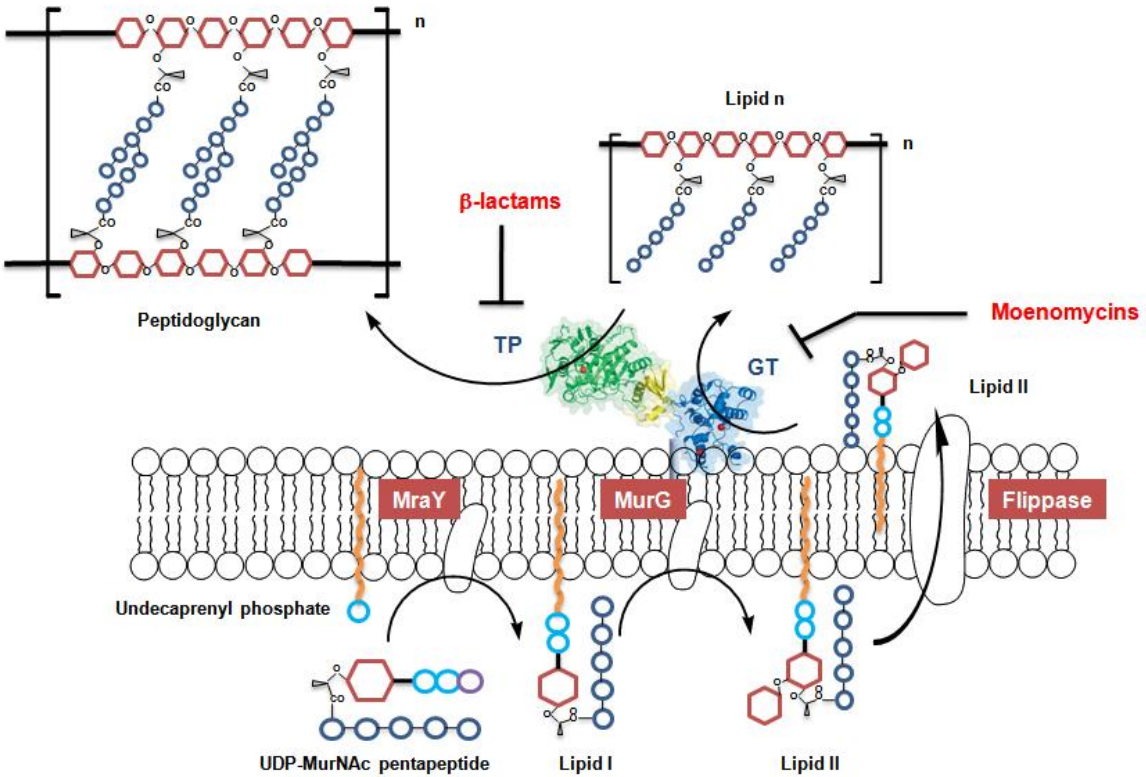

Fig. 1.3 The bacterial biosynthesis of murein (peptidoglycan) [19]. Red hexagons = hexoses; blue circles = phosphates; deep blue circle = amino acids (refers to Fig. 1.2); purple circle = uridine; orange zigzags = undecaprenyl lipids. The protein crystal structure at outer plasma membrane refers to *S. aureus* PBP2 (PDB ID 2OLV).

Table 1.2 Summary of some typical β-lactam antibiotics and their corresponding resistance mechanisms.

β-lactams	Corresponding resistance mechanisms	References
Penicillin	Penicillinase	[13]
Methicillin	PBP2a	[27]
Ampicillin	Penicillinase (TEM-1)[a]	[28]
Cephalothin	Cephalosporinase (AmpC)[b]	[29]
Clavulanic acid (non-antibacterial)	Inhibitor-resistant TEM (IRTs)[c]	[30-31]
Cefotaxime	Cefotaximase (CTX-M)[d]	[32]
Imipenem	Carbapenemase (NDM-1)[e]	[25-26]

[a] The designation of TEM refers to Temoneira, the first patient where the resistant *E. coli* strain was isolated; [b] AmpC refers to the expressing gene ampC; [c] IRT refers to Inhibitor-resistant TEM; [d] CTX refers to the hydrolytic activity against cefotaxime, and [e] NDM refers to New Delhi metallo-beta-lactamase.

1.5 GT as novel antibacterial drug target

The development of resistance (Table 1.2) in bacteria has equipped them with mechanisms to defense against β-lactam antibiotics. The drug companies realized that continuous modification of β-lactam antibiotics cannot help too much in restoring their antibacterial activity. At the beginning of the 21st century, they started to pay attention to non-β-lactam antibiotics to treat those highly resistant bacterial infections. For example, tigecycline, a third-generation tetracycline [33], was developed for the treatment of carbapenem-resistant *Acinetobacter* infections [34]. Despite its observable side effect and safety concerns [35], approval was still given to tigecycline by U.S. Food and Drug Administration (FDA) in 2005 [35-36]. However, resistance to tigecycline was also found within 10 years of administration [37], indicating the seriousness of antibiotic resistance problem.

As modification of the structure of β-lactam antibiotics is not efficient enough to fight against the drug resistance problem, scientists are now interested in searching for new antibacterial mechanisms, especially new drug targets located outside the cytoplasm. The inhibition of bacterial transglycosylation, the penultimate step of peptidoglycan synthesis [38], has become a hot topic for the development of novel

antibiotics.

1.5.1 Mechanism of peptidoglycan transglycoslation and its inhibition

Peptidoglycan glycosyltransferase (GT) is an "inverting" enzyme catalyzing the S_N2 transglycosylation reaction [39]. Using PBP2 as an example, the E114 residue first activates the hydroxyl group of acceptor lipid II, following a nucleophilic attack to the C1 carbon of the donor lipid chain. The donor phosphate is stabilized by Mg^{2+} - E171 residue during the transition state and is finally removed from C1. The resulting product (lipid n) has inverted stereochemistry relative to the original lipid tail (Fig. 1.4) [40].

Moenomycins are the only known natural inhibitors of GT [41]. It occupies both donor and acceptor sites of GT to stop transglycosylation which is bactericidal. Potency persists even after it has been discovered for more than 40 years. It has a high binding affinity towards GT by structurally mimicking its substrate lipid IV (Fig. 1.5). [22, 40, 42]

Although moenomycin is non-toxic to animals, it has a poor pharmacokinetic

property in humans, hypothetically due to its poor absorption from gastrointestinal tract [42]. Currently there is no clinically available GT inhibitor for human use and moenomycin can only serve as agricultural food additive (sold as flavomycin) [42].

1.5.2 Production of lipid II is a major barrier in GT inhibitor development

Lipid II is a central component in bacterial cell wall synthesis [43]. It is the substrate for peptidoglycan transglycosylation, and also an antibacterial drug target [44]. Vancomycin is a non-β-lactam antibiotic effective on curing MRSA infections. It inhibits the bacterial transpeptidation by binding to lipid II [44-46], but resistance has been found for *S. aureus* after 43 years of administration [3, 47]. Despite the effort on searching novel antibiotics with similar antibacterial mechanism, other lipid II-binding agents, such as nisin [48-50] and teixobactin [51], are complex cyclic peptides that are extremely difficult to synthesize [52-54].

On the other hand, the progress of development of GT inhibitors is slow. Apart from the natural inhibitor moenomycins, only a few research groups reported some potential inhibitors with promising inhibitory properties (refers to Fig. 1.6) [55-56]. The slow progress is primarily because of the absence of an effective assay due to the

difficulty in producing lipid II. Although lipid II can be obtained by total synthesis or enzymatic synthesis, both methods require extensive resources and manpower to achieve, and the product yield is very low. The total synthesis of lipid II requires 12 complicated reaction steps [57] while the enzymatic synthesis of lipid II requires 12 purified enzymes to proceed [18]. It is extremely difficult to repeat the procedures in conventional synthetic laboratory, not to mention in medical laboratories. Without the lipid II substrate (or its derivatives), *in vitro* transglycosylation assay is difficult to conduct.

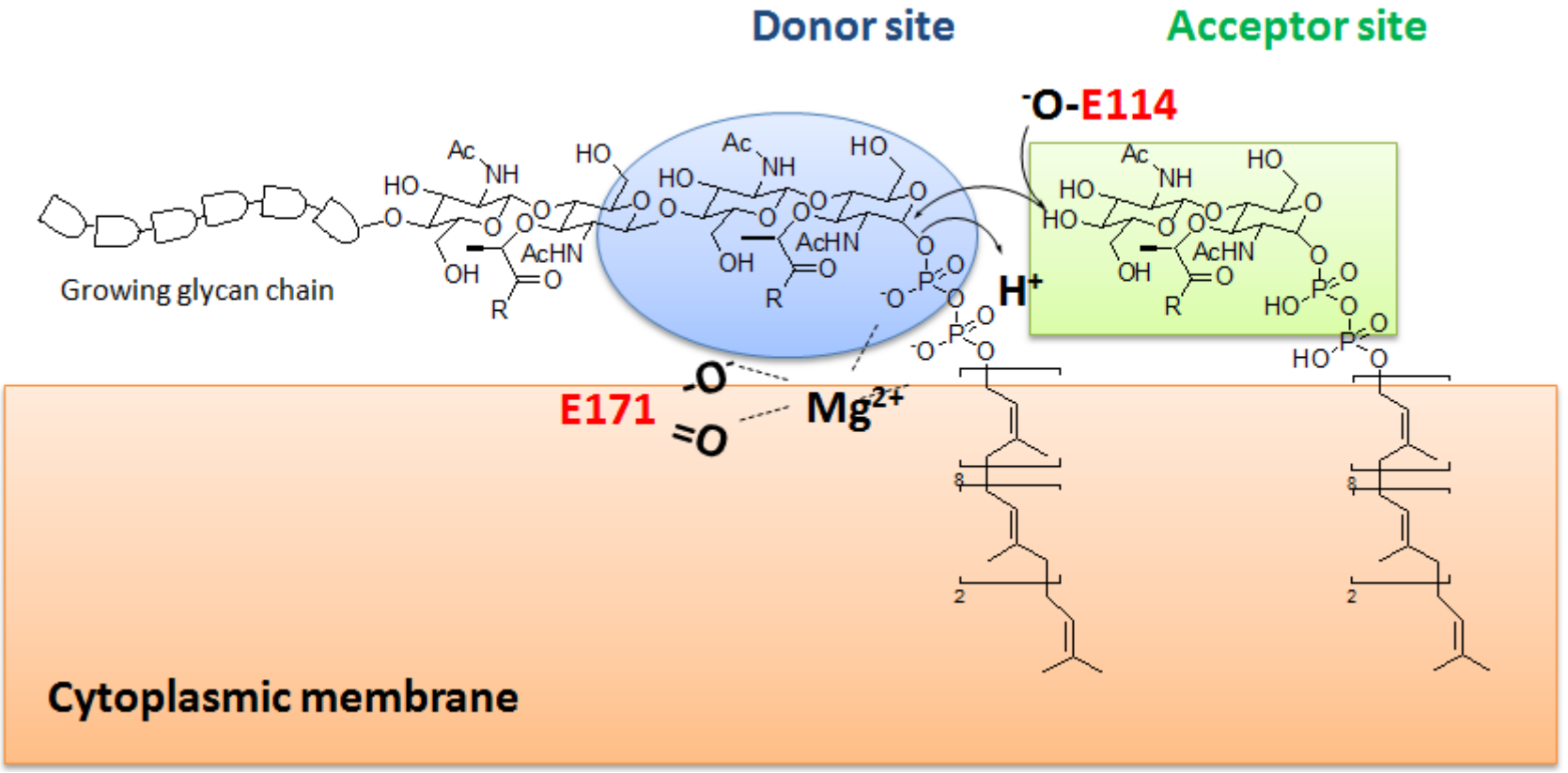

Fig. 1.4 Proposed mechanism of peptidoglycan transglycosylation by PBP2 [40]. The GT of PBP2 catalyses the formation of glycosidic linkage between 2 lipid II molecules by removing the phospholipid tail of lipid II at the donor site. R = pentapeptide (refers to Fig. 1.2).

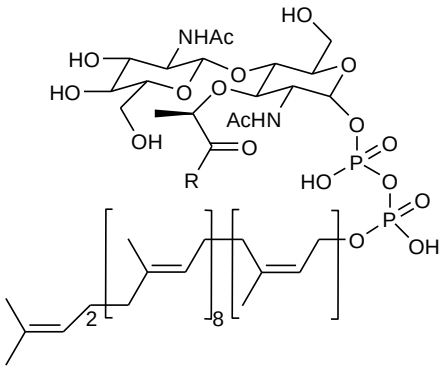

(a)

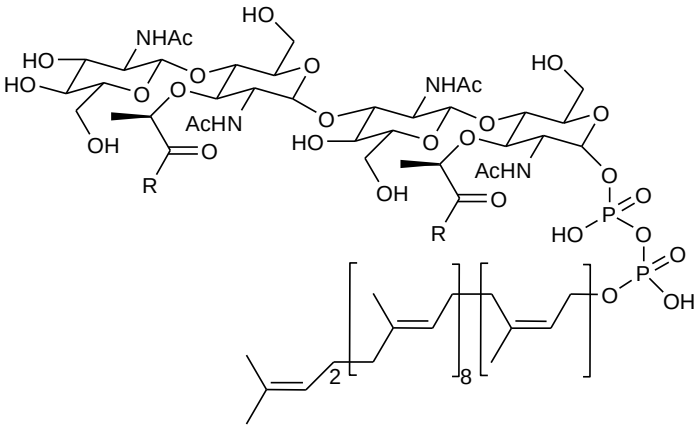

(b)

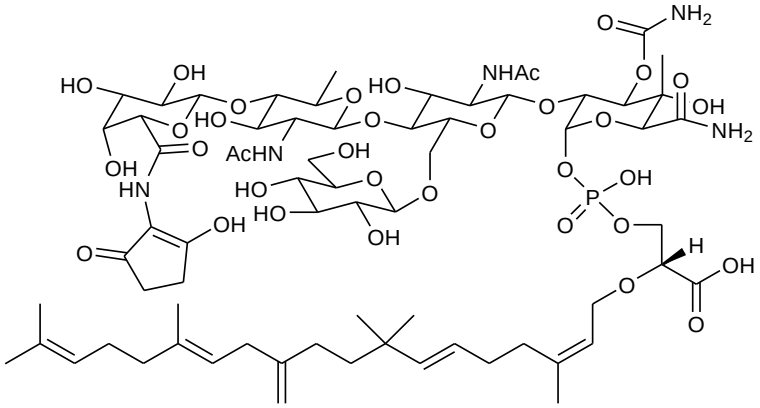

(c)

Fig. 1.5 Structures of (a) lipid II, (b) lipid IV and (c) moenomycin A. Moenomycin A structurally imitates lipid IV by conserving a phospholipid tail linked to an oligosaccharide. R = pentapeptide (refers to Fig. 1.2)

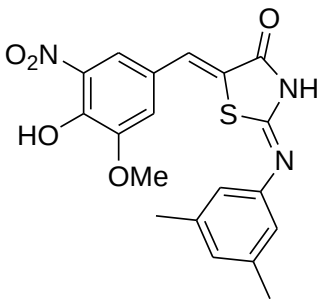

(a)

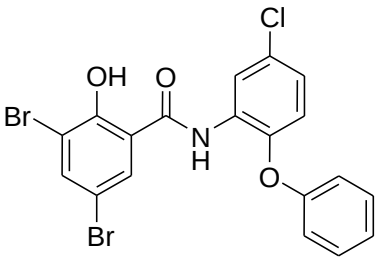

(b)

Fig. 1.6 Examples of novel GT inhibitors. (a) GT inhibitor reported by Gampe et al. IC_{50} = 12 μM [55]; and (b) GT inhibitor reported by Cheng et al. IC_{50} = 37.5 μM [56]. *S. aureus* penicillin-binding protein was used in the transglycosylation activity assays.

1.6 Methods to screen potential GT inhibitors without using lipid II

Ligand binding assay is an alternative method to investigate potential GT inhibitors without using the lipid II substrate. The interaction between GT and ligands can be revealed by various detection methods as described below [58-60]. A conventional means to screen potential structures before assay is computational virtual screening.

1.6.1 Structure-based virtual screening for GT inhibitors

Structure-based virtual screening is conducted by computer simulation mimicking the *in vitro* binding between small molecule ligands and their target biomolecule in solution. The binding affinities are calculated and visualized as scores [61]. The top-scoring ligands will be selected as potential binders ("hit compounds") for further characterization *in vitro*. In this way, potential hit compounds can be screened out from numerous non-binders without conducting physical measurements.

Virtual screening is particularly useful in GT inhibitors research when the peptidoglycan transglycosylation assay is unavailable. By screening out non-binders

from a library of usually more than 1 million compounds, the valuable lipid II can be reserved for assays for the top-scoring compounds only. The first batch of GT "hit compounds" were found by Yang et al. using Surflex-Dock [62] and FlexX-Pharm [63] docking programs against the DrugBank [64] and Life Chemical databases of ~174,000 compounds [65], but they were unable to conduct further *in vitro* characterizations. Derouaux et al. also found a "hit compound" using eHiTS 6.0 [66] against the NCl databases of > 250,000 compounds [67].

Wong and co-workers also reported an isatin structure as hit compound using ICM docking software (Molsoft L.L.C., San Diego, CA, USA) against a library of ~ 3,000,000 compounds [68]. The antibacterial activity was further improved by a serious of structure-based modifications. The final structure, **10b-27** (Fig. 1.7a), has a *S. aureus* MIC of 48 μg/mL [68]. The interaction between GT has been confirmed by STD-NMR spectroscopy [68].

1.6.2 Surface plasmon resonance (SPR) spectroscopy

SPR is a powerful tool to detect ligand-biomolecule interactions. It consists of a ligand-immobilized sensor chip with continuous flow of analyte solution. Binding of

analytes to the ligand increase the degree of total internal reflection (θ) of the sensor chip surface and the results are detected by a light source [69]. The first SPR-based GT binding assay was developed by Stembera et al. at 2002 using Biacore 3000 (GE Healthcare) based on competitive binding with moenomycin A derivatives [70]. Bury et al. and Cheng et al. also used SPR to confirm the binding affinity of modified moenomycins [71-72].

1.6.3 Fluorescence anisotropy

Fluorescence anisotropy is a dimensionless measurement of the extent of polarization of the emission from a fluorescent species [73]. When a fluorescent species of small size in solution is excited by a polarized light source, only those absorption dipoles parallel to the light will be excited and disordered, resulting in reduced population of the parallel dipoles. With sufficient time, all the species with parallel dipole are disordered so that the measured fluorescence anisotropy approaches zero. When the fluorescent species is bound to a macromolecule (for example, GT), it has a slower rate of rotational diffusion and the excited molecules become less disordered. The measured fluorescence anisotropy becomes higher than that without GT binding. In order to test non-fluorescent compounds, scientists

incubate fluorescent moenomycin A into GT before adding test compounds. Potential GT inhibitor can displace moenomycin A out of the GT active-site, resulting in reduction of the fluorescent anisotropy. [55-56, 72]

1.6.4 Saturation-transfer difference (STD)-NMR spectroscopy

STD-NMR is a popular technique in studying protein-ligand interactions. It is a non-destructive technique as it does not require chemical modification or pre-treatment of protein or ligands such as immobilization or labeling. It measures the difference of ligand resonance signals when the nearby protein experiences a selective signal saturation. In a mixture of solution containing protein and weak ligand, there is an equilibrium between bound and unbound state. When the ^{1}H NMR signals of the ligand is measured with additional radiation applied to the protein nuclei, those nuclei are excited to their high energy state and they will attempt to transfer the energy to the nearby ligand nuclei. The process is called the Nuclear Overhauser Effect (NOE). When the ligand nuclei accept the energy and keep at the high energy state, the resulting ligand resonance signal intensities will decrease. Since NOE happens only when the two nuclei are within 5 Å, a positive STD-NMR result can confirm the interaction between ligand and protein [74]. Rühl et al. used STD-NMR to study the interaction between moenomycin derivatives and *E. coli* PBP1b [75].

1.7 Aims and objectives

In their effort to develop novel antibacterial agents, Wong's group has identified a potential GT inhibitor **10b-27** (Fig. 1.7a). It has moderate antibacterial activities among Gram-positive bacteria (*S. aureus* MIC = 48 μg/mL), and the STD-NMR results confirmed the interaction between GT and **10b-27** [68]. The STD-NMR results also suggested that **10b-27** shared the same active-site pocket with moenomycin A. The binding pose [constructed by ICM version 3.6-1c (Molsoft L.L.C., San Diego, CA, USA)] between GT and **10b-27** suggested that the aminoguanidyl group interacted with the K155 and S160 residues while the 2 phenyl groups interacted with the I195, V233 and P234 residues, respectively (Fig. 1.7b) [68].

However, the MIC value of **10b-27** is not good enough to allow it to be an effective antibiotic. This thesis aims to improve its antibacterial activities by studying its structure-activity relationship (SAR). To achieve this goal, 20 new derivatives have been synthesized with reference to the binding pose of **10b-27** to the GT crystal structure (PDB ID 2OLV) [40]. The detailed synthetic procedures will be described in chapter 2; the SAR studies will be reported in chapter 3 and the interactions between GT and the new structure will be reported in chapter 4.

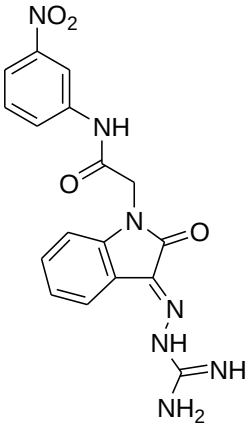

(a)

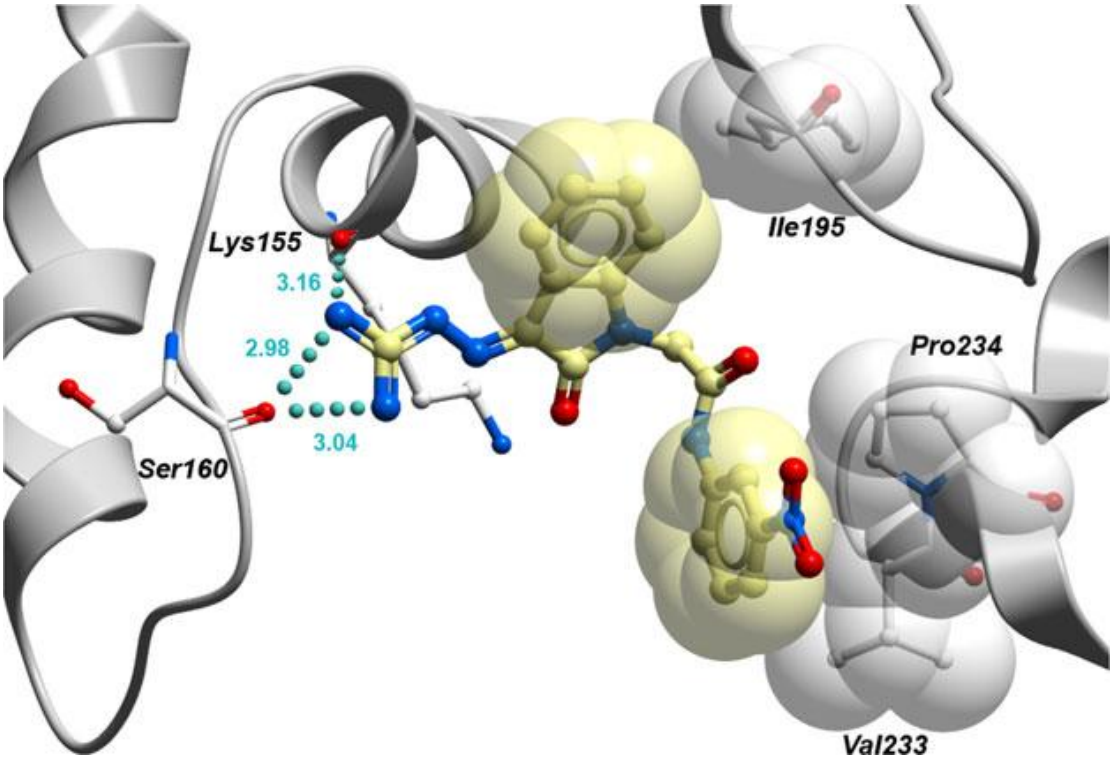

(b)

Fig. 1.7 (a) Structure of **10b**-**27** and (b) the binding pose between *S. aureus* GT (PDB ID 2OLV) and **10b**-**27**. Image adopted from reference [68].

Chapter 2

Synthesis and Characterization of Isatin Derivatives

2.1 Introduction

Isatin (IUPAC name: 1H-indole-2,3-dione) was first discovered by oxidation of indigo [76], and later it was found existing in nature including fruits of cannon ball trees and secretions of *Bufo* frogs [77]. Isatin and its derivatives are known to display pharmaceutical activities, including anticancer [77], anticonvulsant [78] and antibacterial [79], but the mechanisms are not fully understood.

Recently, Wang et al. synthesized an isatin-based derivative **10b-27** (Fig. 1.7a) targeting at the GT domain of PBP2 [68, 80]. However, the antibacterial activities of **10b-27** are only moderate in comparison to many commonly used antibiotics. Therefore, lead optimization is required to raise its potency [68, 80]. The isatin core, R_1 and R_2 groups of **10b-27** (Fig. 2.1) were modified in this project. The isatin core and the R_1 group were first modified and tested, experimental MIC results inspired further modifications of the R_2 group. The design strategies are explained below.

Previous studies on **10b-27** suggested that the aminoguanidyl group plays an important role in antibacterial activities and cannot be replaced, but there were no attempts on the modification of the isatin core [68, 80]. As seen in the binding pose of **10b-27** to the active site of GT domain (Fig. 1.7b), the C5 position of the isatin core

points to a space in the active site and there is no observable interactions with any GT residues. By inserting side groups to the isatin C5 carbon, it could create new interactions with the GT residues. As a result, **10c-27** with 5-methylisatin core was designed and synthesized.

The binding pose also suggested that the 4-nitrophenyl group of **10b-27** interacted with the GT residues V233 and P234 which are hydrophobic in nature. One would expect that the interactions will be enhanced if the nitro group was changed to some hydrophobic groups. Therefore three compounds with hydrophobic side groups were designed and synthesized (named as **10b-04**, **10b-19**, **10b-20** respectively**)**. The measured MICs (refers to Table 3.1) also agreed with the prediction that compound **10b-19** with hydrophobic naphthyl group showed enhanced potency against Gram-positive bacteria. This result inspired the further removal of the hydrophilic methanediylamidyl group. Hence, 16 new derivatives were further designed with side groups of different hydrophobicities, including alkyl, aryl, alkoxyl and hydroxyl groups.

In this thesis, 5-methylisatin derivatives were designated with a letter "c", derivatives with the methanediylamidyl group conserved were designated with a letter "b" whereas derivatives with the methanediylamidyl group removed were designated

with no alphabet letters (Table 2.2). Some derivatives were given smaller numbers than the mother compound **10b-27** because they were previously designated for docking purpose. This chapter will describe the synthetic pathways and characterization of the 20 new isatin derivatives. The structures of these derivatives are shown in Table 2.2.

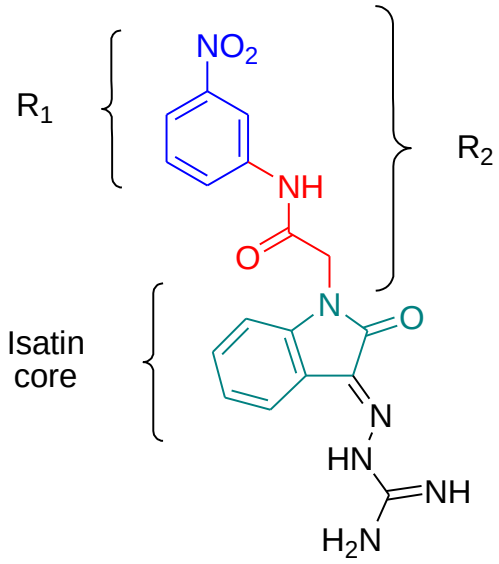

Fig. 2.1 Chemical modification of **10b-27** [80]. R_1 refers to the region shown in cyan; R_2 refers to the region shown in cyan and red; the isatin core is shown in green.

Table 2.1 Summary of previous MIC results of the hit compounds. [68, 80]

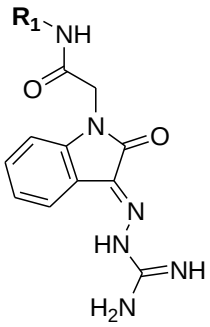

R_1	MIC (μg/mL)		
	S. aureus ATCC 29213	*B. subtilis* 168	*E. coli* ATCC 25922
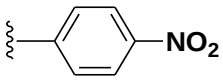	> 96	> 96	> 96
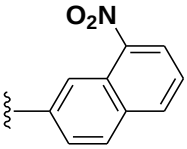	> 96	48	> 96
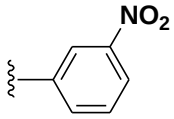 **(10b-27)**	48	24	96
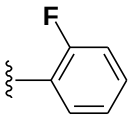	> 96	> 96	>96
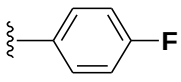	96	48	96
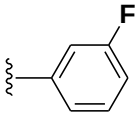	96	48	48

Table 2.2 Structures of **10b-27** (mother compound) and its 20 new derivatives.

Original hit (mother compound)
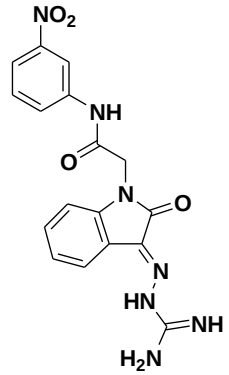
10b-27

With methanediylamidyl linkage conserved (designated with a letter "b")		
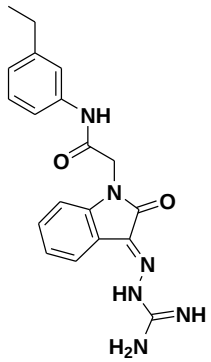	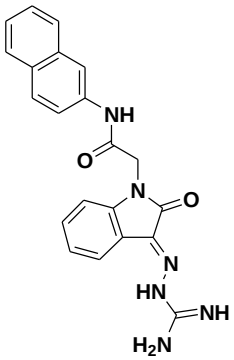	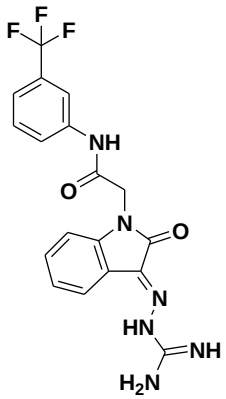
10b-04	**10b-19**	**10b-20**

Modification of the isatin core (designated with a letter "c")
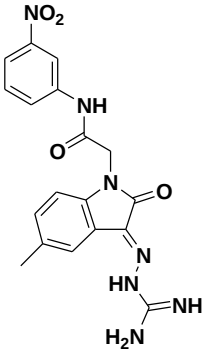
10c-27

With methanediylamidyl linkage deleted (designated with no alphabet letters)		
With hydrophobic substituents		
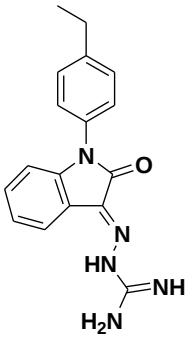 **10-31**	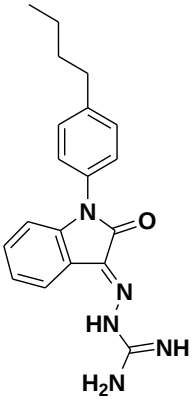 **10-32**	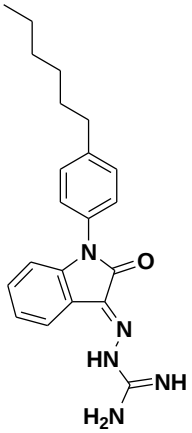 **10-33**
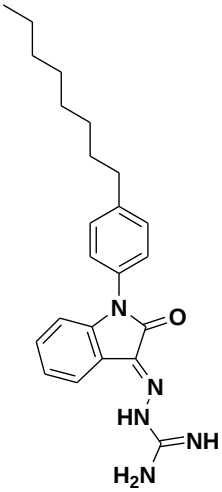 **10-34**	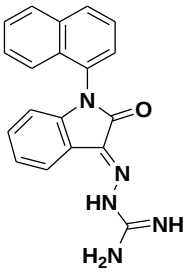 **10-35**	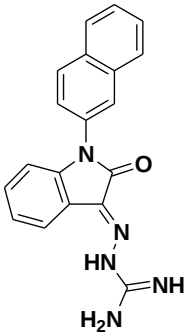 **10-36**
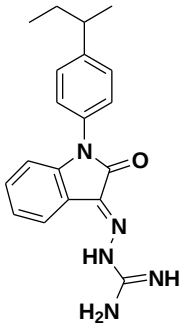 **10-42**		

With alkoxyl substituents		
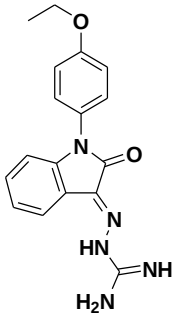 **10-37**	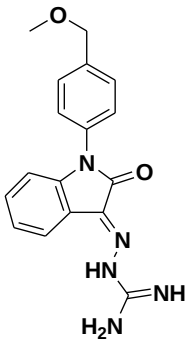 **10-38**	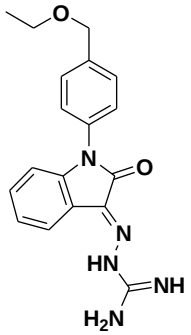 **10-39**
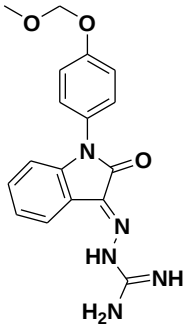 **10-40**	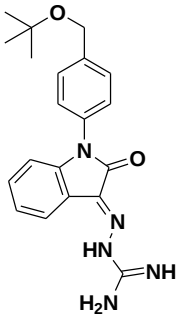 **10-41**	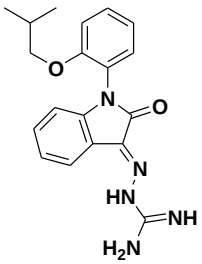 **10-46**

With hydroxyl substituents		
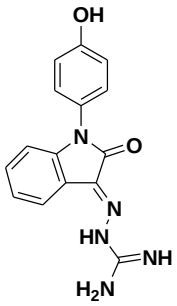 **10-43**	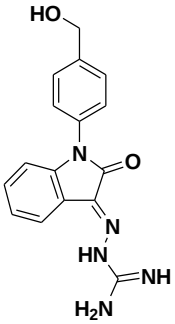 **10-44**	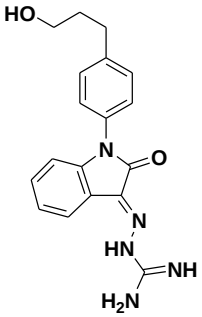 **10-45**

2.2 Experimental

2.2.1 Chemicals

Isatin, 5-methylisatin, aminoguanidine HCl, sodium chloride, potassium carbonate and various phenylboronic acids were purchased from Aldrich. Analytical grade solvents were purchased from Oriental Chemicals. Chloracetyl chloride was purchased from International Laboratory. Sodium sulfate was obtained from SciChem. Silica gel 60 (63-200 μm) used as stationary phase in column chromatography was purchased from Bio-Gene.

2.2.2 Instrumentation

2.2.2.1 Liquid chromatography

Liquid chromatography was used for purification of products after reactions. Silica gel 60 (63-200 μm) powder was first added to the appropriate mobile phase (solvent) and stirred to remove any bubbles. The suspension was loaded into a liquid chromatography column and allowed to sediment. Samples were first dissolved in a minimum amount of solvent and some dry silica gel powder was added into the solution, followed by removal of solvent using a rotary evaporator under vacuum for

complete adsorption of sample onto the silica gel surface. The silica gel was loaded into the liquid chromatography column. Mobile phase solvent was added to the column to elute the sample. The less polar fractions were eluted first and the more polar fractions were eluted as the polarity of mobile phase increased. Sample fractions were collected using test tubes and the product in each fraction was identified using thin-layer chromatography (TLC).

2.2.2.2 ^{1}H nuclear magnetic resonance (NMR) spectroscopy

All reaction intermediates and products were characterized by ^{1}H NMR spectroscopy. Purified products were first completely dried under vacuum. The dried products were dissolved in 600 μL of suitable deuterated solvents, and were added to NMR sample tubes. The ^{1}H-NMR spectra were collected using a Bruker Advance-III 400 MHz FT-NMR spectrometer. The products were re-collected after measurements.

2.2.2.3 Mass spectrometry (MS)

All final products were also characterized by mass spectrometry. Products were dissolved into suitable solvents with a concentration ~ 1 μM, and solutions were

injected into a Waters Acquity ESI mass spectrometry with single quadrupole detector (LRMS) or an Agilent 6460 Ultra High Performance Liquid Chromatography-Electrospray Ionization-Triple Quadrupole Mass Spectrometer (HRMS) at a flow of 200 μL/min.

2.2.3 Synthetic procedures

2.2.3.1 Synthesis of 10b-04, 10b-19, 10b-20 and 10c-27

1 (1.0 g) and potassium carbonate (1.2 g) were dissolved in acetonitrile (10 mL). Chloroacetyl chloride (700 μL) was added dropwisely and the reaction mixture was allowed to stir for 3 h at room temperature. Deionized water (20 mL) was added to the reaction mixture and the mixture was then extracted by ethyl acetate (3 x 20 mL). The ethyl acetate fractions were collected, washed with concentrated sodium chloride solution and dried by anhydrous sodium sulphate. The solvent was removed to yield a white solid **2**.

To 10 mL of dimethylformamide in an ice bath, isatin or 5-methylisatin (1.0 g) and potassium carbonate (1.0 g) were dissolved. The mixture was then stirred for 1 h at room temperature. **2 (**1.0 g) dissolved in minimum amount of dimethylformamide

was added to the reaction mixture, followed by addition of potassium iodide (0.5 g). The reaction mixture was stirred overnight at 80^{o}C. Afterwards, 2M hydrochloric acid (35 mL) was added to the mixture and the product was extracted by ethyl acetate (3 x 20 mL). The ethyl acetate fractions were washed with concentrated sodium chloride solution and dried by anhydrous sodium sulphate. After removal of solvent by a rotary evaporator, the product was purified by silica gel liquid chromatography using a mobile phase of ethyl acetate : petroleum ether (1:4), yielding **3** as a reddish solid.

3 (0.11 g) and aminoguanidine HCl (0.075 g) were dissolved in acetic acid (20 mL) and the reaction was performed under reflux for 2 h. After cooling to room temperature, diethyl ether (200 mL) was added to precipitate the reaction product. The product was collected by centrifugation, washed with diethyl ether (2 x 40 mL) and further purified by silica gel liquid chromatography using a mobile phase of methanol : dichloromethane (1:4), yielding the final product as a yellowish solid. The synthetic scheme for **10b-04**, **10b-19, 10b-20** and **10c-27** is given in Figure 2.2.

(10b-04). Yield 56 %. ^{1}H NMR (400 MHz, CD_3OD) δ: 1.23 (t, *J* = 7.6 Hz, 3H, CH_3CH_2), 2.64 (q, *J* = 7.6 Hz, 2H, CH_3CH_2), 4.71 (s, 2 H), 7.00 (d, *J* = 8.1 Hz, 1H, Ar-*H*), 7.09 (d, *J* = 8.0 Hz, 1H, Ar-*H*), 7.23 (q, *J* = 7.5 Hz, 2H, Ar-*H*), 7.38 - 7.43 (m,

2H, Ar-*H*), 7.51 (t, *J* = 7.9, 1H, Ar-*H*), 7.82 (d, *J* = 7.5 Hz, 1H, Ar-*H*). HRMS calculated for $C_{19}H_{21}N_6O_2$: m/z: 365.17 $[M+H]^+$; found 365.17.

(10b-19). Yield 62 %. ^{1}H NMR (400 MHz, CD_3OD) δ: 4.78 (s, 2H, NHCOC*H*$_2$), 7.13 (d, *J* = 7.9 Hz, 1H, Ar-*H*), 7.24 (t, *J* = 7.6 Hz, 1H, Ar-*H*), 7.41 - 7.54 (m, 3H, Ar-*H*), 7.59 (d, *J* = 8.9, 1H, Ar-*H*), 7.77-7.87 (m, 4H, Ar-*H*), 8.20 (s, 1H, Ar-*H*). HRMS calculated for $C_{21}H_{19}N_6O_2$: m/z: 387.16 $[M+H]^+$, found 387.16.

(10b-20). Yield 61 %. ^{1}H NMR (400 MHz, CD_3OD) δ: 4.75 (s, 2H, NHCOC*H*$_2$), 7.10 (d, *J* = 8.0 Hz, 1H, Ar-*H*), 7.23 (t, *J* = 7.6 Hz, 1H, Ar-*H*), 7.43 (d, *J* = 7.9 Hz, 1H, Ar-*H*), 7.49-7.57 (m, 2H, Ar-*H*), 7.78-7.84 (m, 2H, Ar-*H*), 8.01 (s, 1H, Ar-*H*). HRMS calculated for $C_{18}H_{16}F_3N_6O_2$: m/z: 405.13 $[M+H]^+$, found 405.13.

(10c-27). Yield 52 %. ^{1}H NMR (400 MHz, CD_3OD) δ: 2.40 (s, 3H, Ar-C*H*$_3$), 4.73 (s, 2H, NHCOC*H*$_2$), 6.97 (d, *J* = 8.1 Hz, 1H, Ar-*H*), 7.31 (d, *J* = 7.6 Hz, 1H, Ar-*H*), 7.59 (t, *J* = 8.2 Hz, 1H, Ar-*H*), 7.66 (s, 1H, Ar-*H*), 7.92 (d, *J* = 8.1 Hz, 1H, Ar-*H*), 8.02 (d, *J* = 8.1 Hz, 1H, Ar-*H*), 8.61 (s, 1H). HRMS calculated for $C_{18}H_{18}N_7O_4$: m/z: 396.14 $[M+H]^+$, found 396.14.

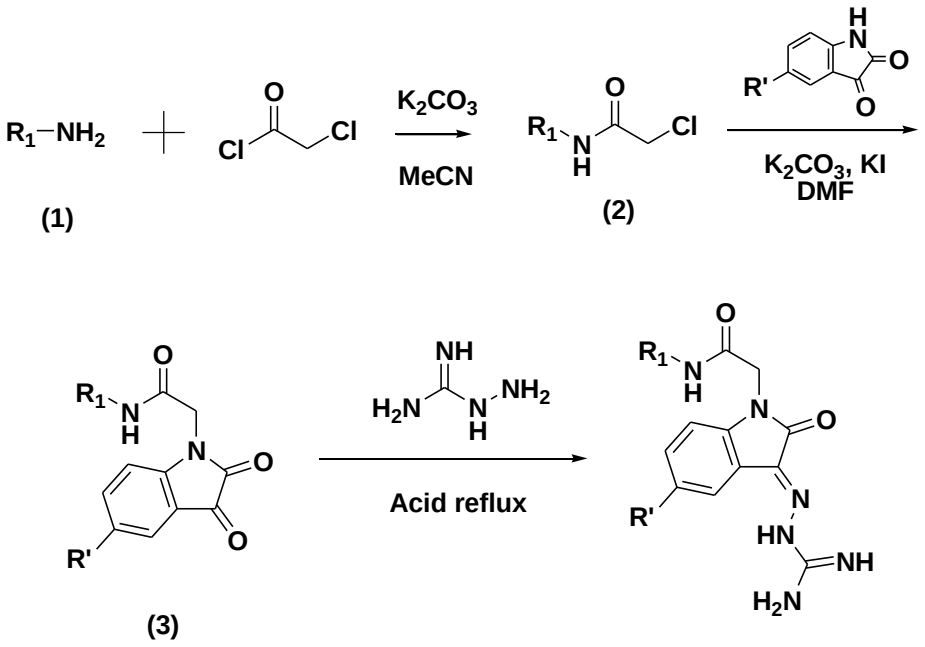

Fig. 2.2 Synthetic pathway for compounds **10b-04**, **10b-19**, **10b-20** and **10c-27**.

2.2.3.2 Synthesis of 10-31 to 10-46

4 (0.05 g), isatin (0.05 g) and dried $Cu(OAc)_2$ (0.055 g) were added to triethylamine (125 μL) in the presence of dry molecular sieves (4Å) and dichloromethane (10 mL). The $Cu(OAc)_2$ and molecular sieves were previously dried in an oven overnight at 100^{o}C. The reaction mixture was allowed to stir for 48-72 h at room temperature. Solid impurities were filtered, and excessive isatin was removed by silica gel liquid chromatography using a mobile phase of ethyl acetate : petroleum ether (1:4), yielding **5** as a yellowish solid.

5 (0.03 g) and aminoguanidine HCl (0.03 g) were added to acetic acid (20 mL) and stirred for 2 h at room temperature. Afterwards, diethyl ether (200 mL) was added to precipitate the reaction product. The product was collected by centrifugation, washed with diethyl ether (2 x 40 mL) and further purified by silica gel liquid chromatography (methanol : dichloromethane = 1:4), yielding the final product as a yellowish solid. The synthetic scheme for **10-31** to **10-46** is given in Figure 2.3.

(10-31). Yield 55 %. ^{1}H NMR (400 MHz, CD_3OD) δ: 1.29 (t, 3H, *J* = 7.6 Hz, CH_2CH_3), 2.74 (q, 2H, *J* = 7.6 Hz, CH_2CH_3), 6.84 (d, *J* = 8.0 Hz, 1H, Ar-*H*), 7.20 (t, *J*

= 7.5 Hz, 1H, Ar-*H*), 7.35 - 7.43 (m, 5H, Ar-*H*), 7.84 (d, *J* = 7.5, 1H, Ar-*H*). HRMS calculated for $C_{17}H_{18}N_5O$: m/z: 308.15 $[M+H]^+$, found 308.15.

(10-32). Yield 54 %. ^{1}H NMR (400 MHz, CD_3OD) δ: 0.97 (t, 3H, *J* = 7.4 Hz, CH_2CH_3), 1.40 (sex, 2H, *J* = 7.4 Hz, $CH_2CH_2CH_3$), 1.65 (quin, *J* = 7.4 Hz, 2H, $CH_2CH_2CH_2$), 2.70 (t, *J* = 7.5 Hz, 2H, Ar-CH_2CH_2), 6.83 (d, *J* = 8.0 Hz, 1H, Ar-*H*), 7.20 (t, *J* = 7.6 Hz, 1H, Ar-*H*), 7.33 - 7.41 (m, 5H, Ar-*H*), 7.83 (d, *J* = 7.5, 1H, Ar-*H*). HRMS calculated for $C_{19}H_{22}N_5O$: m/z: 336.18 $[M+H]^+$, found 336.18.

(10-33). Yield 52 %. ^{1}H NMR (400 MHz, CD_3OD) δ: 0.94 (t, 3H, *J* = 6.9 Hz, CH_2CH_3), 1.38 (m, 6H, $CH_2CH_2CH_2CH_2CH_3$), 1.70 (quin, *J* = 7.3 Hz, 2H, Ar-$CH_2CH_2CH_2$), 2.74 (t, *J* = 7.7 Hz, 2H, Ar-CH_2CH_2), 6.89 (d, *J* = 8.0 Hz, 1H, Ar-*H*), 7.23 (t, *J* = 7.5 Hz, 1H, Ar-*H*), 7.38-7.46 (m, 5H, Ar-*H*), 7.85 (d, *J* = 7.5, 1H, Ar-*H*). HRMS calculated for $C_{21}H_{26}N_5O$: m/z: 364.21 $[M+H]^+$, found 364.21

. **(10-34).** Yield 46 %. ^{1}H NMR (400 MHz, CD_3OD) δ: 0.90 (t, 3H, *J* = 6.7 Hz, CH_2CH_3), 1.30 - 1.36 (m, 10H, $CH_2CH_2CH_2CH_2CH_2CH_2CH_3$), 1.68 (quin, 2H, *J* = 7.0 Hz, Ar-$CH_2CH_2CH_2$), 2.71 (t, *J* = 7.6, 2H, Ar-CH_2CH_2), 6.85 (d, *J* = 8.0 Hz, 1H, Ar-*H*), 7.20 (t, *J* = 7.5 Hz, 1H, Ar-*H*), 7.38 - 7.42 (m, 5H, Ar-*H*), 7.83 (d, *J* = 7.4, 1H,

Ar-*H*). HRMS calculated for $C_{23}H_{30}N_5O$: m/z: 392.24 $[M+H]^+$, found 392.25.

(10-35). Yield 55 %. ^{1}H NMR (400 MHz, CD_3OD) δ: 6.42 (d, *J* = 7.9 Hz, 1H, Ar-*H*), 7.23 (t, *J* = 7.5 Hz, 1H, Ar-*H*), 7.34 (t, *J* = 7.4 Hz, 1H, Ar-*H*), 7.50 - 7.71 (m, 5H, Ar-*H*), 7.92 (d, *J* = 7.4 Hz, 1H, Ar-*H*), 8.06 (d, *J* = 8.2, 1H, Ar-*H*), 8.11 (d, *J* = 8.2, 1H, Ar-*H*). HRMS calculated for $C_{19}H_{16}N_5O$: m/z: 330.13 $[M+H]^+$, found 330.14.

(10-36). Yield 50 %. ^{1}H NMR (400 MHz, CD_3OD) δ: 6.90 (d, *J* = 7.9 Hz, 1H, Ar-*H*), 7.22 (t, *J* = 7.5 Hz, 1H, Ar-*H*), 7.40 (t, *J* = 7.7 Hz, 1H, Ar-*H*), 7.51 - 7.58 (m, 3H, Ar-*H*), 7.85 - 8.04 (m, 5H, Ar-*H*). HRMS calculated for $C_{19}H_{16}N_5O$: m/z: 330.13 $[M+H]^+$, found 330.14.

(10-37). Yield 42 %. ^{1}H NMR (400 MHz, CD_3OD) δ: 1.45 (t, *J* = 7.0 Hz, 3H, CH_2CH_3), 4.14 (q, *J* = 6.9 Hz, 2H, OCH_2CH_3), 6.84 (d, *J* = 8.0 Hz, 1H, Ar-*H*), 7.12 (d, *J* = 8.4, 2H, Ar-*H*), 7.22 (t, *J* = 7.6 Hz, 1H, Ar-*H*), 7.38 - 7.45 (m, 3H, Ar-*H*), 7.84 (d, *J* = 7.2, 1H, Ar-*H*). HRMS calculated for $C_{17}H_{18}N_5O_2$: m/z: 324.15 $[M+H]^+$, found 324.15.

(10-38). Yield 41 %. ^{1}H NMR (400 MHz, CD_3OD) δ: 3.46 (s, 3H, OCH_3), 4.58

(s, 2H, C*H*$_2$OCH$_3$), 6.91 (d, *J* = 8.4 Hz, 1H, Ar-*H*), 7.24 (t, *J* = 7.6, 1H, Ar-*H*), 7.43 - 7.51 (m, 3H, Ar-*H*), 7.60 (d, *J* = 8.4 Hz, 2H, Ar-*H*), 7.86 (d, *J* = 7.2, 1H, Ar-*H*). HRMS calculated for $C_{17}H_{18}N_5O_2$: m/z: 324.15 $[M+H]^+$, found 324.15.

(10-39). Yield 41 %. ^{1}H NMR (400 MHz, CD_3OD) δ: 1.28 (t, *J* = 7.0 Hz, 3H, CH$_2$C*H*$_3$), 3.64 (q, *J* = 7.0 Hz, 2H, OC*H*$_2$CH$_3$), 4.63 (s, 2H, Ar-C*H*$_2$O), 6.91 (d, *J* = 8.0 Hz, 1H, Ar-*H*), 7.24 (t, *J* = 7.6, 1H, Ar-*H*), 7.43 - 7.51 (m, 3H, Ar-*H*), 7.60 (d, *J* = 8.2 Hz, 2H, Ar-*H*), 7.86 (d, *J* = 7.8, 1H, Ar-*H*). LRMS calculated for $C_{18}H_{20}N_5O_2$: m/z: 338.16 $[M+H]^+$, found 338.10.

(10-40). Yield 35 %. ^{1}H NMR (400 MHz, CD_3OD) δ: 3.52 (s, 3H, OC*H*$_3$), 5.29 (s, 2H, OC*H*$_2$O), 6.86 (d, *J* = 8.0 Hz, 1H, Ar-*H*), 7.20 - 7.28 (m, 3H, Ar-*H*), 7.40 - 7.46 (m, 3H, Ar-*H*), 7.84 (d, *J* = 7.6, 1H, Ar-*H*). LRMS calculated for $C_{17}H_{18}N_5O_3$: m/z: 340.14 $[M+H]^+$, found 340.11.

(10-41). Yield 42 %. ^{1}H NMR (400 MHz, CD_3OD) δ: 1.35 [s, 9H, C(C*H*$_3$)$_3$], 4.60 (s, 2H, Ar-C*H*$_2$O), 6.90 (d, *J* = 8.0 Hz, 1H, Ar-*H*), 7.24 (t, *J* = 7.6 Hz, 1H, Ar-*H*), 7.43 - 7.48 (m, 3H, Ar-*H*), 7.59 (d, *J* = 8.4 Hz, 2H, Ar-*H*), 7.86 (d, *J* = 7.6 Hz, 1H, Ar-*H*). LRMS calculated for $C_{20}H_{24}N_5O_2$: m/z: 366.19 $[M+H]^+$, found 366.25.

(10-42). Yield 56 %. ^{1}H NMR (400 MHz, CD_3OD) δ: 0.90 (t, *J* = 7.4 Hz, 3H, CH_2CH_3), 1.32 (d, *J* = 7.2 Hz, 3H, $CHCH_3$), 1.70 (quin, *J* = 7.3 Hz, 2H, $CHCH_2CH_3$), 2.74 (sex, *J* = 7.0 Hz, 1H, CH_3CHCH_2), 6.90 (d, *J* = 8.0 Hz, 1H, Ar-*H*), 7.23 (t, *J* = 7.6 Hz, 1H, Ar-*H*), 7.41 - 7.47 (m, 5H, Ar-*H*), 7.86 (d, *J* = 7.2 Hz, 1H, Ar-*H*). HRMS calculated for $C_{19}H_{22}N_5O$: m/z: 366.18 $[M+H]^+$, found 336.18.

(10-43). Yield 32 %. ^{1}H NMR (400 MHz, CD_3OD) δ: 6.83 (d, *J* = 8.0 Hz, 1H, Ar-*H*), 7.00 (d, *J* = 8.8 Hz, 2H, Ar-*H*), 7.21 (t, *J* = 7.6 Hz, 1H, Ar-*H*), 7.28 (d, *J* = 8.8 Hz, 2H, Ar-*H*), 7.44 (t, *J* = 7.6 Hz, 1H, Ar-*H*), 7.84 (d, *J* = 7.2 Hz, 1H, Ar-*H*). HRMS calculated for $C_{15}H_{14}N_5O_2$: m/z: 296.11 $[M+H]^+$, found 296.12.

(10-44). Yield 29 %. ^{1}H NMR (400 MHz, CD_3OD) δ: 4.73 (s, 2H, CH_2OH), 6.90 (d, *J* = 8.0 Hz, 1H, Ar-*H*), 7.24 (t, *J* = 7.5 Hz, 1H, Ar-*H*), 7.43 - 7.50 (m, 3H, Ar-*H*), 7.58 - 7.62 (m, 2H, Ar-*H*), 7.86 (d, *J* = 7.4 Hz, 1H, Ar-*H*). LRMS calculated for $C_{16}H_{16}N_5O_2$: m/z: 310.33 $[M+H]^+$, found 310.24.

(10-45). Yield 36 %. ^{1}H NMR (400 MHz, CD_3OD) δ: 1.92 (quin, *J* = 7.1 Hz, 2H, $CH_2CH_2CH_2$), 2.82 (t, *J* = 7.6 Hz, 2H, Ar-CH_2CH_2), 3.64 (t, *J* = 6.2 Hz, 2H, CH_2OH), 6.90 (d, *J* = 8.0 Hz, 1H, Ar-*H*), 7.24 (t, *J* = 7.6 Hz, 1H, Ar-*H*), 7.40 - 7.49 (m, 5H,

Ar-*H*), 7.86 (d, *J* = 7.2 Hz, 1H, Ar-*H*). LRMS calculated for $C_{18}H_{20}N_5O_2$: m/z: 338.16 $[M+H]^+$, found 338.14.

(10-46). Yield 48 %. ^{1}H NMR (400 MHz, CD_3OD) δ: 0.79 [dd, *J* = 10.16, 6.8 Hz, 6H, $CH_2CH(CH_3)_2$], 1.85 [nonet, 1H, *J* = 6.4 Hz, $CH_2CH(CH_3)_2$], 3.79 [m, 2H, $CH_2CH(CH_3)_2$], 6.59 (d, *J* = 8.0 Hz, 1H, Ar-*H*), 7.14 - 7.26 (m, 3H, Ar-*H*), 7.40 - 7.41 (m, 2H, Ar-*H*), 7.54 (t, *J* = 8.0 Hz, 1H, Ar-*H*), 7.84 (d, *J* = 7.2 Hz, 1H, Ar-*H*). HRMS calculated for $C_{19}H_{22}N_5O_2$: m/z: 352.18 $[M+H]^+$, found 352.18.

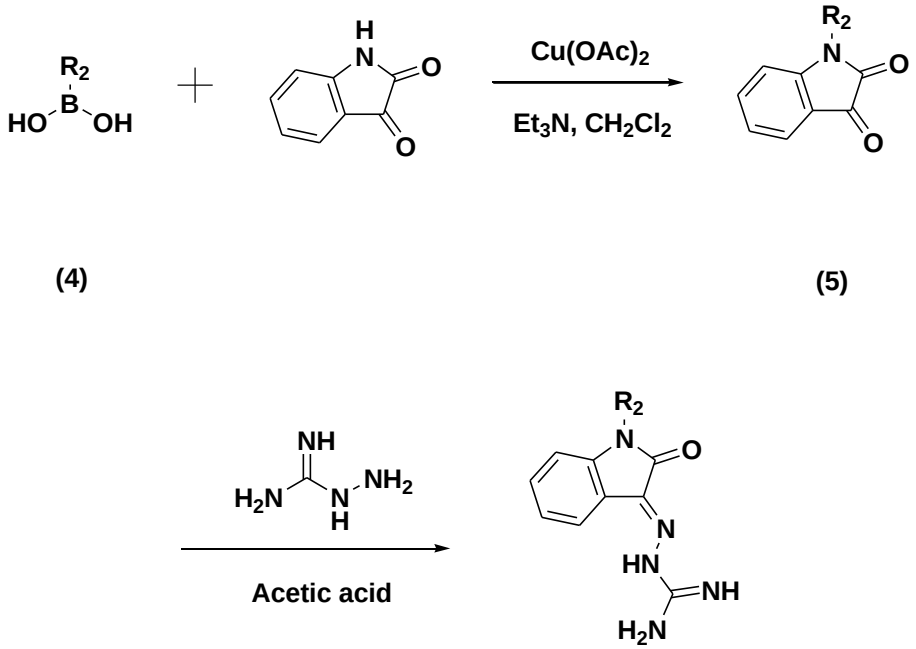

Fig. 2.3 Synthetic pathway for compounds **10-31** to **10-46**.

2.3 Results and discussions

The 20 new isatin derivatives have been synthesized and the structures were characterized by ^{1}H NMR spectroscopy. The number of protons integrated and the peak multiplicities in each spectrum were consistent with the corresponding structures. Compounds with the methanediylamidyl linkage conserved (**10b-04**, **10b-19**, **10b-20** and **10c-27**) showed extra singlet peaks at $\delta \sim 4.7$ ppm, assignable to the 2 methanediyl protons. The amino and hydroxyl protons are NMR-inactive since the protons can exchange between the deuterium in methanol-d_6. For MS characterization, positive electrospray ionization were applied in all measurements. The major $[M+1]^+$ peaks were observed in all the spectra, with some of them contained minor $[M+Na]^+$ and $[2M+H]^+$ peaks. All NMR and mass spectra can be found in Appendix I.

Previous MIC results suggested that the aminoguanidyl group of the hit compounds are essential to the antibacterial activities [68, 80]. Derivatives with R_1 at the *meta*-position of the phenyl ring are more potent than that at the *ortho*- and *para*-positions, in which the *meta*-nitrophenyl derivative is more effective against Gram-positive bacteria while the *meta*-fluorophenyl derivative is more effective against Gram-negative bacteria (Table. 2.1) [68, 80]. In this regards, 3 more

derivatives (assigned as **10b-04**, **10b-19** and **10b-20**) of new R_1 groups (shown in cyan, Fig. 2.1) were synthesized. Moreover, a **10b-27** derivative with methylation at C5 position of the isatin core (named as **10c-27**) was also synthesized. The synthetic procedures were the same except isatin that was replaced by 5-methylisatin. The yields of the four products were ~ 60 %.

In addition, 16 more isatin derivatives with the methanediylamidyl linkage removed (shown in red, Fig. 2.1) were designed and synthesized in order to increase the hydrophobicity of the compounds. The *N*-phenylisatins were formed by the Chan-Evans-Lam coupling reactions using copper(II) acetate as catalyst [81-83]. Although the coupling can also be done by the Buchwald-Hartwig reaction with palladium as catalyst [84-86], copper(II) acetate is less expensive and more environmentally friendly and therefore was preferred.

The reactions between isatin compounds and aminoguanidine are condensation reactions in the presence of acetic acid. The condensation reaction is accelerated under reflux [68, 80], but reduced yields were found for alkoxyl and hydroxyl derivatives. Upon analyzing the unpurified reaction product of **10-44** by mass spectrometry, an additional mass peak at 352.1 $[M+H]^+$ (Fig. 2.4) was found, which

was assigned as the esterified side product (Fig. 2.5).

To optimize the reaction conditions, the condensation reaction of **10-40** was performed at room temperature for 4 hours. An overall yield of 35% was obtained. However, when the reaction was performed under reflux for 4 hours, no **10-40** was obtained. The hydrolyzed **10-40** was obtained as the major product instead (Fig. 2.5).

These findings suggested that the alkoxy and hydroxyl groups of the compounds can react with acetic acid and generate side products under high temperature. In order to minimize the side reaction, it is recommended to conduct the condensation reaction with alkoxyl and hydroxyl derivatives at room temperature.

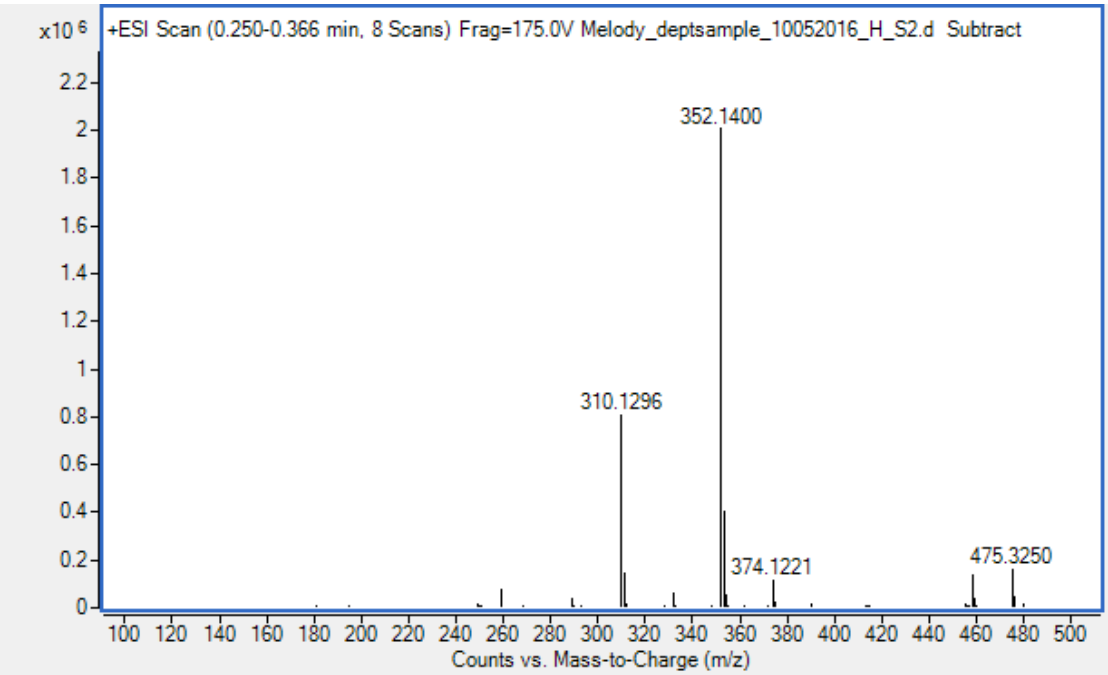

Fig. 2.4 ESI-MS spectrum of the unpurified reaction product of **10-44** after acetic acid reflux. The mass 310.13 $[M+H]^+$ refers to compound **10-44** and the mass 352.14 $[M+H]^+$ refers to esterified side product (Fig. 2.5).

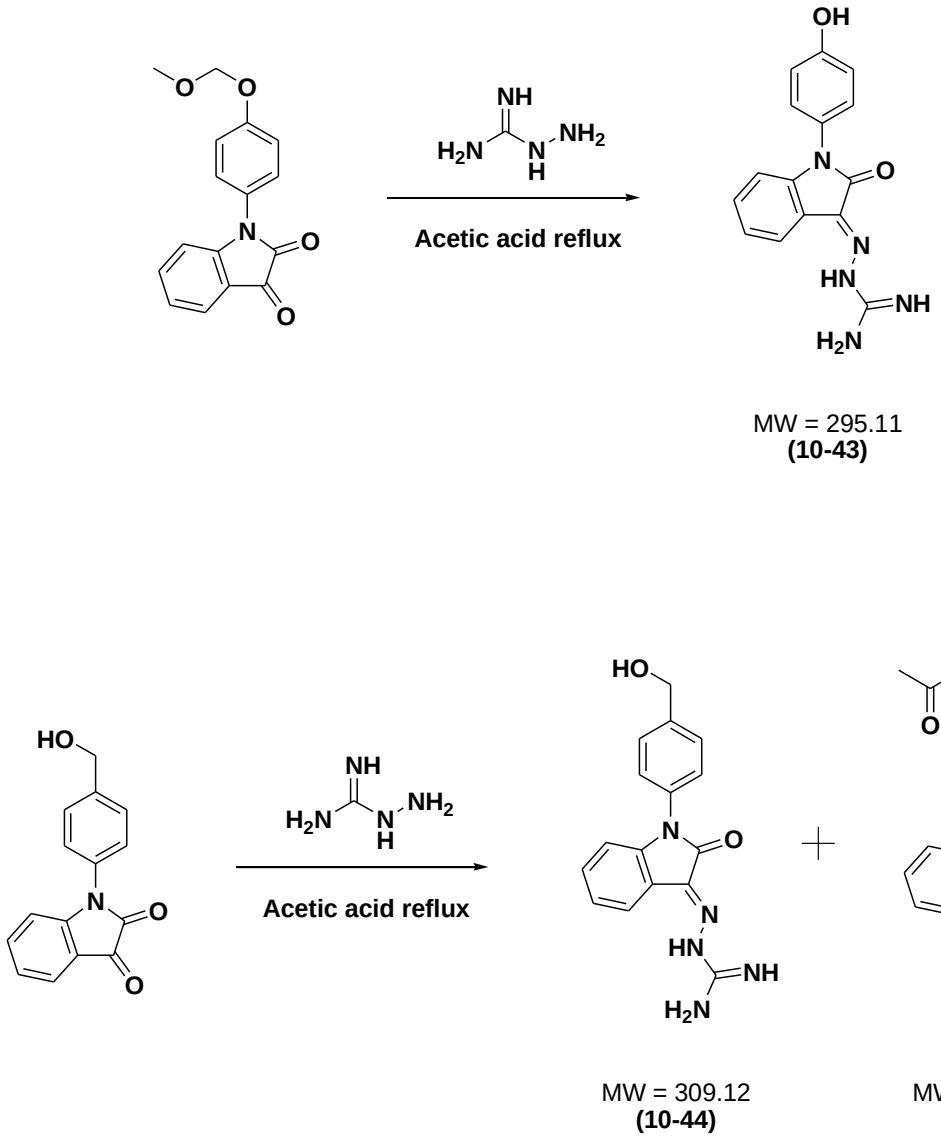

Fig. 2.5 Side reactions found for the condensation reactions for **10-40** and **10-44** under acetic acid reflux.

2.4 Concluding remarks

With reference to the binding pose of **10b**-**27** to the *S. aureus* GT binding site (Fig. 1.7b), 20 new isatin derivatives were designed and synthesized. The reactions conditions involving alkoxyl and hydroxyl groups have been optimized and considerable yields were obtained for the reactions at room temperature. The products are methanol-soluble yellowish solid and have been characterized by ^{1}H NMR and ESI-MS (all spectra are available at Appendix I). The derivatives were dried and stored at -20^{o}C for further SAR and STD-NMR studies. All of them have a shelf life of more than 1 month (stored at -20^{o}C) without observable degradation detected by ESI-MS.

Chapter 3

Structure-Activity Relationship (SAR) Studies of the Isatin Derivatives

3.1 Introduction

Structure-activity relationship (SAR) is the relationship between a chemical structure and its biological activity [5]. It provides important information for the structure-based drug design. Since *in vitro* transglycosylation assay for GT inhibitors is limited by the availability of lipid II, the SAR study was performed by testing the MIC values of the 20 derivatives against Gram-positive and Gram-negative bacteria.

Two important observations were obtained in previous studies: the aminoguanidyl group was important for the exhibition of antibacterial activity, and the side groups attached to the *meta*-position showed the best antibacterial activities (Table 2.1) [68, 80]. The SAR studies of the new isatin derivatives will be reported in this chapter. The modification strategies have been discussed in Chapter 2.1. Each side group was designed based on the MIC results of the previous derivatives, and also with reference to the 2 powerful substituents predicting tools: Craig plot and Topliss scheme. Craig plot provides information about the hydrophobicity and the electron-withdrawing or donating ability of a substituent [87] while Topliss scheme provides guidelines to new substituents based on the SAR results of previous substituents [88].

The 20 new derivatives have been designed and synthesized as reported in Chapter 2, their MIC will be measured against Gram-positive *S. aureus*, *B. subtilis* and Gram-negative *E. coli*, including the clinically significant MRSA (ATCC® BAA-41™). The structures of these derivatives are shown in Table 2.2.

3.2 Experimental

3.2.1 Chemicals and reagents

Bacterial strains were purchased from American Type Culture Collection (ATCC). Culture media were bought from Oxoid. Ampicillin was obtained from Sigma, and moenomycin A was isolated from flavomycin purchased from International Laboratory as described [89].

3.2.2 Minimum inhibitory concentration (MIC)

Procedures were referenced to the standard method M7-A7 [90]. MHB was the medium for *B. subtilis* and *E. coli* while CA-MHB was the medium for *S. aureus*. Frozen stock bacterial strains were streaked on a TSA plate and incubated at 37^{o}C for 16 h. A single colony was picked and added to a fresh autoclaved liquid medium at 37^{o}C for 5 h at 250 rpm. It was further diluted by adding 2 μL of the culture solution into 5 mL of fresh autoclaved medium.

Isatin derivatives were first dissolved in DMSO (9.6 mg/mL) and serially diluted (concentration by half) to give a serious of solutions with concentrations ranged from

9.6 mg/mL to 0.075 mg/mL. A solution of each concentration (1 μL) was added into 2 separate wells of a 96-well microplate (as duplicate results), followed by addition of diluted culture solution (99 μL) in each well, the working isatin derivative concentrations were ranged between 96 μg/mL to 0.75 μg/mL. Negative control wells were made by addition of DMSO (1 μL) and bacteria-free medium (99 μL) while positive control wells were made by addition of DMSO (1 μL) and diluted culture solution (99 μL). Solutions were well mixed and incubate at 37^{o}C for 18 h, and ODs of all wells were measured at 600 nm using BioRad 680 Microplate Reader.

MIC is the lowest drug concentration with a calculated bacterial inhibition ≥ 90 % [91]. The percentage bacterial inhibition can be calculated using the following equation.

$$\%\ \text{bacterial inhibition} = \frac{\text{OD of positive control} - \text{OD of drug solution}}{\text{OD of positive control} - \text{OD of negative control}}\ \text{x}\ 100\%$$

3.3 Results and discussions

The MIC values of all 20 isatin derivatives were measured and shown in Table 3.1. Among all 20 new derivatives, **10-32** showed the most promising MIC against both Gram-positive and Gram-negative bacteria, in which the *S. aureus* MIC was 8 folds more potent than the mother compound **10b-27** (Table 3.1). **10-42** showed even better potency on *B. subtilis* but decreased potency on *E. coli*. All analogues with alkoxyl (**10-37** to **10-41**) and hydroxyl (**10-43** to **10-45**) substituents did not show any improvement on MIC to the mother compound (**10b-27**), except **10-46** which is an *ortho*-substituted analogue with aliphatic carbon chain (n = 4). The findings suggested that hydrophobic substituents are important on the antibacterial activities.

The deletion of the methanediylamidyl group showed improvement in the antibacterial activities. For example, **10b-04** and **10-31** both carry an ethyl substituent, **10b-04** (with methanediylamidyl group conserved) showed no improvement compared to the mother compound (**10b-27**) while **10-31** (with methanediylamidyl group deleted) was more potent to *B. subtilis* and *E. coli* (Table 3.1).

All analogues with hydrophobic substituents and methanediylamidyl group

deleted (**10-31** to **10-36** and **10-42**) showed improved potencies compared to the mother compound (**10b-27**), in which analogues with aliphatic substituents are more potent than those of aromatic substituents, except **10-31** with short alkyl chain (n = 2). It can be explained by the binding pose of **10-32** to GT (Fig. 3.1). The alkyl chain of **10-32** (n = 4) was long enough to interact with the V233 and P234 residues of GT, whereas further increase in the alkyl chain length (**10-33**, n = 6 and **10-34**, n = 8) did not exhibit additional advantages in interacting with the GT residues, thus they displayed similar potencies against Gram-positive bacteria. **10-31** had a shorter alkyl chain (n =2) which was too short to interact with the V233 and P234 residues of GT, resulting in reduced potency compared to **10-32** to **10-34**.

Compounds **10-32**, **10-33** and **10-34** showed promising MIC results against Gram-positive bacteria, but **10-33** and **10-34** showed progressive reduction of potencies against Gram-negative *E. coli.* as the alkyl chain length increased (red line, Fig. 3.2). This could be due to the difference in cell wall structure between the Gram-positive and Gram-negative bacteria. Since the cell surface of Gram-negative bacteria include an extra outer-membrane, this outer-membrane may act as a physical barrier so that compounds with longer alkyl chain lengths were less able to diffuse (or through porins) to the plasma membrane, thus reducing the drug potency.

Gram-positive bacteria do not include outer-membrane, compounds can directly diffuse to the plasma membrane regardless to the lipophilicity or molecular size, so compounds with different alkyl chain lengths displayed similar MIC value against Gram-positive bacteria (blue line, Fig. 3.2).

Although the analogues with methanediylamidyl group conserved (**10b-04**, **10b-19** and **10b-20**) were less potent comparing to those with the methanediylamidyl group deleted, their SAR were still studied using substituent hydrophobicity constant (π) and Hammett substituent constant (σ) (Table 3.2). π is a measurement of hydrophobicity of a substituent [92]; σ is a measurement of electron-withdrawing or electron-donating ability of a substituent [93]. In this study, there was no observable relationship between σ and antibacterial activity, but the two analogues with improved activities (**10b-19** and **10b-20**) have higher π values than the others, with **10b-19** showing a very high π value of 1.23. This finding is consistent to the promising antibacterial activities of **10-31** to **10-36** which contain hydrophobic substituents.

Considering the 2 analogues **10b-27** and **10c-27**, the additional methyl group at the isatin core showed neither improvement nor suppression on the antibacterial activities. This means future modification on the methyl group could be possible to

further enhance the antibacterial activities.

The 20 new derivatives were also docked to the donor site of GT using *S. aureus* PBP2 (PDB ID 2OLV) and the binding affinities were calculated using Autodock Vina [94]. The binding affinities ranged from -6.4 to -7.7 kcal/mol and no direct relationship was observed between the ligand binding affinity and the antibacterial activities. The results were understandable because the software simulated the binding affinities in aqueous solution, it might not be fully compatible to membrane proteins which bind to ligands in the hydrophobic membrane (phospholipid) region. The binding affinities obtained by docking are shown in Table 3.3.

Table 3.1 MIC values of the 20 new isatin derivatives. Structures refer to Table 2.2.

Name	MIC (μg/mL)			
	S. aureus (ATCC 29213)	*S. aureus* (ATCC BAA-41)	*B. subtilis* 168	*E. coli* (ATCC 25922)
10b-27*	48	N.D.	24	96
10b-04	48	48	24	>96
10b-19	12	12	12	>96
10b-20	24	24	12	48
10c-27	48	48	24	96
10-31	48	48	12	48
10-32	6	6	6	12
10-33	6	6	6	48
10-34	6	6	6	>96
10-35	48	48	24	48
10-36	24	24	12	48
10-37	96	>96	24	96
10-38	>96	>96	>96	>96
10-39	>96	>96	96	>96
10-40	>96	>96	96	>96
10-41	96	96	48	>96
10-42	6	6	3	48
10-43	>96	>96	96	>96
10-44	>96	>96	>96	>96
10-45	>96	>96	>96	>96
10-46	24	48	12	>96
MoeA	<0.75	<0.75	1.5	>96
Amp	<0.75	>96	<0.75	6

Analogues with improved MIC to the mother compound (**10b-27**) were highlighted in blue.

MoeA = moenomycin A; Amp = ampicillin.

*Adopted from reference [68].

Table 3.2 Substituent hydrophobicity constant (π) and Hammett substituent constant (σ) of substituents (aromatic substituents, *meta*-position). **10b-19** and **10b-20** (highlighted in blue) have high π values and improved MIC values.

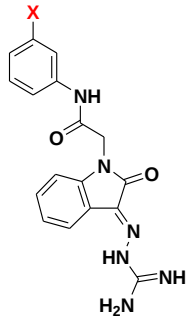

Substituent (X)	π	σ	MIC (*S. aureus*)
-H	0 [87]	0 [93]	>192 μg/mL [68]
-OCH_3	0.12 [87]	0.115 [95]	192 μg/mL [68]
-CN	-0.57 [87]	0.56 [95]	>192 μg/mL [68]
-CH_3	0.51 [87]	-0.069 [95]	192 μg/mL [68]
-Cl	0.76 [87]	0.373 [95]	>192 μg/mL [68]
-NO_2 (**10b-27**)	0.11 [87]	0.710 [95]	48 μg/mL [68]
-F	0.13 [87]	0.337 [95]	96 μg/mL [68]
-CH_2CH_3 (**10b-04**)	0.97 [87]	-0.07 [93]	48 μg/mL
-C_4H_4 (*m*,*p*-naphthyl) (**10b-19**)	1.23 [96]	0.17 [93]	12 μg/mL
-CF_3 (**10b-20**)	1.07 [87]	0.43 [95]	24 μg/mL

Table 3.3 Docking of the 20 isatin derivatives to the donor site of GT using *S. aureus* PBP2 (PDB ID 2OLV).

Name	Best mode binding affinity (kcal/mol)
10b-27	-7.6
10b-04	-6.7
10b-19	-7.6
10b-20	-7.4
10c-27	-7.6
10-31	-6.6
10-32	-6.5
10-33	-6.8
10-34	-6.6
10-35	-7.7
10-36	-7.5
10-37	-6.4
10-38	-6.5
10-39	-6.5
10-40	-6.6
10-41	-6.6
10-42	-6.8
10-43	-7.4
10-44	-6.7
10-45	-6.8
10-46	-7.1

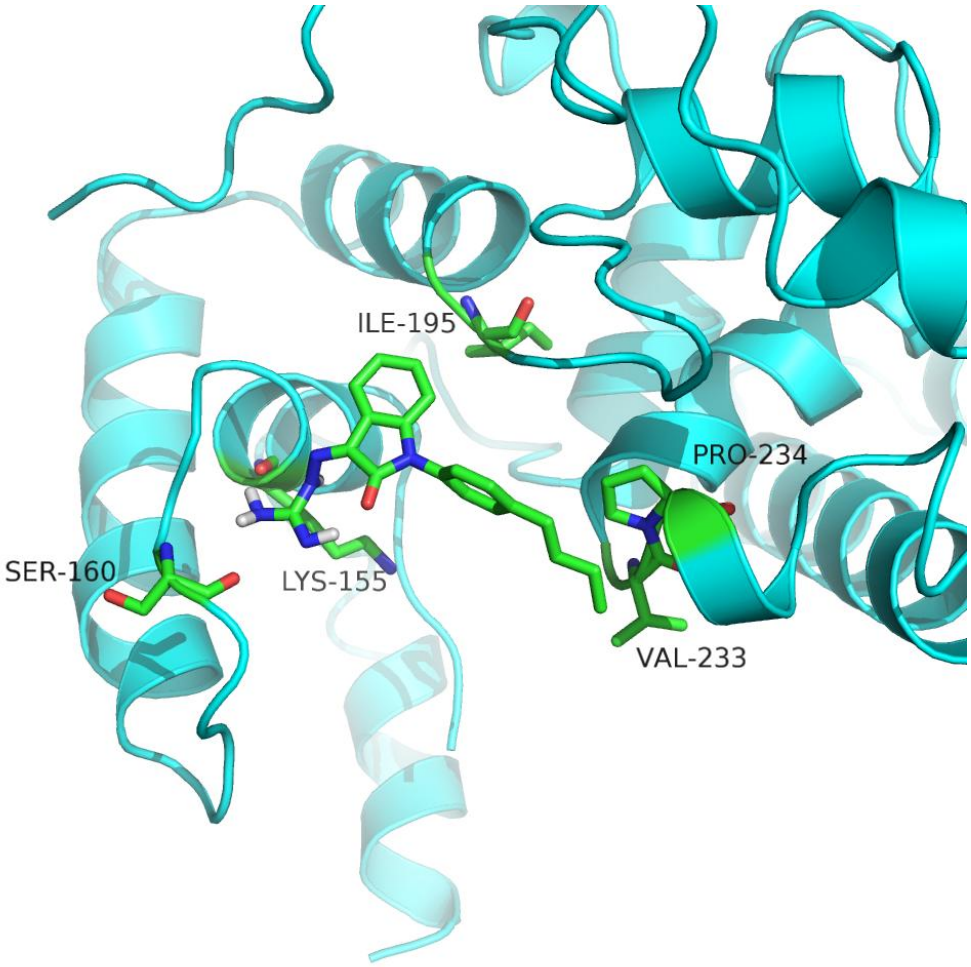

Fig. 3.1 Binding pose of **10-32** to the donor site of *S. aureus* GT (PDB ID 2OLV).

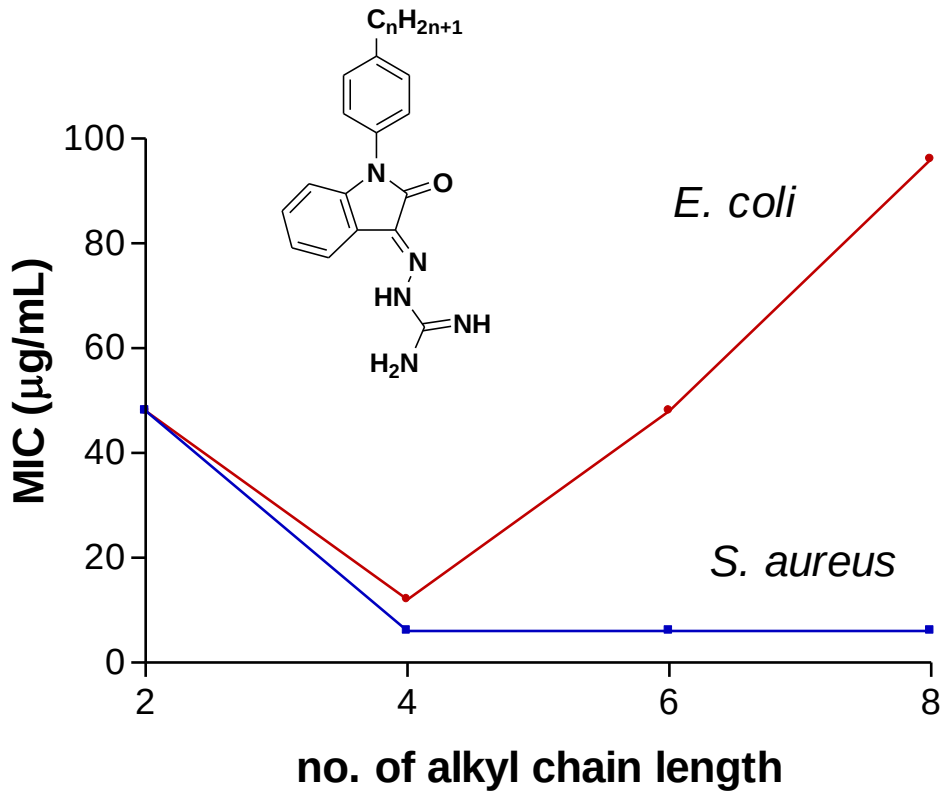

Fig. 3.2 Relationship between no. of alkyl chain length (n) on the isatin derivative and MIC values on Gram-positive *S. aureus* (blue) and Gram-negative *E. coli* (red). The measured MIC of **10**-**34** (n = 8) for *E. coli* is > 96 μg/mL, but plotted as 96 μg/mL for easy reference.

3.4 Concluding remarks

The SAR of the new 20 isatin-based derivatives had been studied. A promising derivative, **10-32**, which showed promising antibacterial activities against both Gram-positive and Gram-negative bacteria was discovered. Interestingly, **10-32** is also effective in treating the clinically significant MRSA (ATCC® BAA-41™). Thus **10-32** is a potential new antibiotic in treating multi-drug resistant bacteria.

The hydrophobic side group in isatin is confirmed to be an important factor to display antibacterial activities. The SAR results were consistent with the predicted binding pose to the *S. aureus* GT binding site (Fig. 3.1). Moreover, the 5-methylisatin derivative (**10c-27**) showed the same MIC value as its mother compound (**10b-27**). It opens a new direction for the modification of new derivatives.

The *in vitro* binding studies between GT and **10-32** had been studied by STD-NMR experiments. Experimental details, including the expression of *S. aureus* GT, are described in chapter 4.

Chapter 4

In vitro Binding Studies between *S. aureus* GT and 10-32 using Saturation-Transfer Difference (STD)-NMR

4.1 Introduction

Saturation-transfer difference (STD)-NMR is one of the most popular techniques to study ligand-protein interactions. It only measures the ligand signals and does not require labeling of the macromolecules [97-99], and it works well for weak binding ligands (K_D from 10^{-7} to 10^{-3} mol/L) [100].

The first NMR-based method for studying protein-ligand interactions was reported by Shuker et al. in 1996 [101] by detecting the change in ^{1}H and ^{15}N-amide chemical shifts in two-dimensional ^{15}N-heteronuclear single-quantum correlation (HSQC) spectra [102]. Although the chemical-shift mapping (measuring the signals of proteins) is rather fast and simple, it requires large quantity of isotope labeled protein per measurement (250 - 500 μg) [103-104]. STD-NMR measurement can somehow overcome this disadvantage, as it only measures the signals of ligands, and a small amount of unlabeled protein is sufficient [103-104]. Hence it is suitable for high-throughput screening of small molecule ligands.

STD-NMR is the observation of sample Nuclear Overhauser Effect (NOE) generated from saturating a nearby target resonance. It is defined as the resonance

signal intensity change of one species when the spin transitions of another are somehow disturbed from their equilibrium populations [105]. By applying selective radiation (e.g. 0 to -1 ppm) to the macromolecule nucleus (*S*), the nucleus becomes saturated (i.e. at high-energy state, β). If a ligand nucleus (*I*) is close enough to the macromolecule nucleus (*S*), the high energy can be transferred from *S* to *I* through NOE, giving a higher population of I_β compared to its equilibrium state. This process is called the zero quantum transition (W_o) [74]. The bound ligand nuclei (*I*) tend to stay at high energy state (I_β) because of the transferred energy, resulting in a net reduction in the *I* spin resonance during relaxation. STD-NMR is the difference between the signal with selective saturation (I_{SAT}) and the signal without saturation (I_o):

$$I_{STD} = I_o - I_{SAT}$$

If interaction exists between ligand and macromolecule (the 2 nuclei are close enough for NOE), the signal intensity of I_{SAT} will be lower than that of I_o, giving a positive I_{STD} signal [74, 106-107]. A zero I_{STD} signal will be observed if there is no such interaction.

Further identification of the specific ligand-binding site can be achieved by addition of a known inhibitor as a competitive probe. The bound ligand will be displaced by the known inhibitor if they share the same ligand-binding site, resulting in reduction of the ligand STD signals.

In this chapter, the interaction between the GT domain of *S. aureus* PBP2 and the most potent derivative (**10-32)** will be studied by ^{1}H STD-NMR. GT, **10-32** and moenomycin A will be served as receptor, ligand and competitive probe, respectively. The experimental details and the results will be discussed.

4.2 Experimental

4.2.1 Chemicals and consumables

All analytical grade solvents were purchased from Oriental Chemicals. Deuterated solvents were obtained from Cambridge Isotope Laboratories. Sodium phosphate and potassium phosphate (monobasic and dibasic), and IPTG were purchased from USB Corporation. Kanamycin, lysozyme, sodium hydroxide and Tris-HCl were obtained from Sigma. Bis-acrylamide and tetramethylethylenediamine (TEMED) were purchased from Bio-rad. Fos-Choline-14 (Sol-grade) was purchased from Anatrace. Syringe filters and amicons were purchased from Merck Millipore. Sodium dodecyl sulfate - polyacrylamide gel electrophoresis (SDS-PAGE) protein marker solution and Bradford solutions were purchased from Bio-Rad.

4.2.2 Over-expression and purification of *S. aureus* GT

The frozen bacterial glycerol stock expressing *S. aureus* GT domain (PBP2 residues 76-243) was a stock in our laboratory. GT was expressed by the *E. coli* strain BL21(DE3) (New England BioLabs) containing the GT gene with the pRSET vector (ThermoFisher, N-terminus 6xHis tag). The bacterium was streaked on a LB agar

plate with kanamycin (working concentration 50 μg/mL) and was incubated at 37 ℃ overnight. A single colony was added to 5 mL of LB medium and incubated at 37^{o}C with shaking at 250 rpm overnight. The overnight culture (1 mL) was transferred into an autoclaved 2xTY medium (200 mL) with the screening antibiotic kanamycin (working concentration 50 μg/mL), followed by incubation at 37 ^{o}C at 250 rpm. 1 M IPTG (1 mL) was added to the culture solution when the OD_{600} reached 0.8. It was further incubated at 25^{o}C at 250 rpm for another 18 h. The cells were harvested by centrifugation at 4 ^{o}C, 10000 rpm for 20 min and then resuspended into 20 mM sodium phosphate buffer (pH 7.4) followed by cell lysis by sonication. The insoluble fractions were collected by centrifugation at 4 ^{o}C, 10000 rpm for 20 min. Membrane proteins were extracted by mild shaking of the cell pellet (without suspension) overnight at 4 ^{o}C in 20 mL buffer A (0.5 M NaCl, 20 mM sodium phosphate, 20 mM Fos-Choline-14; pH 7.4). The supernatant was collected by centrifugation at 12000 rpm for 1 h at 4^{o}C.

The supernatant was purified by affinity chromatography using an ÄKTA purifier equipped with a 5 mL HiTrap chelating column (GE Healthcare) with a linear gradient of 0 - 0.5 M imidazole. The purity of each fraction was confirmed by SDS-PAGE before desalting by dialysis against H_2O (Milli-Q type 1), followed by

concentration using Amicon® (Millipore). The concentration was measured by Bradford assay before storage at -80^{o}C.

4.2.3 STD-NMR experiments

Compound **10-32** was fully dissolved in DMSO-d_6, giving a 10 mM solution. 50 μL of the **10-32** solution was transferred to a 1.5-mL centrifuge tube, and mixed well with 150 μL of DMSO-d_6 and 300 μL of D_2O, resulting in a 1 mM solution dissolved in 40% DMSO-d_6. 5 μL of GT stock solution (1 mM, dissolved in H_2O) was subsequently added to the sample, giving a protein concentration of 10 μM. The ratio of GT and **10-32** was 1:100. The solution mixture was added to a 600-MHz compatible NMR tube and STD-NMR was measured using a Bruker Advance-III 600 MHz FT-NMR spectrometer equipped with a 5-mm QCI cryoprobe. The spectrum was collected at 25^{o}C under a train of 50 ms Gauss-shaped pulses, each separated by a 1 ms delay with successive on- and off- resonances for selective protein irradiation. Protein resonance was suppressed by T1ρ spinlock filter (50 ms). Protein resonance presaturation was achieved by applying an on-resonance irradiation at -0.4 ppm while an off-resonance irradiation was applied at -30 ppm with neither resonances of GT or **10-32**. STD signals were measured by applying a 5 s saturation and measured with a

recovery delay of 5 s to eliminate incomplete relaxation to thermal equilibrium with no less than 128 scans and 16 K data points. The on- and off-resonance spectra were independently treated, and subtracted to give a difference spectrum with positive signal ($I_{STD} = I_{off} - I_{on}$). All data were processed using the TopSpin program suite (Bruker BioSpin Pte Ltd).

Competitive assay was done by titration of **10**-**32**-GT mixture solution with moenomycin A solution. **10-32** (working concentration 1 mM) was first dissolved in 50% DMSO-d_6 / D_2O solution (550 μL) and the STD-NMR spectrum was measured. GT (working concentration 20 μM) was added directly into the NMR tube and shaken well, the STD-NMR spectrum was measured again. Moenomycin A solution (working concentration 50 μM, dissolved in D_2O) was added subsequently into the NMR tube and shaken well, the STD-NMR spectrum was measured again. Addition of moenomycin A was repeated until the difference spectrum showed reduction of **10-32** signal intensities.

4.3 Results and discussions

4.3.1 Purification of GT domain of *S. aureus* PBP2

The first reported STD-NMR experiment on the binding of small molecules to GT was on the interaction between moenomycin derivatives and *E. coli* PBP1b [75]. The experiment simply used the membrane extract as the source of protein, and the inhibitor moenomycin as reference probe. However, the use of membrane extract cannot show binding specificity. In this experiment, the GT domain of *S. aureus* PBP2 was over-expressed and purified as the sole receptor for binding studies.

Because the full-length bifunctional *S. aureus* PBP2 has a MW of 78 kDa, a large protein may create excessive noise to the spectra. In this regard, the GT domain was genetically encoded (residues 76-243) in which the MW was reduced to 20 kDa. Purification was performed using a special detergent Fos-Choline-14 as re-solubilization agent. The purified GT has a yield of 4 mg / L culture, and the purity has been confirmed by SDS-PAGE gel as a single band at 20 kDa (Fig. 4.1b).

The expression of GT domain showed a higher yield over the full length PBP2 (0.4 mg / L culture) using the same expression procedures. Also, the purified

full-length PBP2 showed multiple bands in addition to the band at 78 kDa (see Appendix II). Therefore, the genetically encoded GT domain was used for the subsequent binding studies.

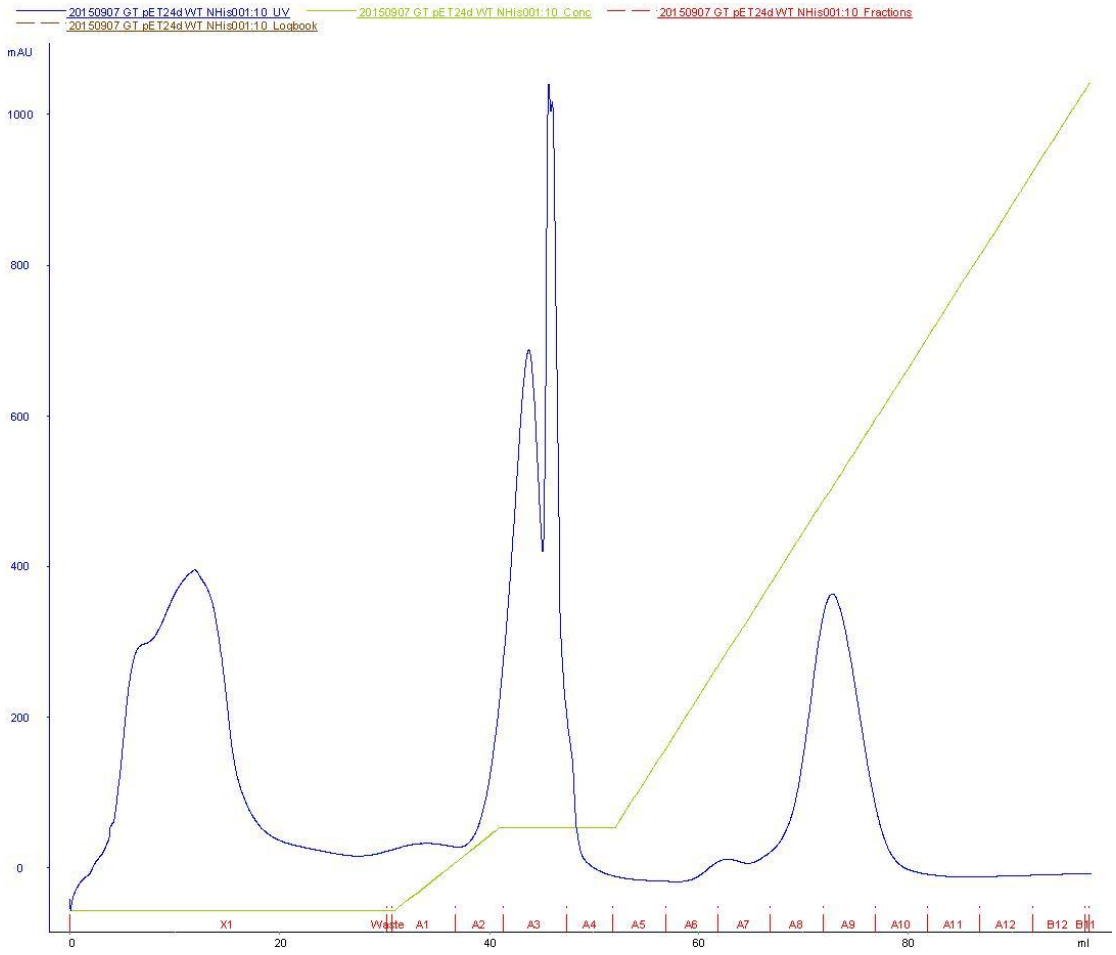

Fig. 4.1(a) ÄKTA purification spectrum of GT domain using 20 mM Fos-Choline-14 as membrane solubilizing detergent. GT was eluted at A8 to A10.

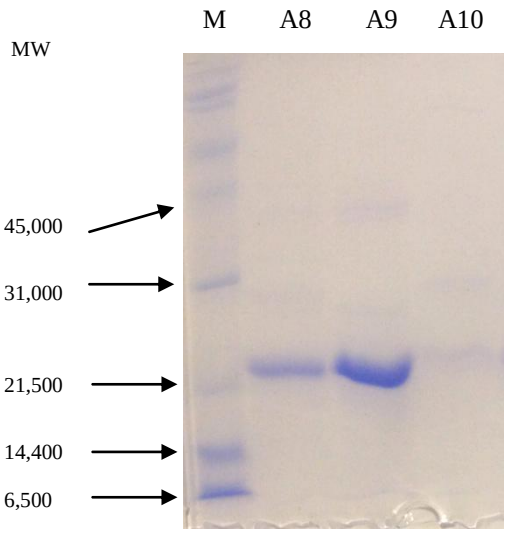

Fig. 4.1(b) SDS-PAGE gel of the GT domain using 20 mM Fos-choline-14 as membrane solubilizing detergent. M refers to low range molecular markers. GT was eluted at A8 to A9.

4.3.2 STD-NMR experiments

The STD-NMR results are shown in Fig. 4.2. The sample mixture consisted of **10-32** (1 mM) and GT (10 μM) in 40% DMSO-d_6 / 60% D_2O solution. The upper spectrum was a negative control experiment measuring the STD signals without applying selective saturation. In this case, there was no observable **10-32** signals in the difference spectrum except solvent peak (δ = 2.71 ppm for DMSO in D_2O [108]). The middle spectrum was the sample STD spectrum with selective saturation. Here, the difference spectrum showed positive STD signals of the compound **10-32**, and all the signal peaks were identified with reference to the ^1H NMR spectrum (the bottom spectrum and Fig. 4.3), suggesting that there was a saturation-transfer between GT and **10-32** through NOE. Since NOE only happened when the ligand nuclei were in close contact with the protein (within 5 Å) [74], hence, the positive results indicated there was an interaction between GT and **10-32**.

Since compound **10-32** is only sparingly soluble in aqueous solution, the solvent DMSO-d_6 concentration was increased to 40% to ensure it was completely dissolved in the reaction mixture without precipitation. Under 40% DMSO-d_6 solution, no precipitation was observed in the sample mixture after 1 day at room temperature.

There is literature reporting that the optimum concentration of DMSO for PBP2a tranglycosylation assays (another penicillin-binding protein found in MRSA) [109] was 30 - 40 % [110], so the PBP2 should also remain active under 40% DMSO-d_6 solution.

System suitability experiment was also conducted based on the detection of binding between bovine serum albumin (protein) and $_L$-tryptophan (ligand) [111-113]. In 40% DMSO-d_6 / 60% D_2O solution, the ^1H reference NMR showed both the signals of tryptophan (at aromatic region) and sucrose (at aliphatic region), but only the signals of tryptophan were found in the STD spectrum, and no signals of sucrose were observed (see appendix III). It was because the bound tryptophan experienced a partial saturation from the protein, giving positive STD signals, whereas sucrose did not bind to the protein and no saturation was transferred, resulting in zero STD signals. The result suggested that the STD-NMR experiment was capable to differentiate between small molecule true binder (tryptophan) and non-binder (sucrose).

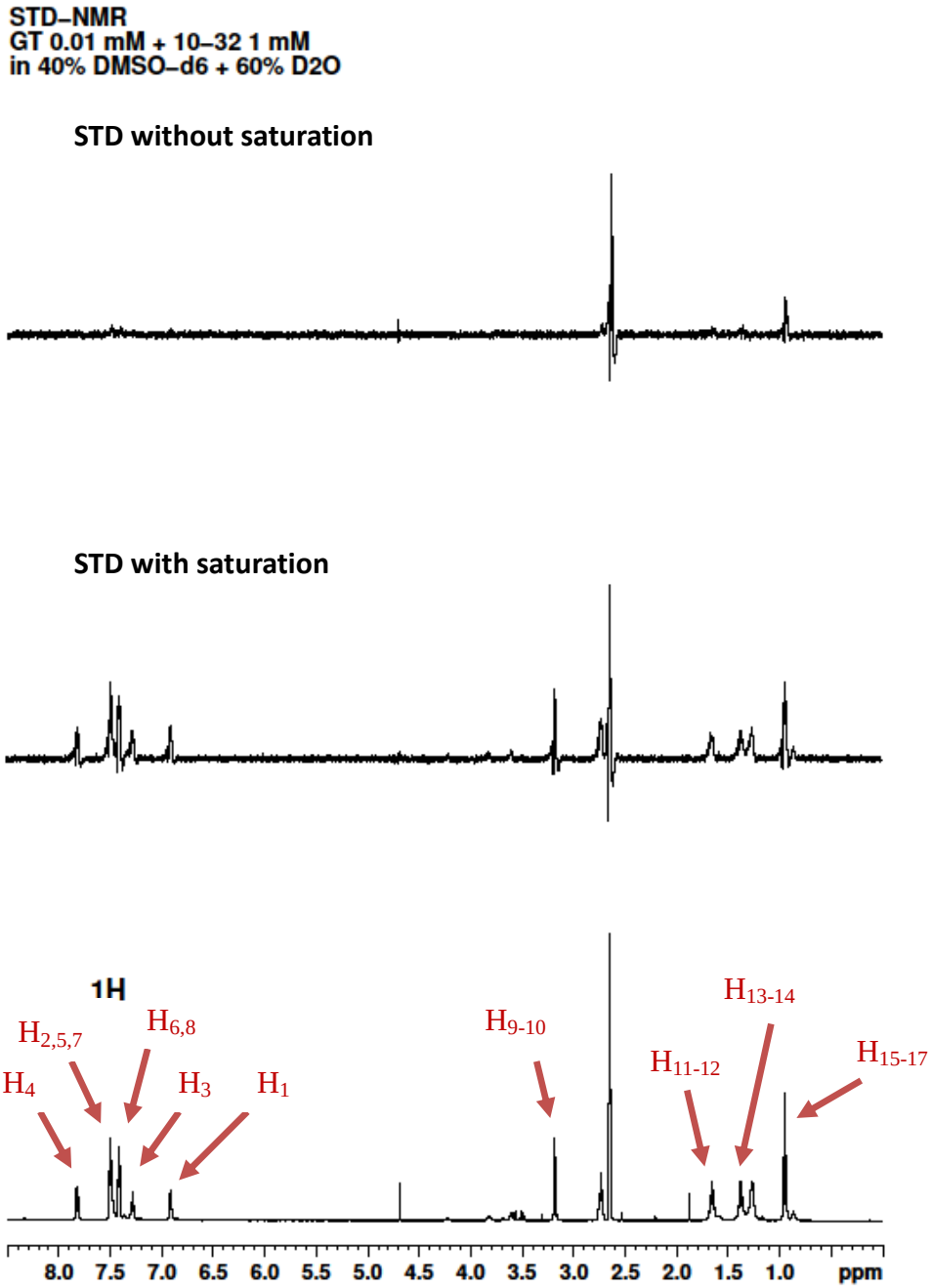

Fig. 4.2 STD-NMR experiment of 1 mM **10-32** in the presence of 10 μM GT. Upper spectrum: STD signals without selective saturation; middle spectrum: STD signals with selective saturation; lower spectrum: reference ^{1}H NMR.

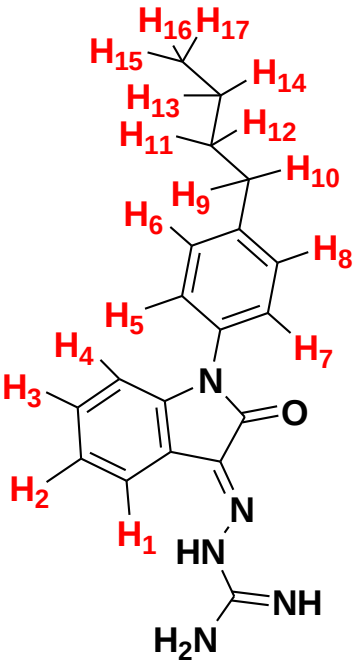

Fig. 4.3 Structure of **10-32**. ^{1}H NMR active protons were indicated in red color.

4.3.3 Competitive STD-NMR experiments

Although the STD-NMR results suggested that there was interaction between **10-32** and GT domain, the site of binding remained unknown. Moenomycin A is a strong inhibitor of GT (IC_{50} of PBP1b = 12 nM; IC_{50} of SgtB = 6 nM [55]), it can compete and displace weak ligands which share the same active-site pocket. This experiment aimed to confirm that **10-32** competes with moenomycin A for the same binding site on GT by displacing the STD signal intensities of **10-32** upon the addition of moenomycin A.

The competitive STD-NMR experiment was done by titrating **10-32**-GT mixture with moenomycin A solution and measured the difference spectra until displacement of the **10-32** signal intensities was observed. The solvent DMSO-d_6 was further increased to 50% in order to prevent any unwanted precipitation during titration.

The results are shown in Fig. 4.4. The first spectrum (Fig. 4.4a) consisted of **10-32** (1 mM) in 50% DMSO-d_6 / D_2O solution. There were no observable STD signals in the absence of GT; the STD signals were only observed after addition of GT (20 μM) to the solution (Fig. 4.4b). Afterwards, the solution was titrated with

moenomycin A solution. The **10-32** signal intensities were slightly displaced when the working concentration of moenomycin A was increased to 200 μM (Fig. 4.4c). The signal intensities were further reduced when the concentration of moenomycin A was increased to 250 μM (Fig. 4.4d). The titration was repeated twice with similar observations. The results indicated that the displacement of **10**-**32** signal intensities were dependent on the concentration of moenomycin A, thus suggesting that **10**-**32** shared the same active-site binding pocket of GT as moenomycin A.

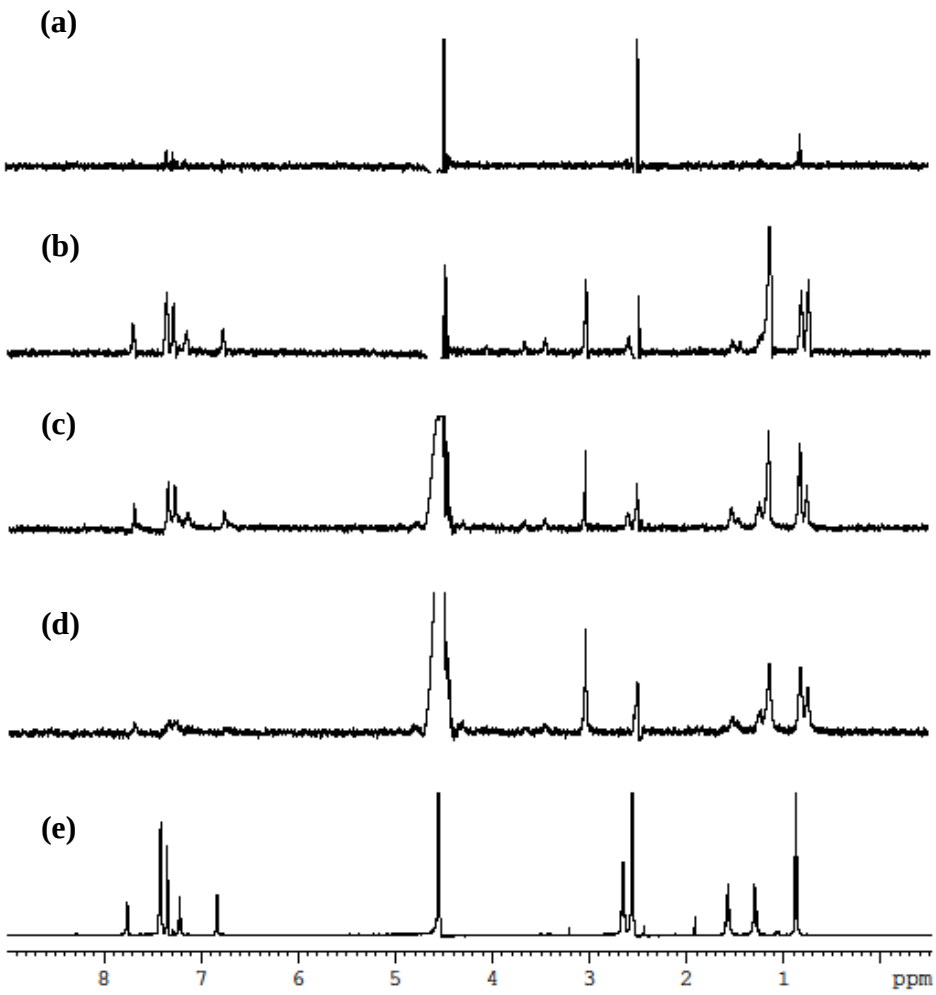

Fig. 4.4 Spectra of competitive STD-NMR experiment. The reaction mixtures in each spectrum were: (a) **10**-**32** (1 mM) only; (b) **10**-**32** (1 mM) + GT (20 μM); (c) **10**-**32** (1 mM) + GT (20 μM) + moenomycin A (200 μM); and (d) **10**-**32** (1 mM) + GT (20 μM) + moenomycin A (250 μM). (e) reference ^{1}H NMR of **10**-**32** (1 mM). All experiments were performed using 50 % DMSO-d_6 / D_2O solution (550 μL).

4.4 Concluding remarks

The results of this chapter confirmed the *in vitro* interactions between bacterial GT and **10-32** using STD-NMR. The GT motif of the *S. aureus* PBP2 were successfully expressed with considerable yield and purity. The STD spectra showed the signals of **10-32** in the presence of GT, confirming the interaction between GT and **10-32**. Further addition of the strong ligand moenomycin A displaced the **10-32** signal intensities, suggesting that **10-32** shared the same active-site binding pocket with meonomycin A.

Chapter 5

Conclusions

To cope with antibacterial resistance, rather than modifying existing antibiotics to restore their biological activities, scientists are searching for new antibiotics with new drug targets. The bacterial peptidoglycan glycosyltransferase domain (GT) is a potential excellent drug target [58, 60, 114]. As GT is equally important for bacterial cell wall biosynthesis as the conventional β-lactam target transpeptidase, inhibition of GT activity becomes an excellent opportunity in the development of antibacterial agents. Scientists already started to develop GT inhibitors based on modification of lipid II (a GT substrate) and moenomycin (a GT inhibitor) [38, 55, 115-117].

Target-based drug discovery is a popular approach [118-119]. It is widely adopted after the GT crystal structure became accessible [40, 120-121]. With the GT as an antibacterial drug target, small molecule inhibitors were screened for high binding affinities. The target-based approach ensures that the antibacterial mechanism is defined at the early stage of drug discovery, yet it is arduous to discover potential hit structures without a hint. With the aid of computational drug screening, small molecules potential drug candidates can be estimated before conducting physical measurements.

This thesis aims to improve the antibacterial potency of the GT inhibitor (**10b**-**27**)

[68] by studying its structure-activity relationship (SAR). 20 new derivatives were designed and synthesized. Derivatives were synthesized by simple condensation reactions between isatin derivatives and aminoguanidine. One of these derivatives (**10-32**) showed much improved antibacterial activities against both Gram-positive bacteria (MIC of *S. aureus* and *B. subtilis* = 6 μg/mL) and Gram-negative bacteria (MIC of *E. coli* = 12 μg/mL). Interestingly, **10-32** showed no detectable resistance against the clinically significant MRSA (ATCC® BAA-41™), demonstrating its potential to be a novel antibiotic to fight against ABR.

The SAR results showed that deletion of the polar methanediylamidyl group showed improvement in the antibacterial potency while derivatives with alkoxyl and hydroxyl substituents showed limited improvement to the potency. Thus, it is believed that the hydrophobicity of the compounds plays an important role on the potency. This is further supported by derivative **10b-19** with naphthyl side group (π = 1.23) which showed 4 times MIC (*S. aureus*) improvement to the mother compound **10b-27** with nitro side group instead (π = 0.11).

Since the *in vitro* transglycosylation activity assay was limited by the availability of the substrate lipid II [122] (or its analogues) [123-125], the interaction between

10-32 and GT was studied by STD-NMR using moenomycin A as a competitive probe. The difference spectrum revealed the signals of **10-32** in the presence of GT (100:1 ratio), suggesting that **10-32** and GT were in close contact (≤ 5Å) [74]. Moreover, the signal intensities of **10-32** were displaced by further addition of moenomycin A (5:1 ratio), suggesting that **10-32** shared the same active-site binding pocket with moenomycin A. Together with its small molecular weight and simple synthetic route, **10-32** is a potential new antibiotic to treat multi-drug resistant infections.

In spite of the promising broad-spectrum antibacterial activities of **10-32**, further hit-to-lead optimization could be possible. One of the major structural differences between **10-32** and the mother compound **10b-27** is the deletion of the methanediylamidyl group, and this new structural core has been studied with alkyl, aryl, alkoxyl and hydroxyl substituents. New analogues could be designed and synthesized with halogenated substituents, for example the 4-chloro substituent suggested by the Topliss scheme [88].

Although the competitive STD-NMR experiments confirmed the interaction between **10-32** and GT, the bacterial transglycosylation assay is still important to

acquire the inhibitory information (Ki and IC_{50}). In order to achieve this ultimate goal, extensive efforts had been put in our laboratory to synthesize lipid II by enzymatic method [126], in which the UDP-MurNAc pentapeptide (a lipid II precursor, Fig. 1.3) had been successfully isolated from *B. cereus* and *S. aureus* cultures as described [127]. Hopefully, the bacterial transglycosylation assay of **10**-**32** can be conducted in the near future.

Appendix I

^{1}H NMR and mass spectra of the isatin-based GT inhibitors

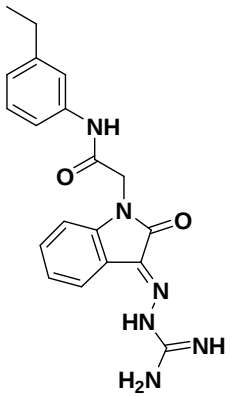
NH
O
N
O
N
HN
NH
H2N

10b-04

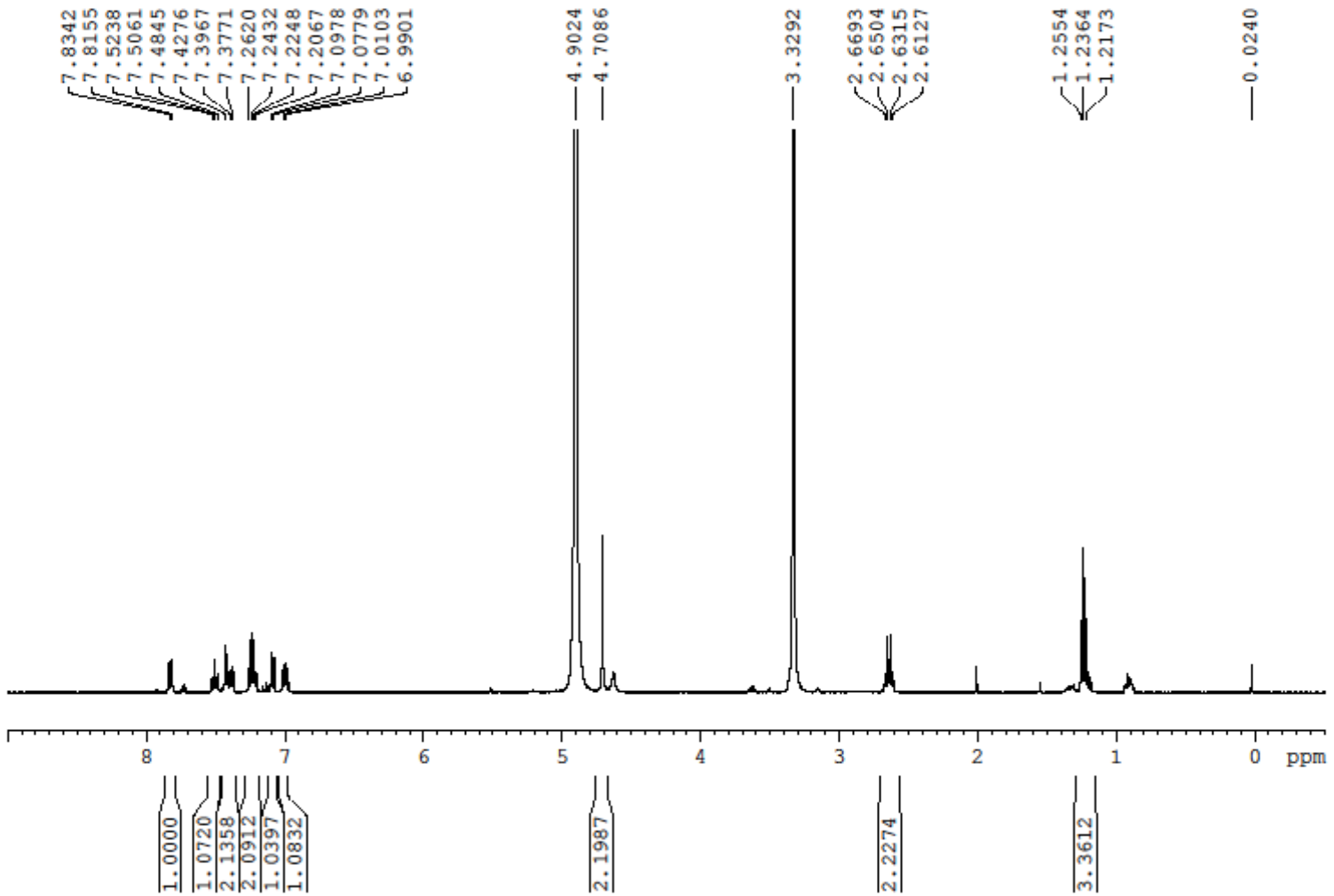
7.8342
7.8155
7.5238
7.5061
7.4845
7.4276
7.3967
7.3771
7.2620
7.2432
7.2248
7.2067
7.0978
7.0779
7.0103
6.9901
4.9024
4.7086
3.3292
2.6693
2.6504
2.6315
2.6127
1.2554
1.2364
1.2173
0.0240
8
7
6
5
4
3
2
1
0
ppm
1.0000
1.0720
2.1358
2.0912
1.0397
1.0832
2.1987
2.2274
3.3612

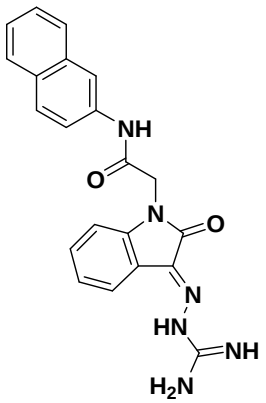
NH
O
N
O
N
HN
NH
H2N

10b-19

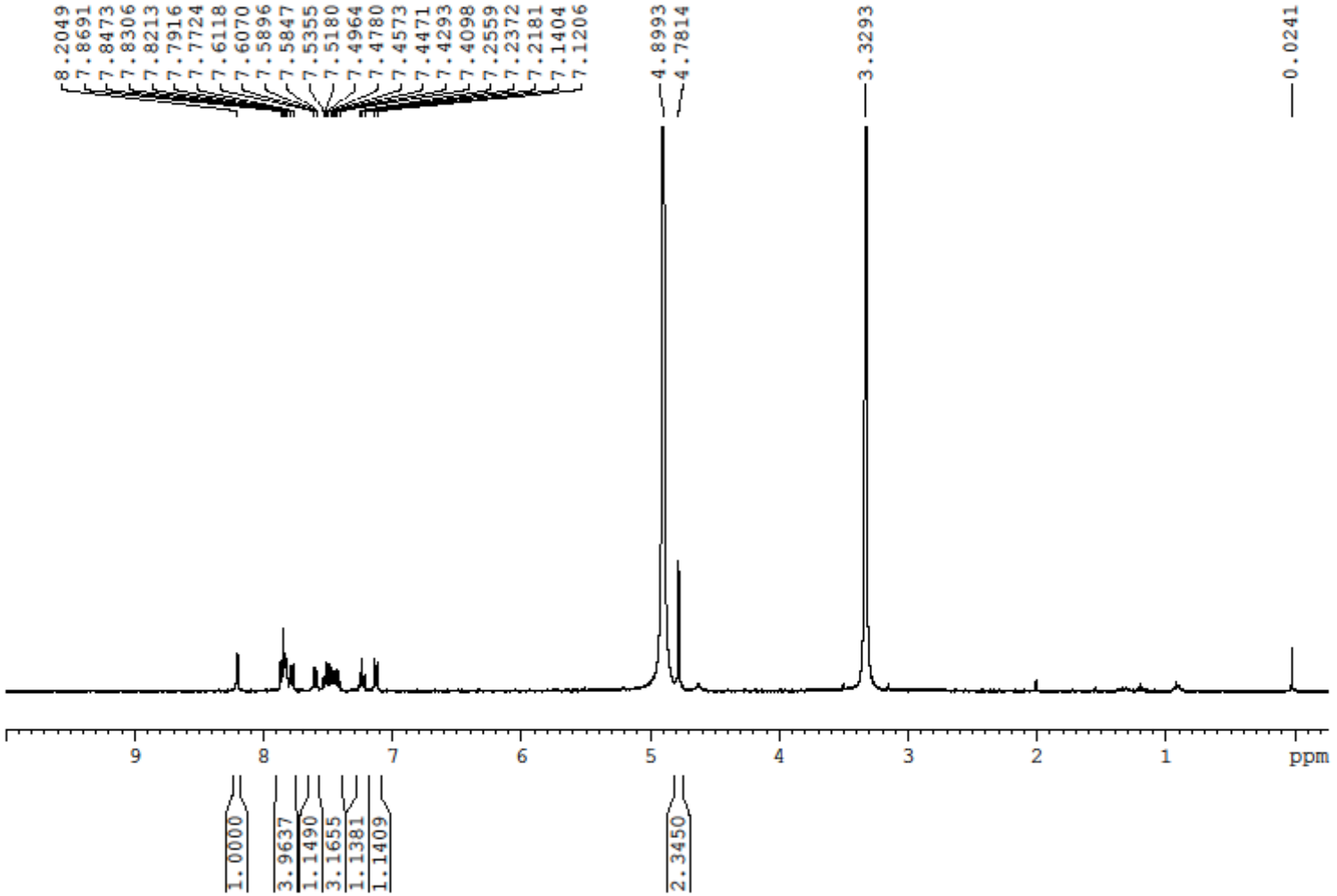
8.2049
7.8691
7.8473
7.8306
7.8213
7.7916
7.7724
7.6118
7.6070
7.5896
7.5847
7.5355
7.5180
7.4964
7.4780
7.4573
7.4471
7.4293
7.4098
7.2559
7.2372
7.2181
7.1404
7.1206
4.8993
4.7814
3.3293
0.0241
9
8
7
6
5
4
3
2
1
ppm
1.0000
3.9637
1.1490
3.1655
1.1381
1.1409
2.3450

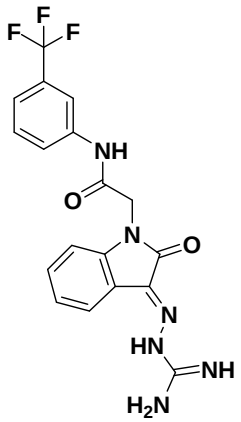
F
F
F
NH
O
N
O
N
HN
NH
H2N

10b-20

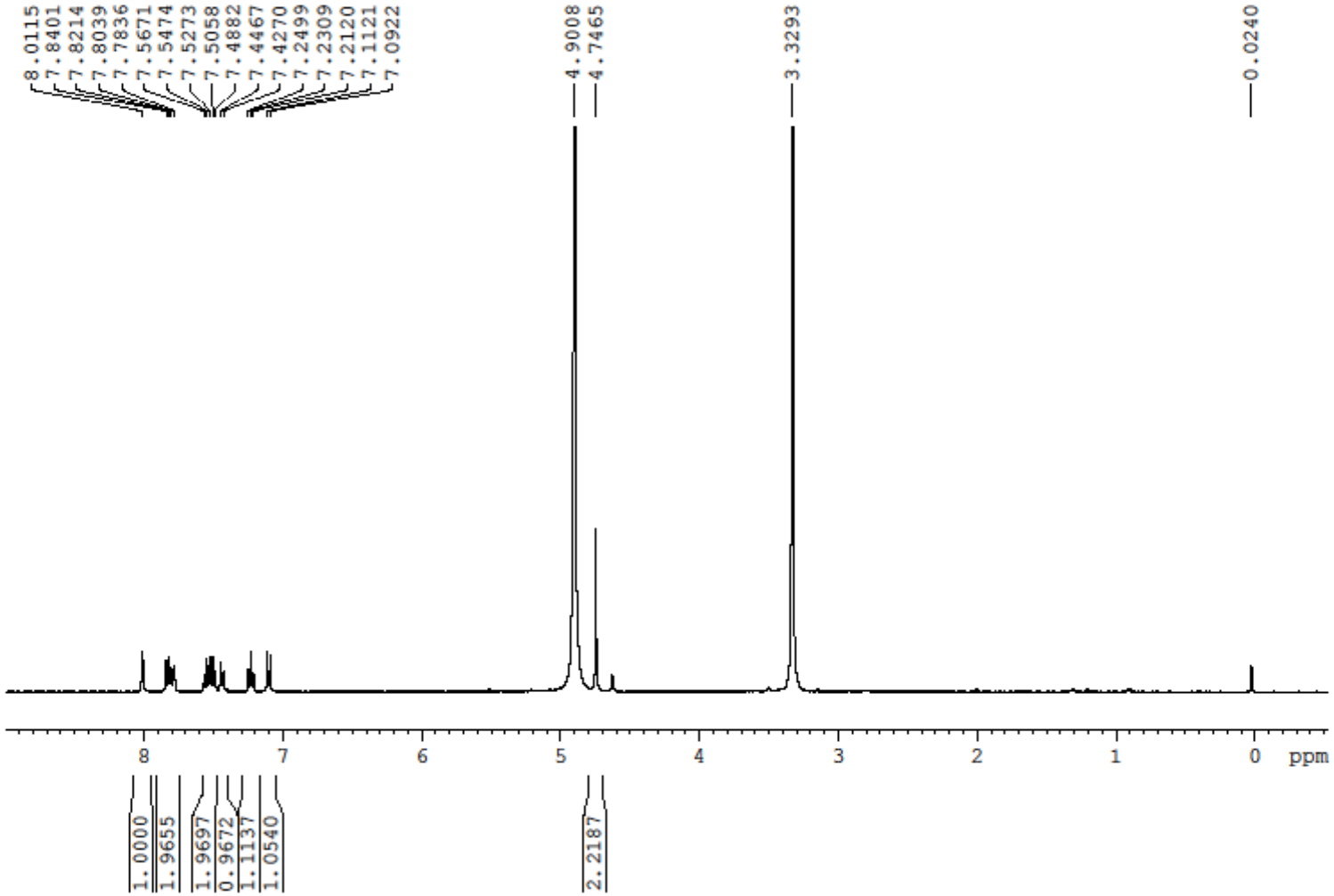
8.0115
7.8401
7.8214
7.8039
7.7836
7.5671
7.5474
7.5273
7.5058
7.4882
7.4467
7.4270
7.2499
7.2309
7.2120
7.1121
7.0922
4.9008
4.7465
3.3293
0.0240
8
7
6
5
4
3
2
1
0
ppm
1.0000
1.9655
1.9697
0.9672
1.1137
1.0540
2.2187

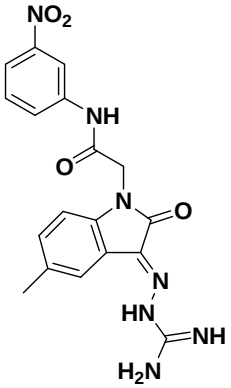
NO2
NH
O
N
O
N
HN
NH
H2N

10c-27

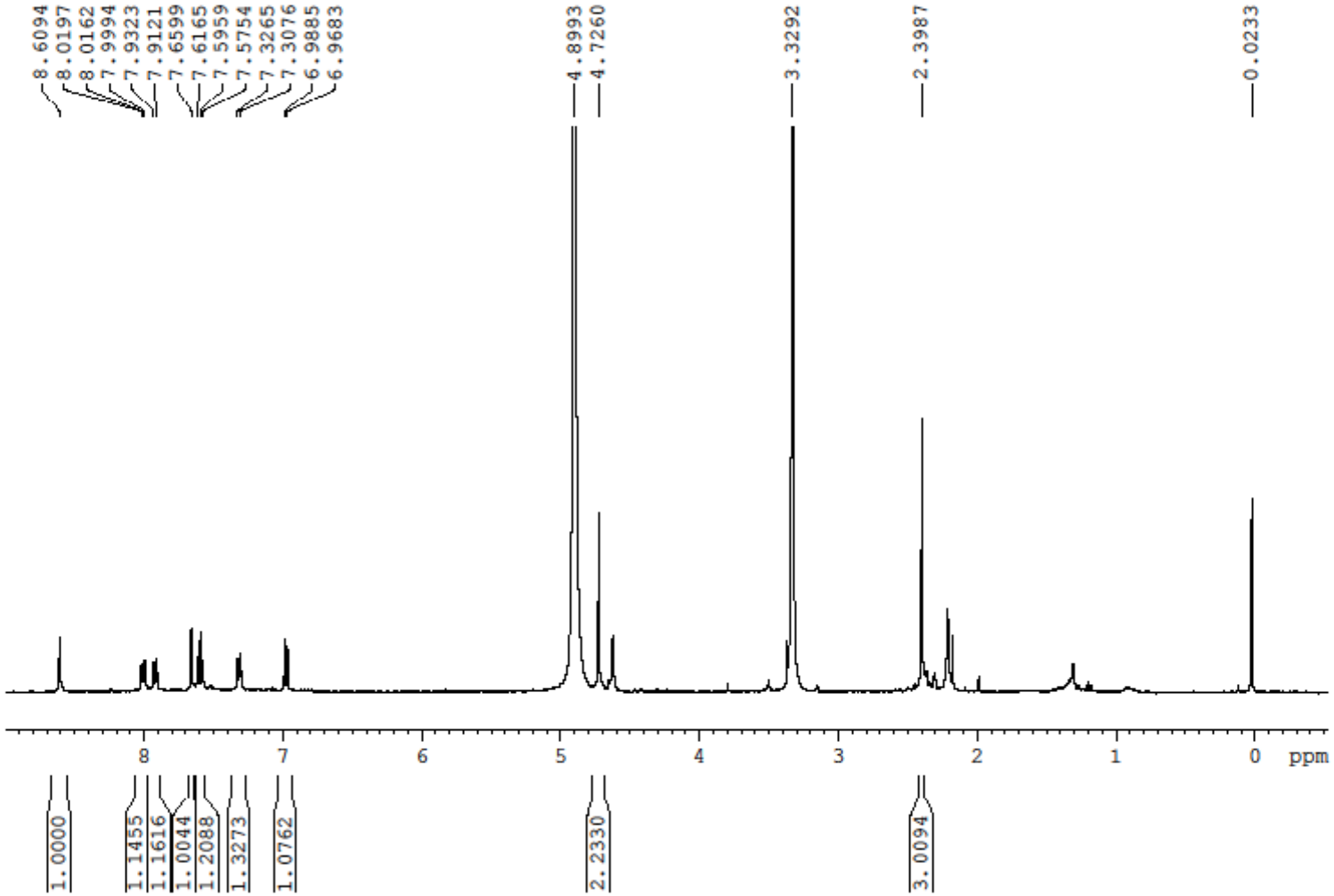
8.6094
8.0197
8.0162
7.9994
7.9323
7.9121
7.6599
7.6165
7.5959
7.5754
7.3265
7.3076
6.9885
6.9683
4.8993
4.7260
3.3292
2.3987
0.0233
8
7
6
5
4
3
2
1
0
ppm
1.0000
1.1455
1.1616
1.0044
1.2088
1.3273
1.0762
2.2330
3.0094

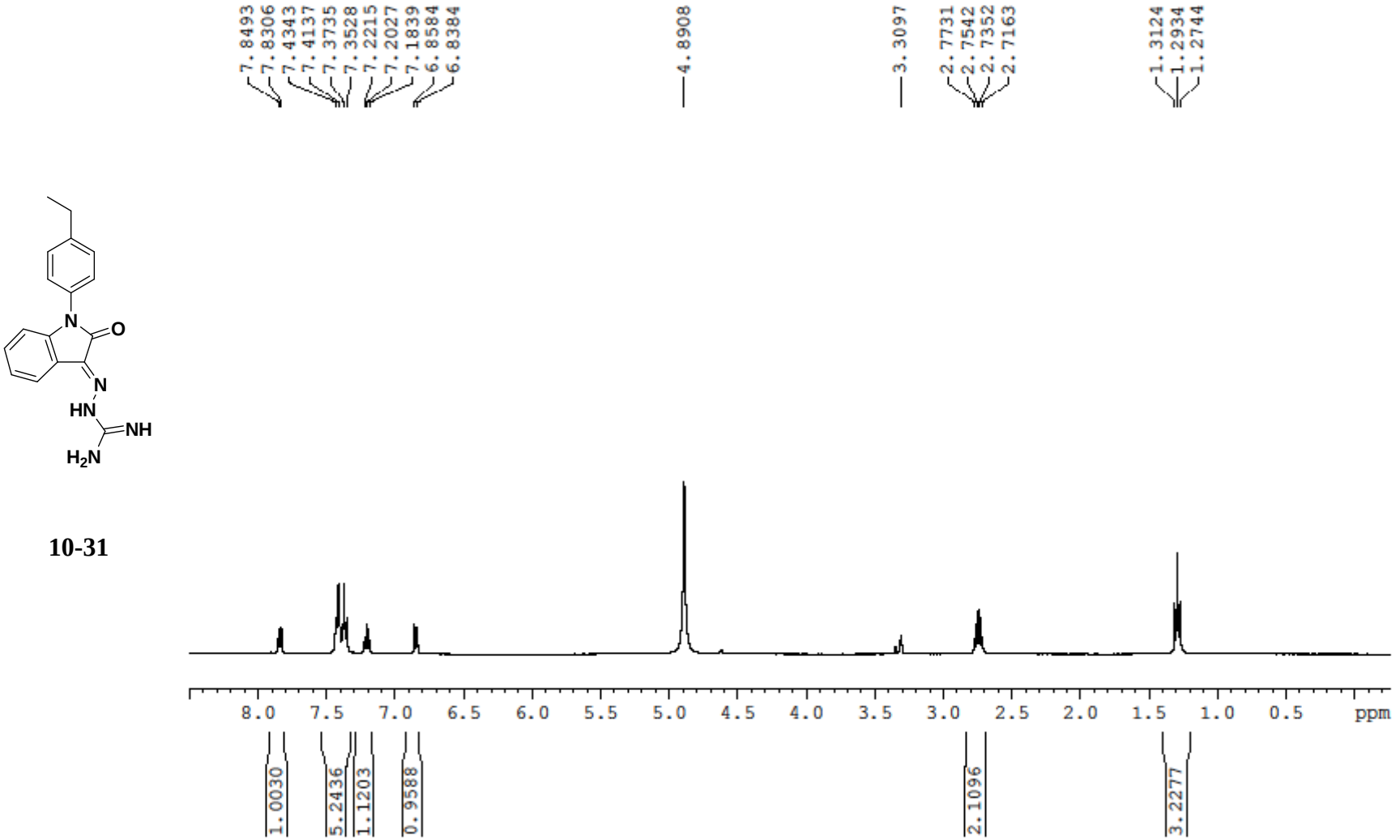
7.8493
7.8306
7.4343
7.4137
7.3735
7.3528
7.2215
7.2027
7.1839
6.8584
6.8384
4.8908
3.3097
2.7731
2.7542
2.7352
2.7163
1.3124
1.2934
1.2744
N
O
N
HN
NH
H2N
8.0
7.5
7.0
6.5
6.0
5.5
5.0
4.5
4.0
3.5
3.0
2.5
2.0
1.5
1.0
0.5
ppm
1.0030
5.2436
1.1203
0.9588
2.1096
3.2277

10-31


7.8425
7.8238
7.4108
7.4077
7.3937
7.3783
7.3737
7.3543
7.3484
7.3332
7.3278
7.2113
7.1923
7.1735
6.8438
6.8239
4.8820
3.3055
2.7182
2.6996
2.6805
1.6896
1.6707
1.6527
1.6348
1.6152
1.4457
1.4273
1.4087
1.3901
1.3718
1.3537
0.9844
0.9660
0.9477

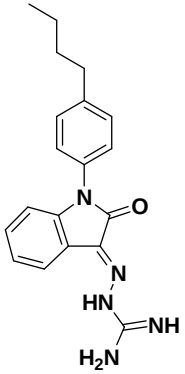
N
O
N
HN
NH
H2N

10-32

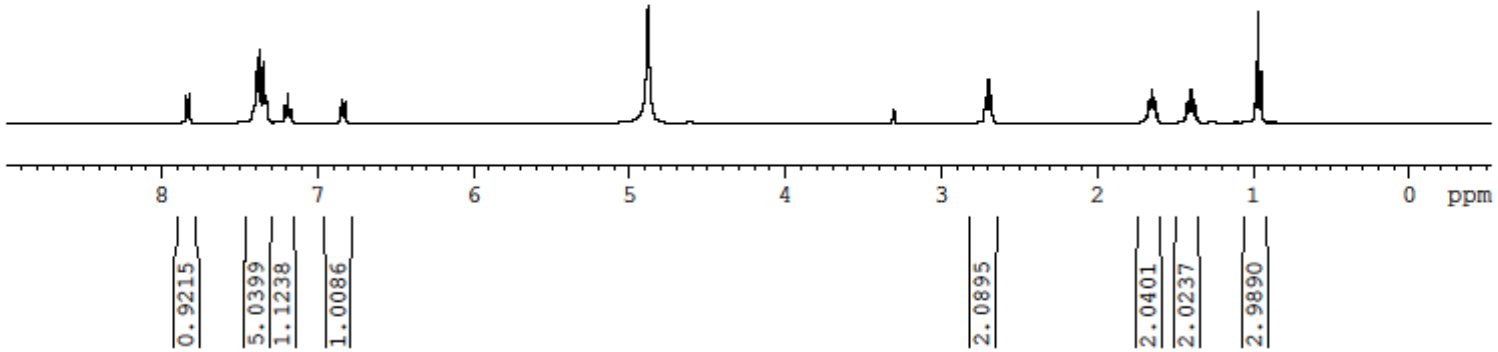
8
7
6
5
4
3
2
1
0
ppm
0.9215
5.0399
1.1238
1.0086
2.0895
2.0401
2.0237
2.9890

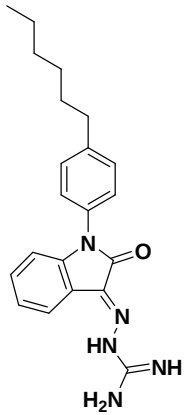
N
O
N
HN
NH
H2N

10-33

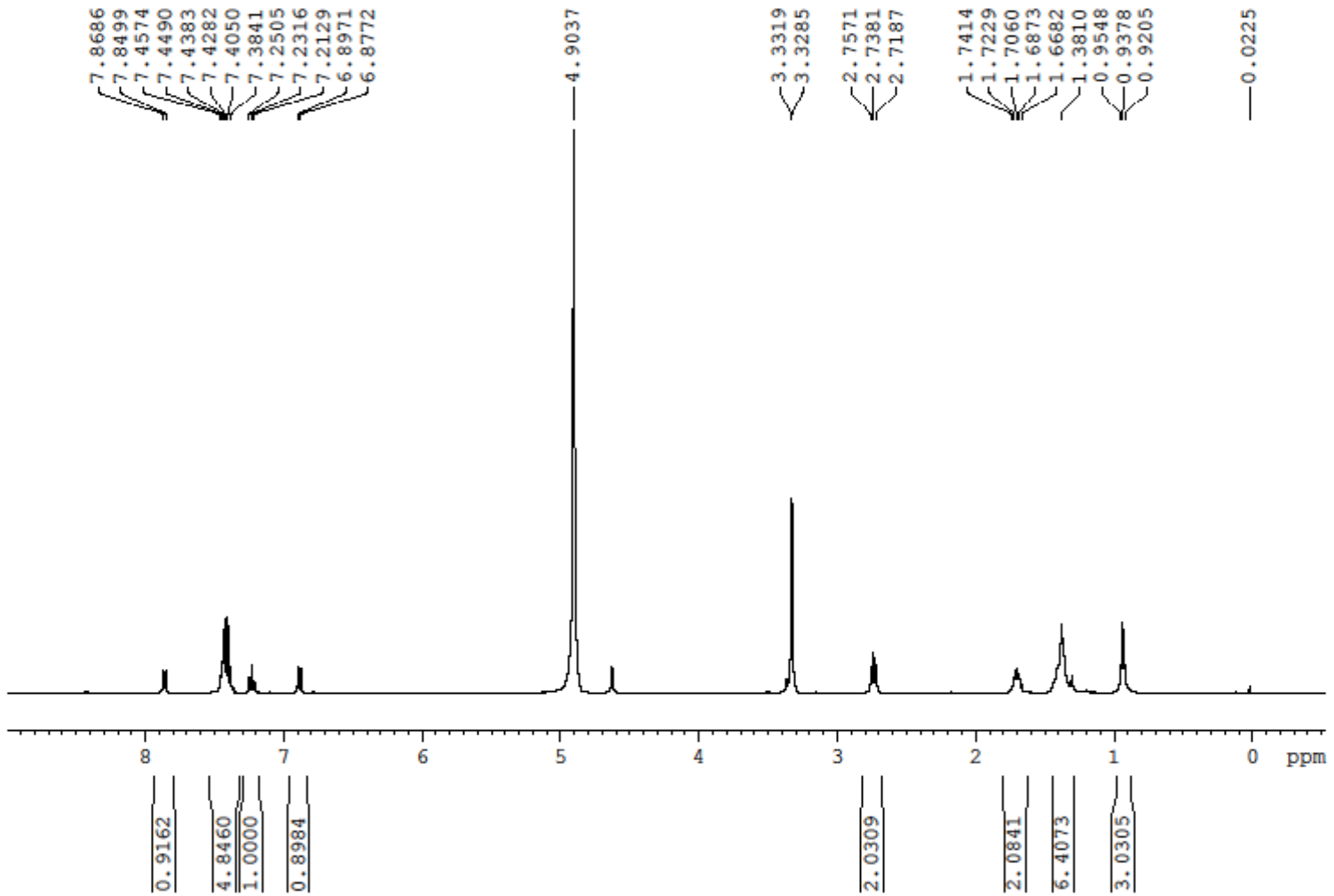
7.8686
7.8499
7.4574
7.4490
7.4383
7.4282
7.4050
7.3841
7.2505
7.2316
7.2129
6.8971
6.8772
4.9037
3.3319
3.3285
2.7571
2.7381
2.7187
1.7414
1.7229
1.7060
1.6873
1.6682
1.3810
0.9548
0.9378
0.9205
0.0225
8
7
6
5
4
3
2
1
0
ppm
0.9162
4.8460
1.0000
0.8984
2.0309
2.0841
6.4073
3.0305

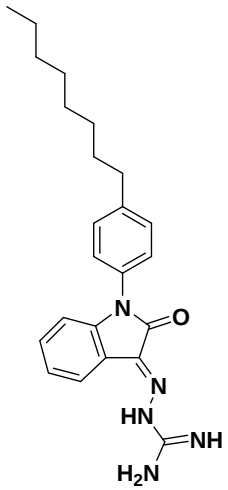
N
O
N
HN
NH
H2N

10-34

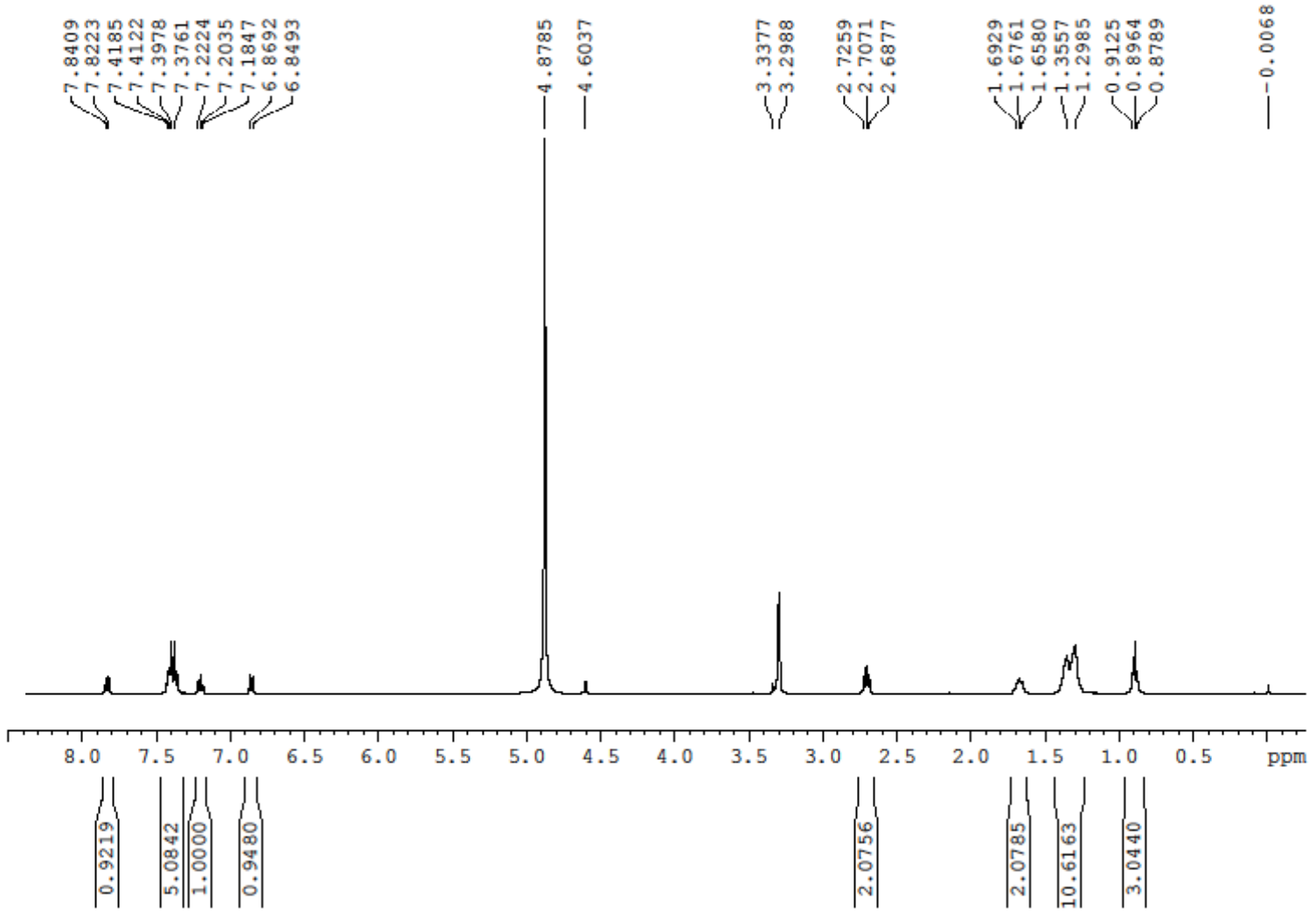
7.8409
7.8223
7.4185
7.4122
7.3978
7.3761
7.2224
7.2035
7.1847
6.8692
6.8493
4.8785
4.6037
3.3377
3.2988
2.7259
2.7071
2.6877
1.6929
1.6761
1.6580
1.3557
1.2985
0.9125
0.8964
0.8789
0.0068
8.0
7.5
7.0
6.5
6.0
5.5
5.0
4.5
4.0
3.5
3.0
2.5
2.0
1.5
1.0
0.5
ppm
0.9219
5.0842
1.0000
0.9480
2.0756
2.0785
10.6163
3.0440

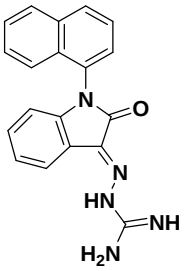
N
O
N
HN
NH
H2N

10-35

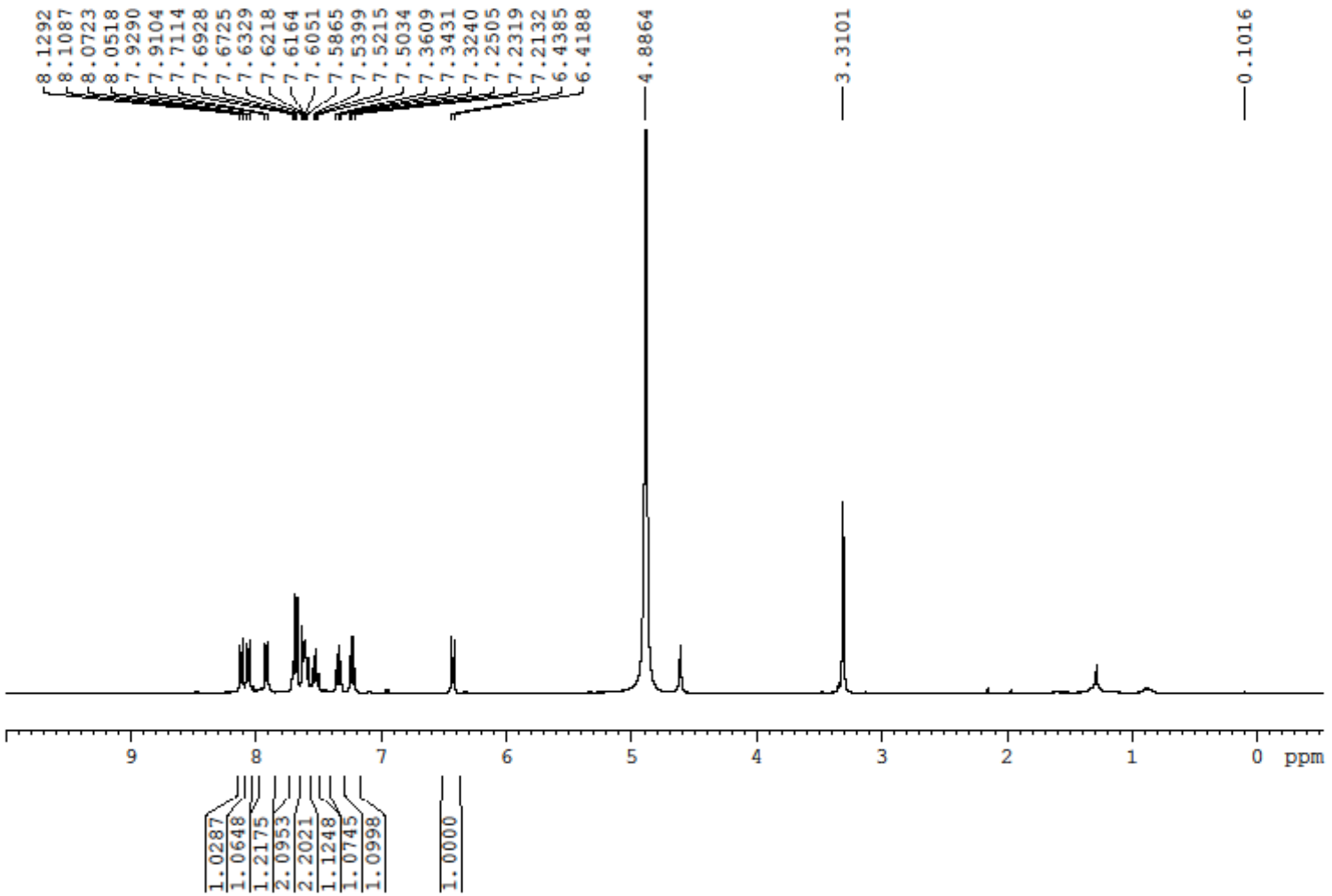
8.1292
8.1087
8.0723
8.0518
7.9290
7.9104
7.7114
7.6928
7.6725
7.6329
7.6218
7.6164
7.6051
7.5865
7.5399
7.5215
7.5034
7.3609
7.3431
7.3240
7.2505
7.2319
7.2132
6.4385
6.4188
4.8864
3.3101
0.1016
9
8
7
6
5
4
3
2
1
0
ppm
1.0287
1.0648
1.2175
2.0953
2.2021
1.1248
1.0745
1.0998
1.0000

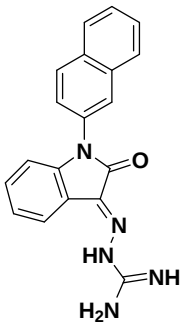
N
O
N
HN
NH
H2N

10-36

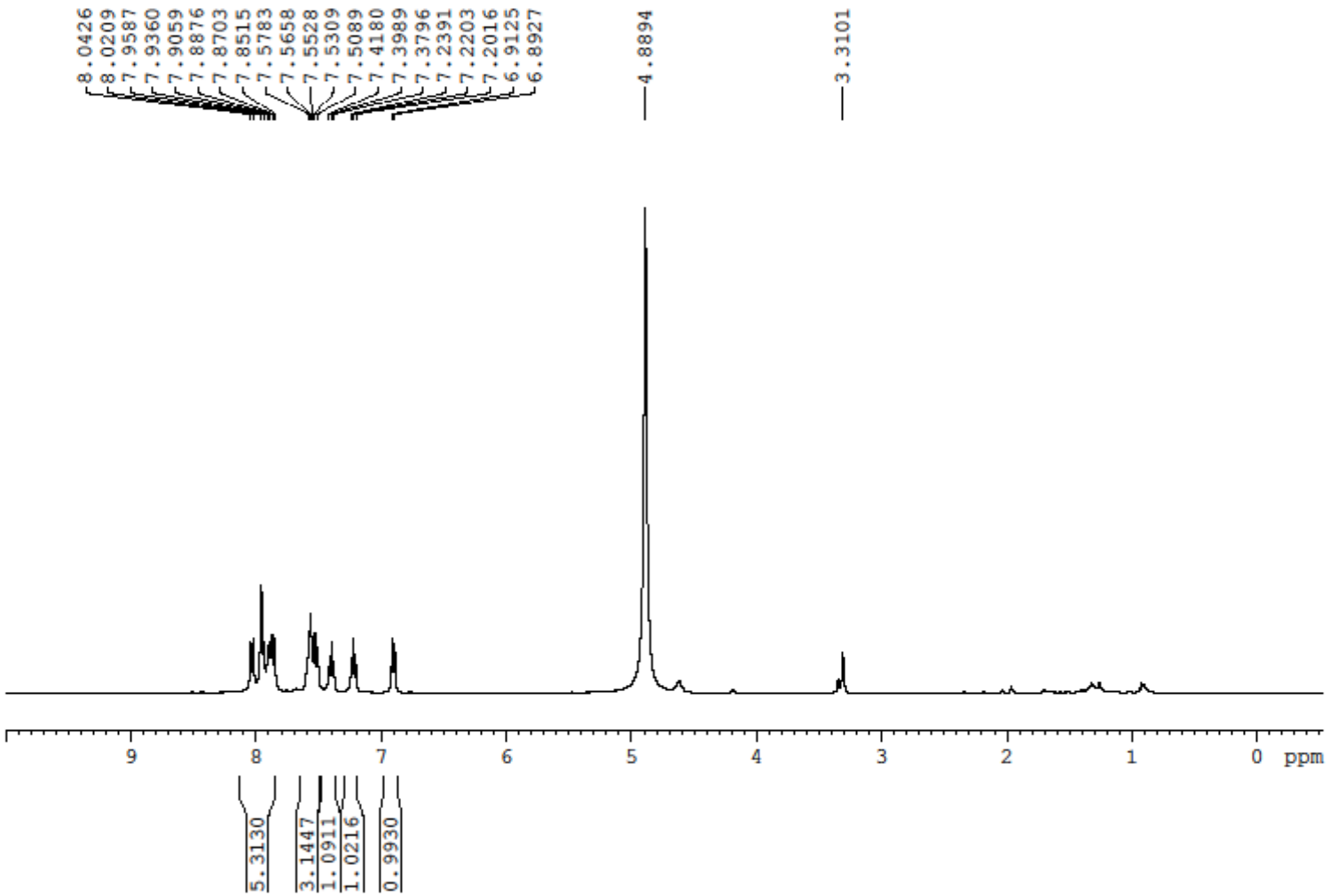
8.0426
8.0209
7.9587
7.9360
7.9059
7.8876
7.8703
7.8515
7.5783
7.5658
7.5528
7.5309
7.5089
7.4180
7.3989
7.3796
7.2391
7.2203
7.2016
6.9125
6.8927
4.8894
3.3101
9
8
7
6
5
4
3
2
1
0
ppm
5.3130
3.1447
1.0911
1.0216
0.9930

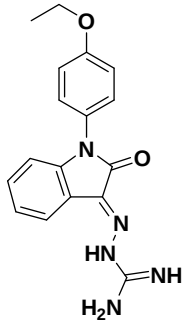
O
N
O
N
HN
NH
H2N

10-37

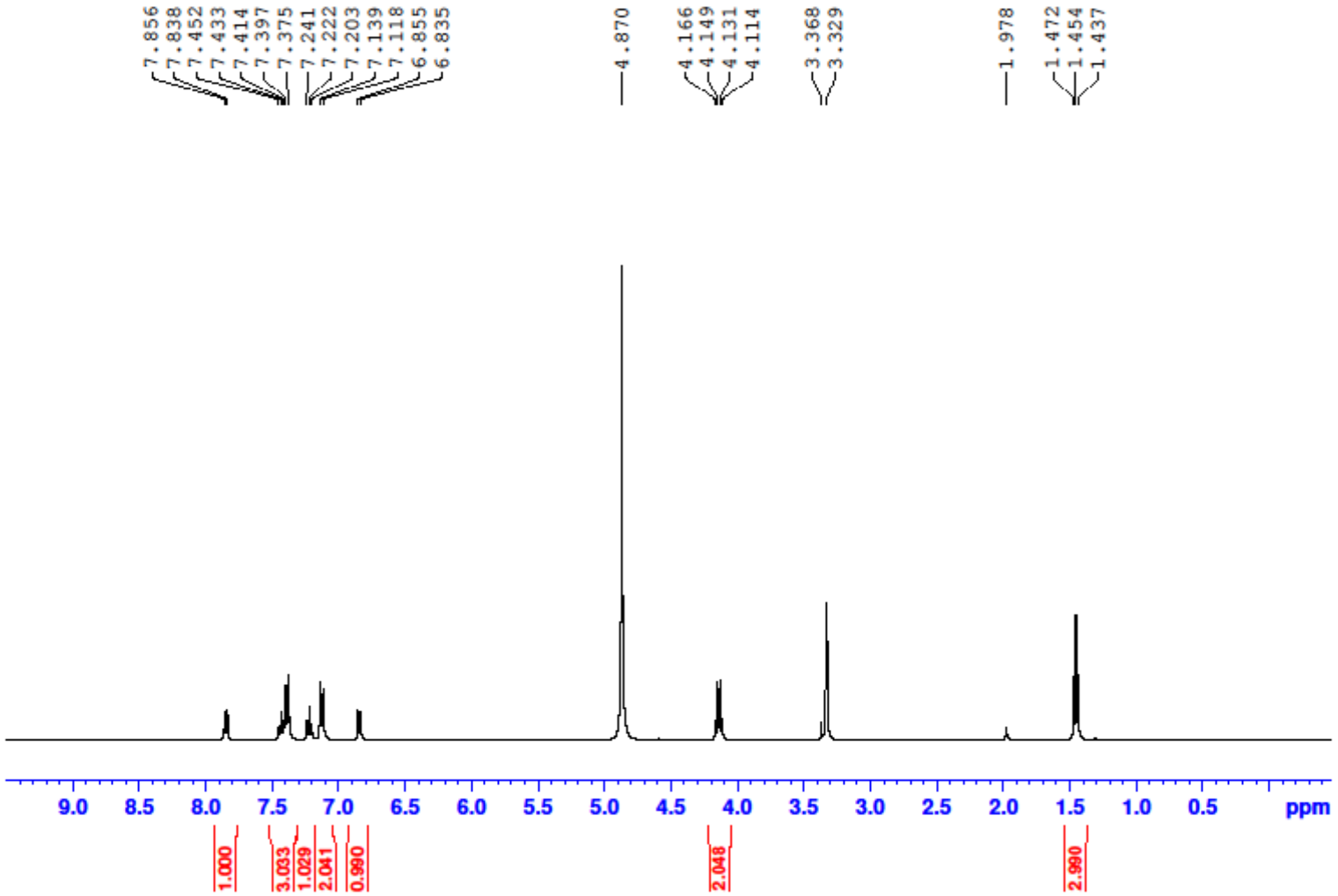
7.856
7.838
7.452
7.433
7.414
7.397
7.375
7.241
7.222
7.203
7.139
7.118
6.855
6.835
4.870
4.166
4.149
4.131
4.114
3.368
3.329
1.978
1.472
1.454
1.437
9.0
8.5
8.0
7.5
7.0
6.5
6.0
5.5
5.0
4.5
4.0
3.5
3.0
2.5
2.0
1.5
1.0
0.5
ppm
1.000
3.033
1.029
2.041
0.990
2.048
2.990

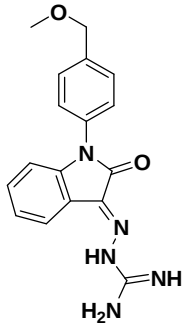
O
N
O
N
HN
NH
H2N

10-38

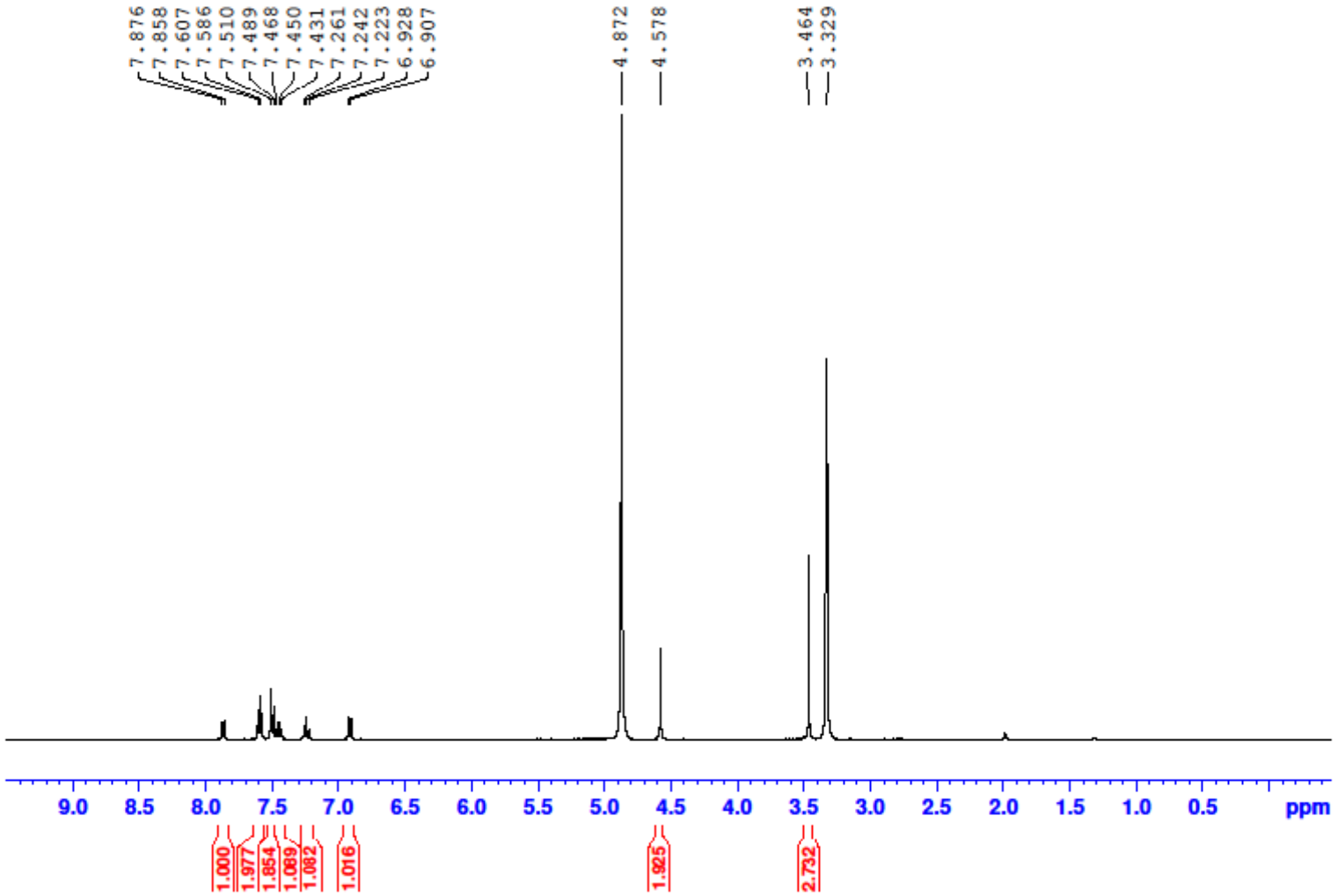
7.876
7.858
7.607
7.586
7.510
7.489
7.468
7.450
7.431
7.261
7.242
7.223
6.928
6.907
4.872
4.578
3.464
3.329
9.0
8.5
8.0
7.5
7.0
6.5
6.0
5.5
5.0
4.5
4.0
3.5
3.0
2.5
2.0
1.5
1.0
0.5
ppm
1.000
1.977
1.854
1.089
1.082
1.016
1.925
2.732

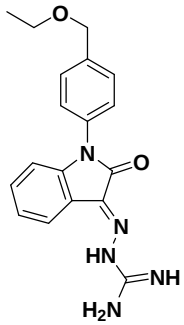
O
N
O
N
HN
NH
H2N

10-39

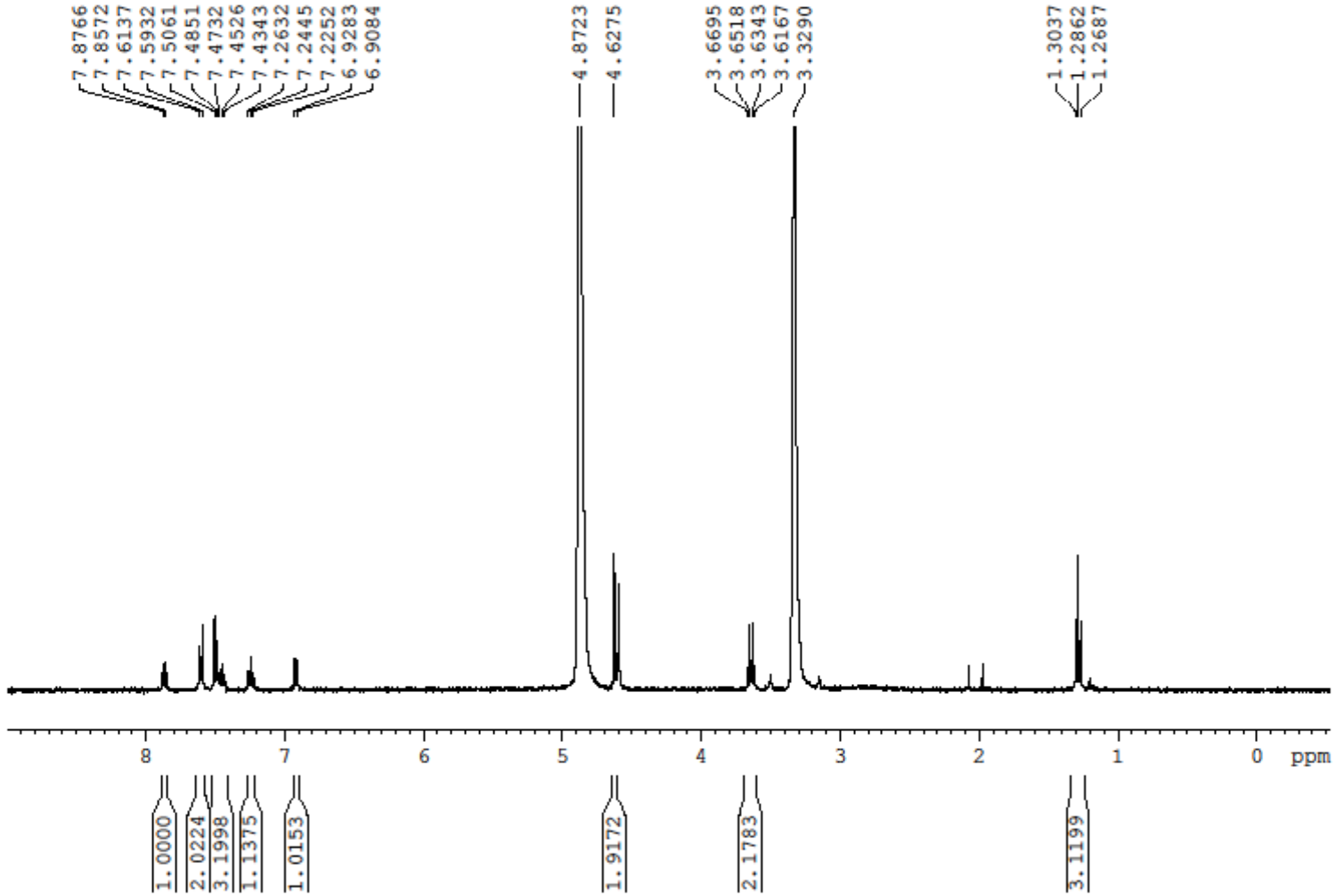
7.8766
7.8572
7.6137
7.5932
7.5061
7.4851
7.4732
7.4526
7.4343
7.2632
7.2445
7.2252
6.9283
6.9084
4.8723
4.6275
3.6695
3.6518
3.6343
3.6167
3.3290
1.3037
1.2862
1.2687
8
7
6
5
4
3
2
1
0
ppm
1.0000
2.0224
3.1998
1.1375
1.0153
1.9172
2.1783
3.1199

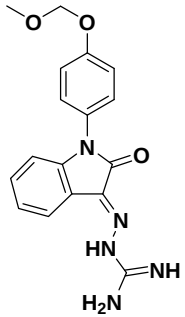
O
O
N
O
N
HN
NH
H2N

10-40

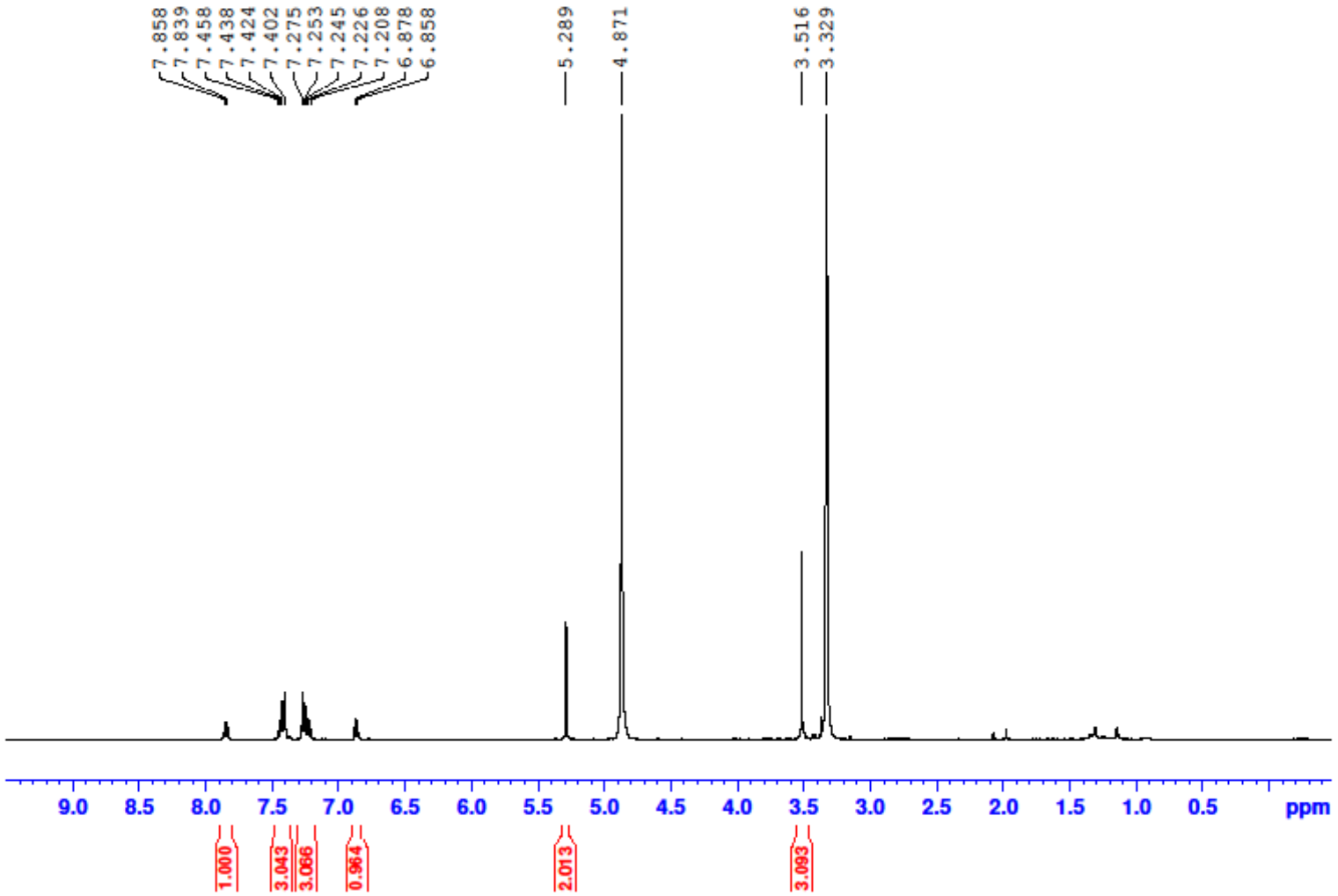
7.858
7.839
7.458
7.438
7.424
7.402
7.275
7.253
7.245
7.226
7.208
6.878
6.858
5.289
4.871
3.516
3.329
9.0
8.5
8.0
7.5
7.0
6.5
6.0
5.5
5.0
4.5
4.0
3.5
3.0
2.5
2.0
1.5
1.0
0.5
ppm
1.000
3.043
3.066
0.964
2.013
3.093

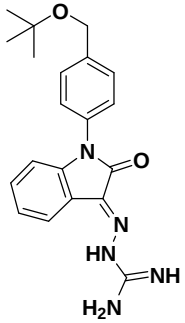
O
N
O
N
HN
NH
H2N

10-41

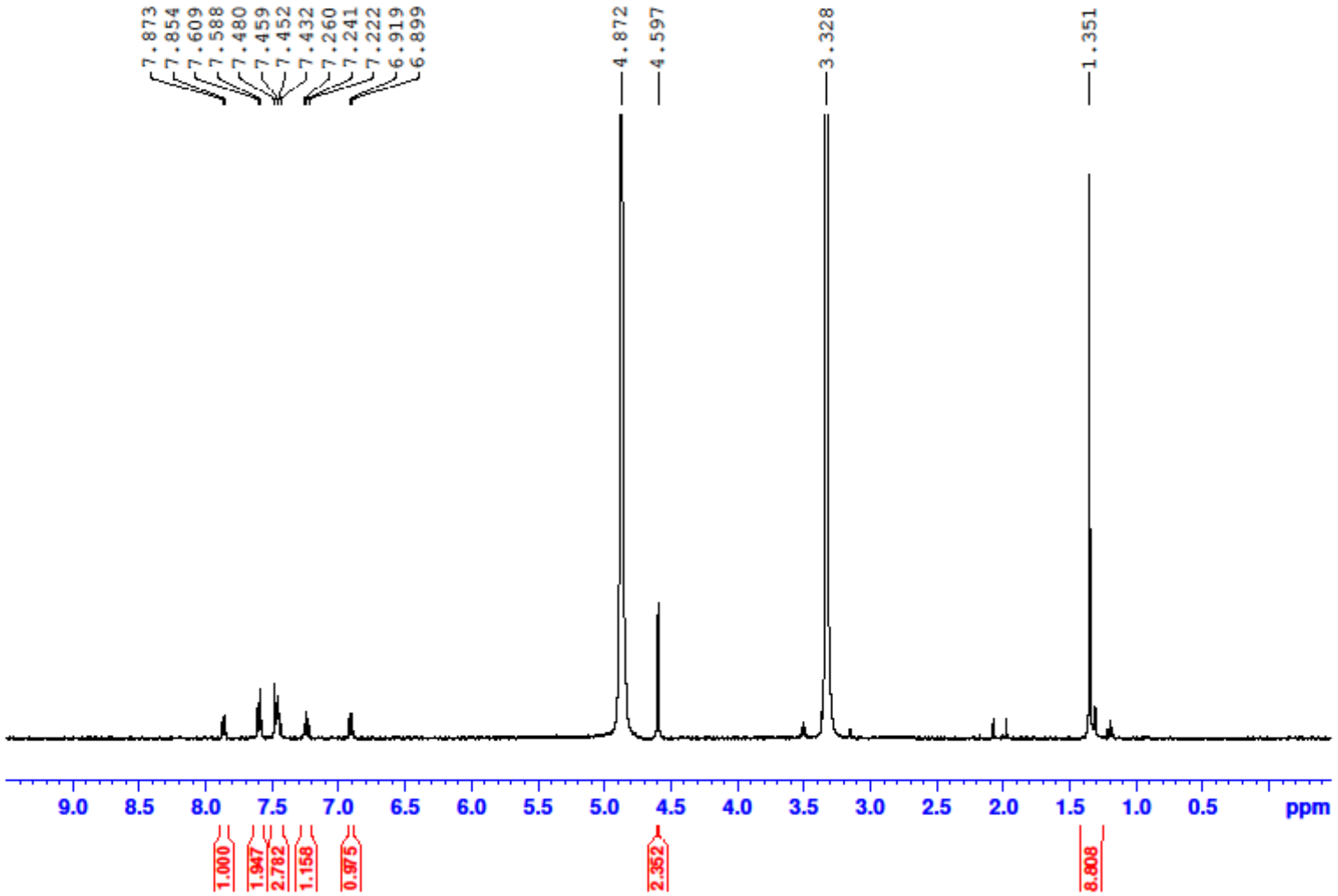
7.873
7.854
7.609
7.588
7.480
7.459
7.452
7.432
7.260
7.241
7.222
6.919
6.899
4.872
4.597
3.328
1.351
9.0
8.5
8.0
7.5
7.0
6.5
6.0
5.5
5.0
4.5
4.0
3.5
3.0
2.5
2.0
1.5
1.0
0.5
ppm
1.000
1.947
2.782
1.158
0.975
2.352
8.808

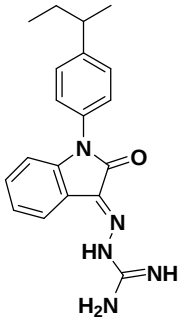
N
O
N
HN
NH
H2N

10-42

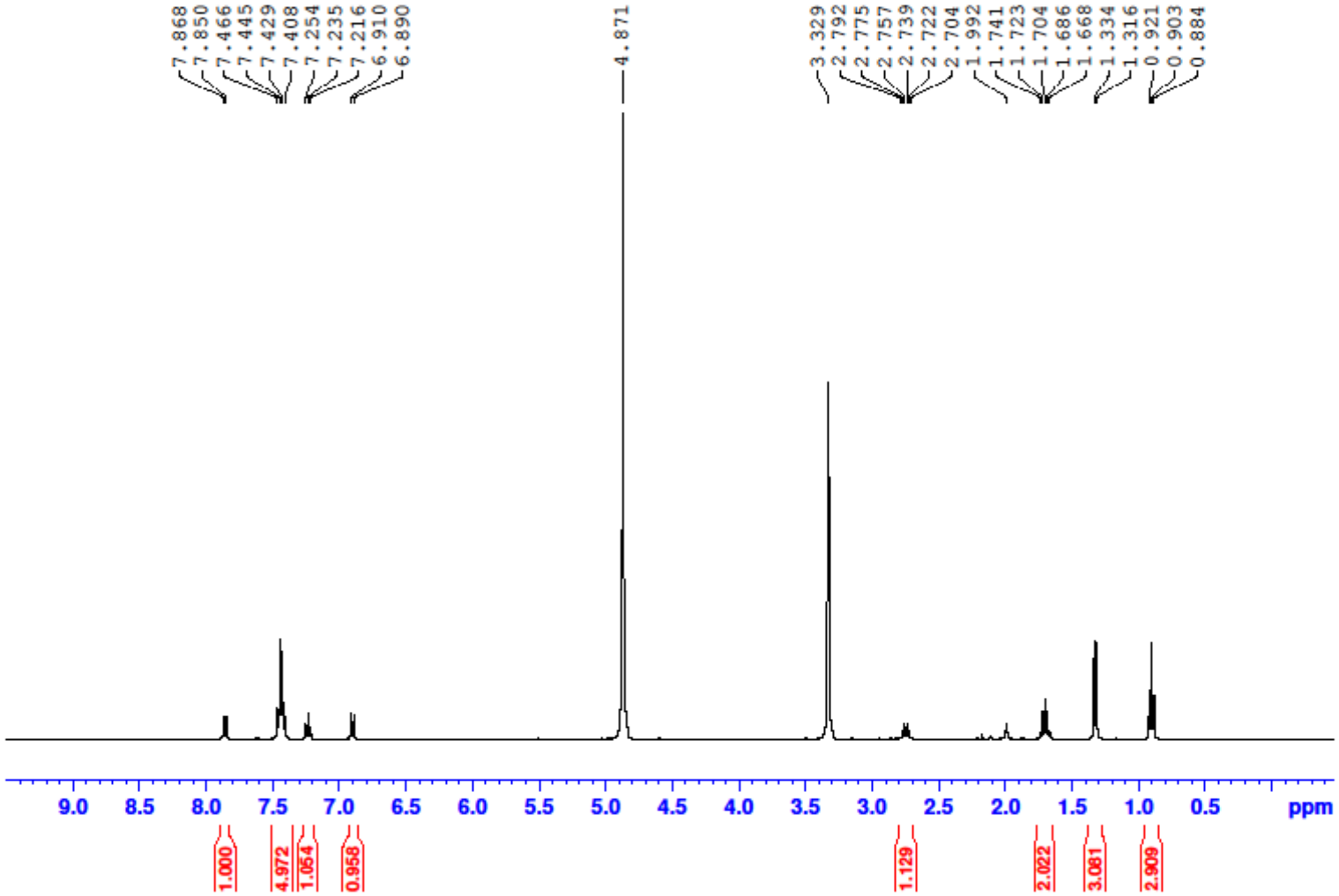
7.868
7.850
7.466
7.445
7.429
7.408
7.254
7.235
7.216
6.910
6.890
4.871
3.329
2.792
2.775
2.757
2.739
2.722
2.704
1.992
1.741
1.723
1.704
1.686
1.668
1.334
1.316
0.921
0.903
0.884
9.0
8.5
8.0
7.5
7.0
6.5
6.0
5.5
5.0
4.5
4.0
3.5
3.0
2.5
2.0
1.5
1.0
0.5
ppm
1.000
4.972
1.054
0.958
1.129
2.022
3.081
2.909

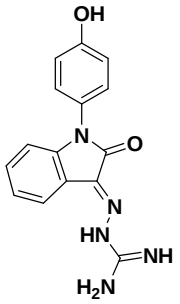
OH
N
O
N
HN
NH
H2N

10-43

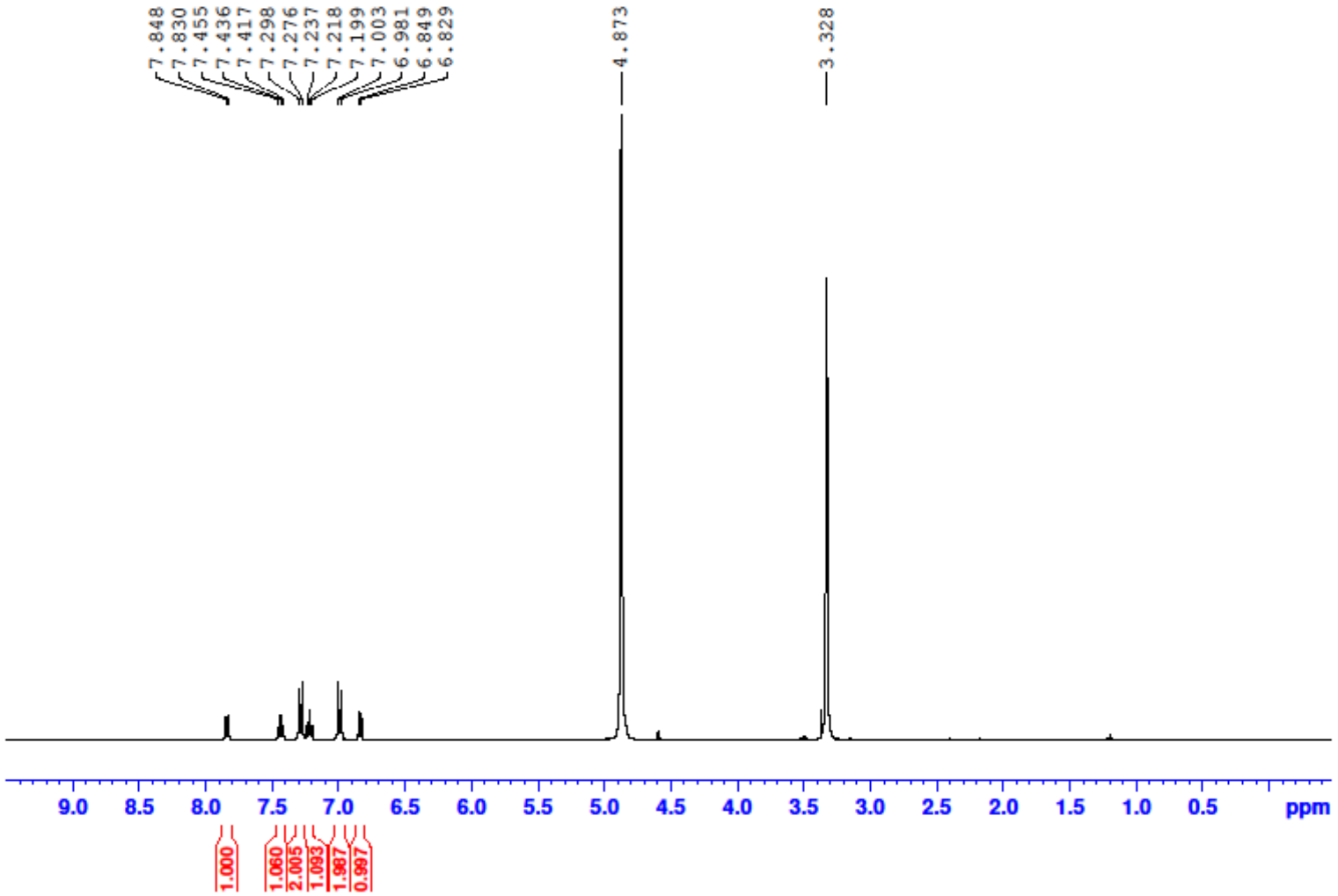
7.848
7.830
7.455
7.436
7.417
7.298
7.276
7.237
7.218
7.199
7.003
6.981
6.849
6.829
4.873
3.328
9.0
8.5
8.0
7.5
7.0
6.5
6.0
5.5
5.0
4.5
4.0
3.5
3.0
2.5
2.0
1.5
1.0
0.5
ppm
1.000
1.060
2.005
1.093
1.987
0.997

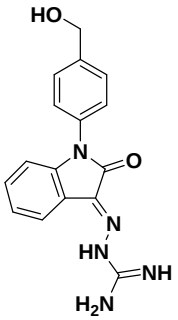
HO
N
O
N
HN
NH
H2N

10-44

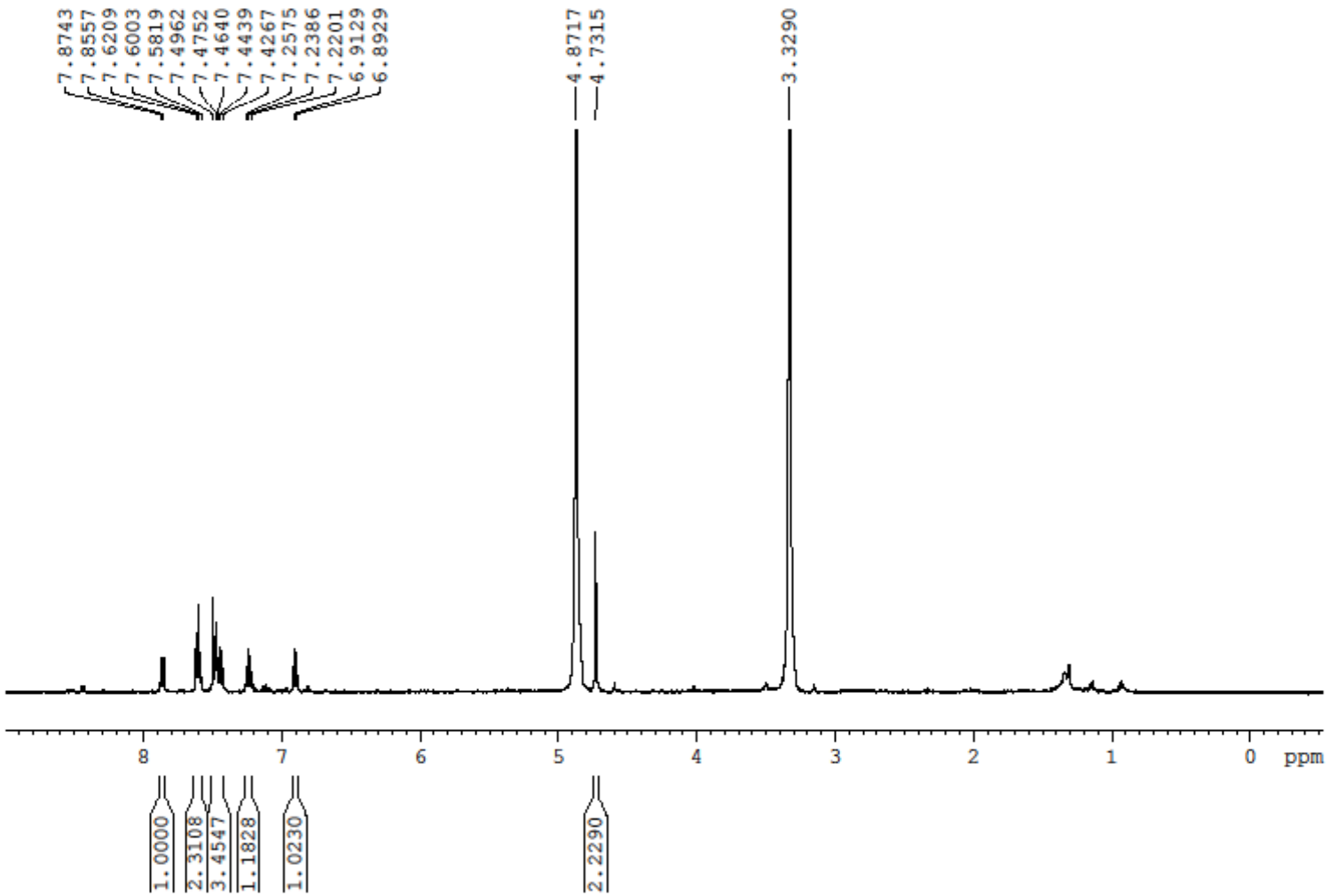
7.8743
7.8557
7.6209
7.6003
7.5819
7.4962
7.4752
7.4640
7.4439
7.4267
7.2575
7.2386
7.2201
6.9129
6.8929
4.8717
4.7315
3.3290
8
7
6
5
4
3
2
1
0
ppm
1.0000
2.3108
3.4547
1.1828
1.0230
2.2290

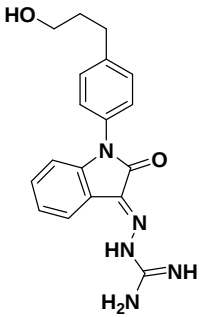
HO
N
O
N
HN
NH
H2N

10-45

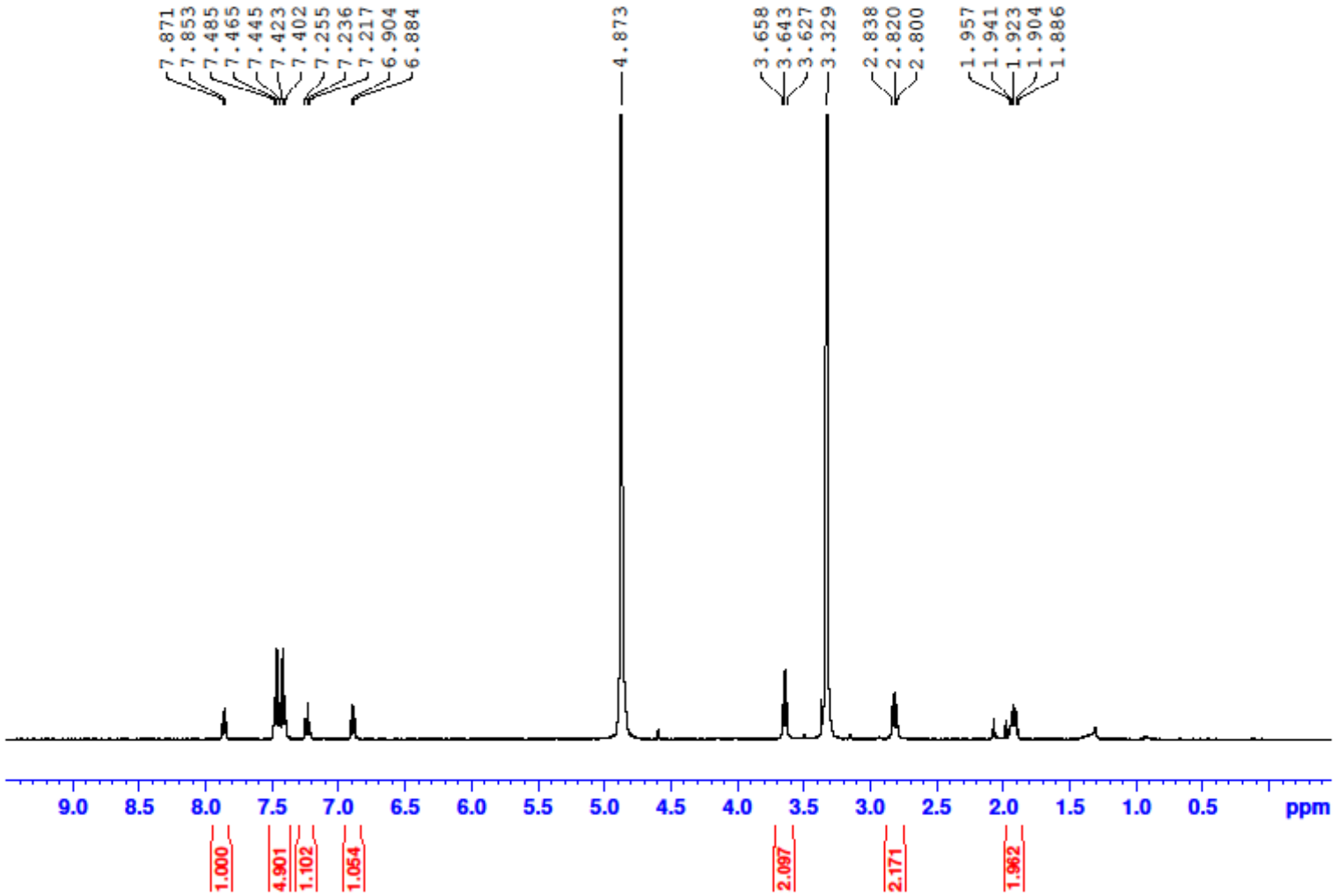
7.871
7.853
7.485
7.465
7.445
7.423
7.402
7.255
7.236
7.217
6.904
6.884
4.873
3.658
3.643
3.627
3.329
2.838
2.820
2.800
1.957
1.941
1.923
1.904
1.886
9.0
8.5
8.0
7.5
7.0
6.5
6.0
5.5
5.0
4.5
4.0
3.5
3.0
2.5
2.0
1.5
1.0
0.5
ppm
1.000
4.901
1.102
1.054
2.097
2.171
1.962

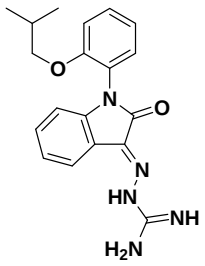
O
N
O
N
HN
NH
H2N

10-46

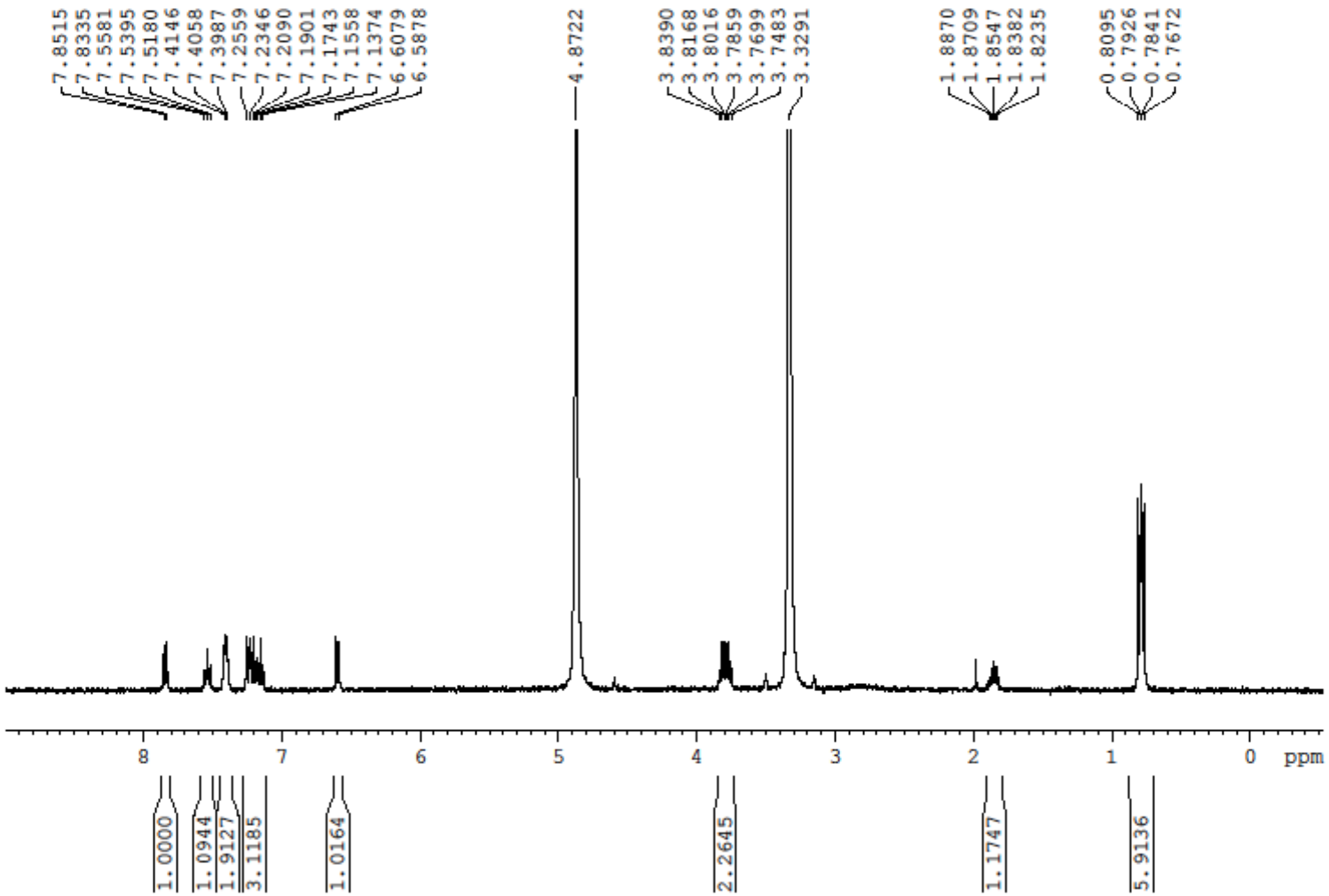
7.8515
7.8335
7.5581
7.5395
7.5180
7.4146
7.4058
7.3987
7.2559
7.2346
7.2090
7.1901
7.1743
7.1558
7.1374
6.6079
6.5878
4.8722
3.8390
3.8168
3.8016
3.7859
3.7699
3.7483
3.3291
1.8870
1.8709
1.8547
1.8382
1.8235
0.8095
0.7926
0.7841
0.7672
8
7
6
5
4
3
2
1
0
ppm
1.0000
1.0944
1.9127
3.1185
1.0164
2.2645
1.1747
5.9136

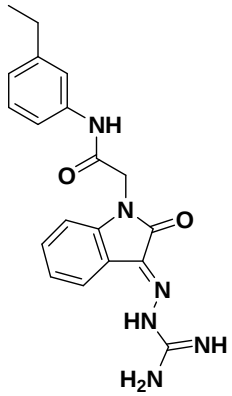
NH
O
N
O
N
HN
NH
H2N

10b-04

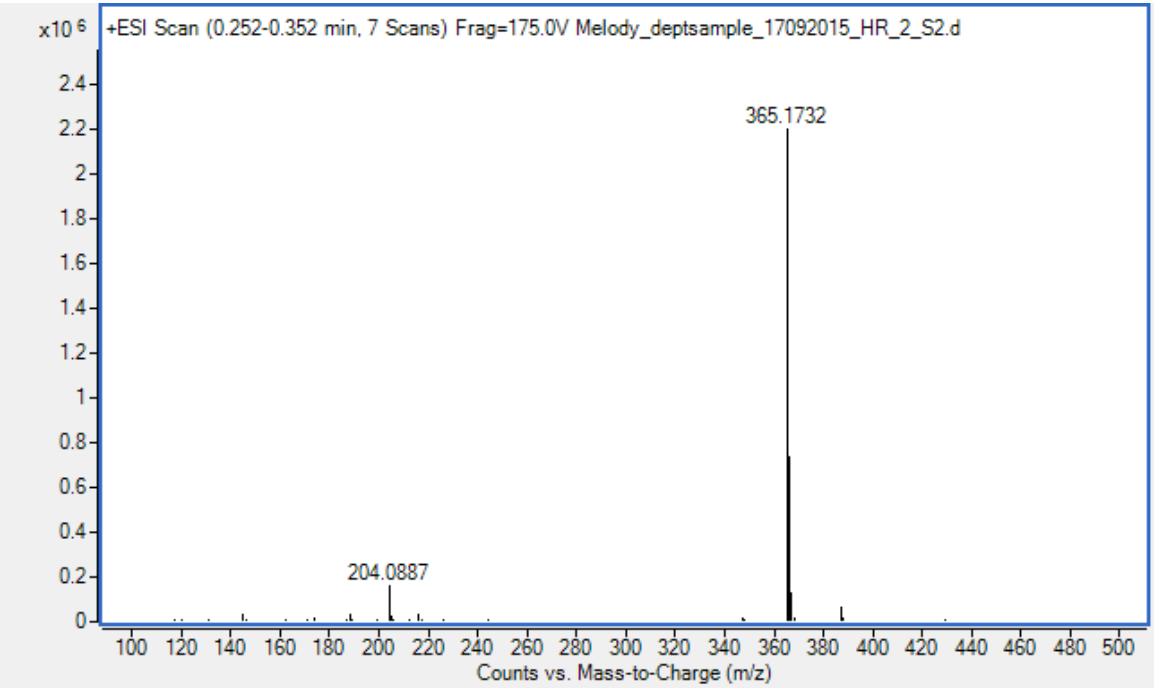
x10 6
+ESI Scan (0.252-0.352 min, 7 Scans) Frag=175.0V Melody_deptsample_17092015_HR_2_S2.d
365.1732
204.0887
2.4
2.2
2
1.8
1.6
1.4
1.2
1
0.8
0.6
0.4
0.2
0
100 120 140 160 180 200 220 240 260 280 300 320 340 360 380 400 420 440 460 480 500
Counts vs. Mass-to-Charge (m/z)

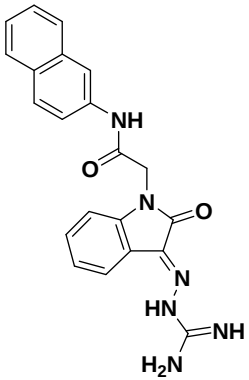
NH
O
N
O
N
HN
NH
H2N

10b-19

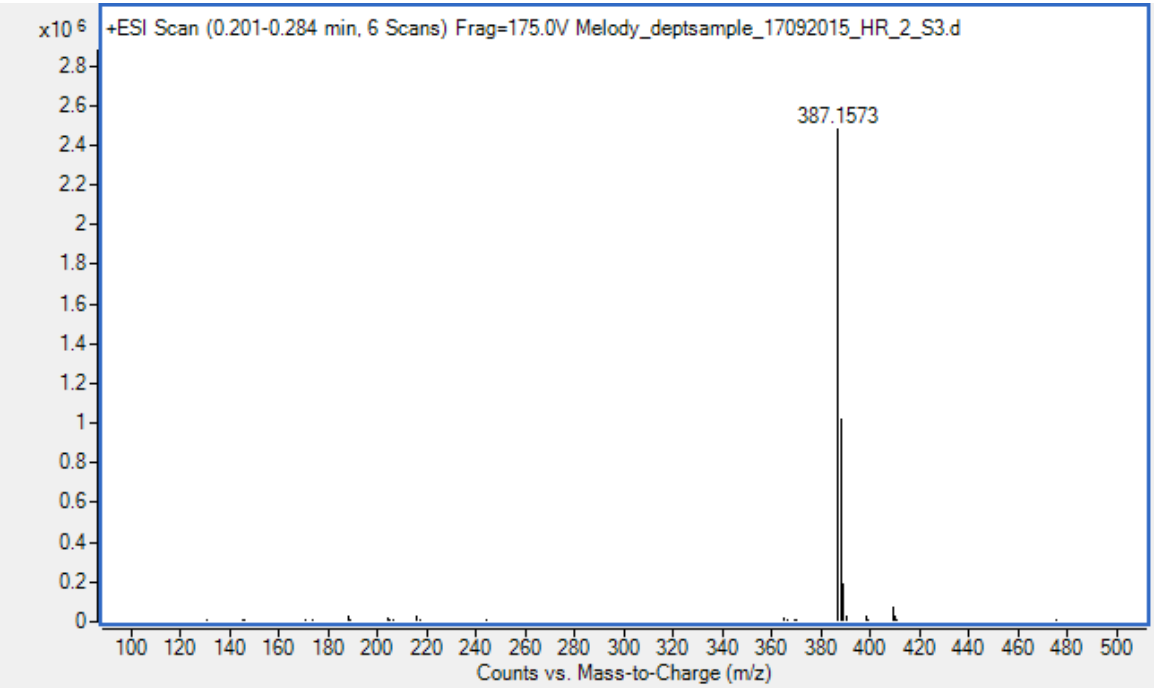
x10 6
+ESI Scan (0.201-0.284 min, 6 Scans) Frag=175.0V Melody_deptsample_17092015_HR_2_S3.d
387.1573
2.8
2.6
2.4
2.2
2
1.8
1.6
1.4
1.2
1
0.8
0.6
0.4
0.2
0
100 120 140 160 180 200 220 240 260 280 300 320 340 360 380 400 420 440 460 480 500
Counts vs. Mass-to-Charge (m/z)

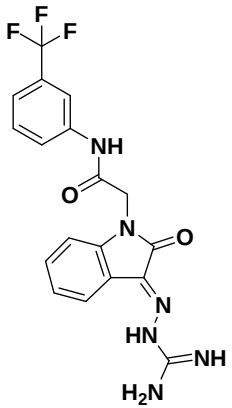
F
F
F
NH
O
N
O
N
HN
NH
H_2N

10b-20

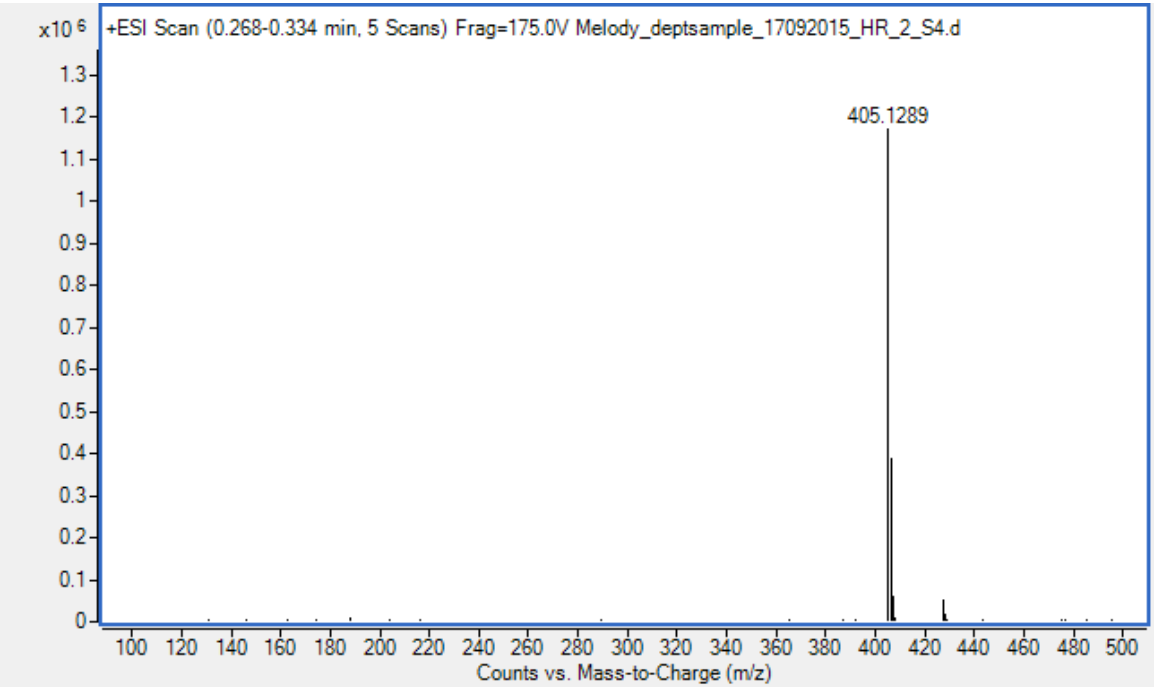
x10 6
+ESI Scan (0.268-0.334 min, 5 Scans) Frag=175.0V Melody_deptsample_17092015_HR_2_S4.d
405.1289
1.3
1.2
1.1
1
0.9
0.8
0.7
0.6
0.5
0.4
0.3
0.2
0.1
0
100 120 140 160 180 200 220 240 260 280 300 320 340 360 380 400 420 440 460 480 500
Counts vs. Mass-to-Charge (m/z)

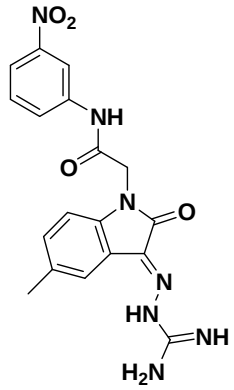
NO2
NH
O
N
O
N
HN
NH
H2N

10c-27

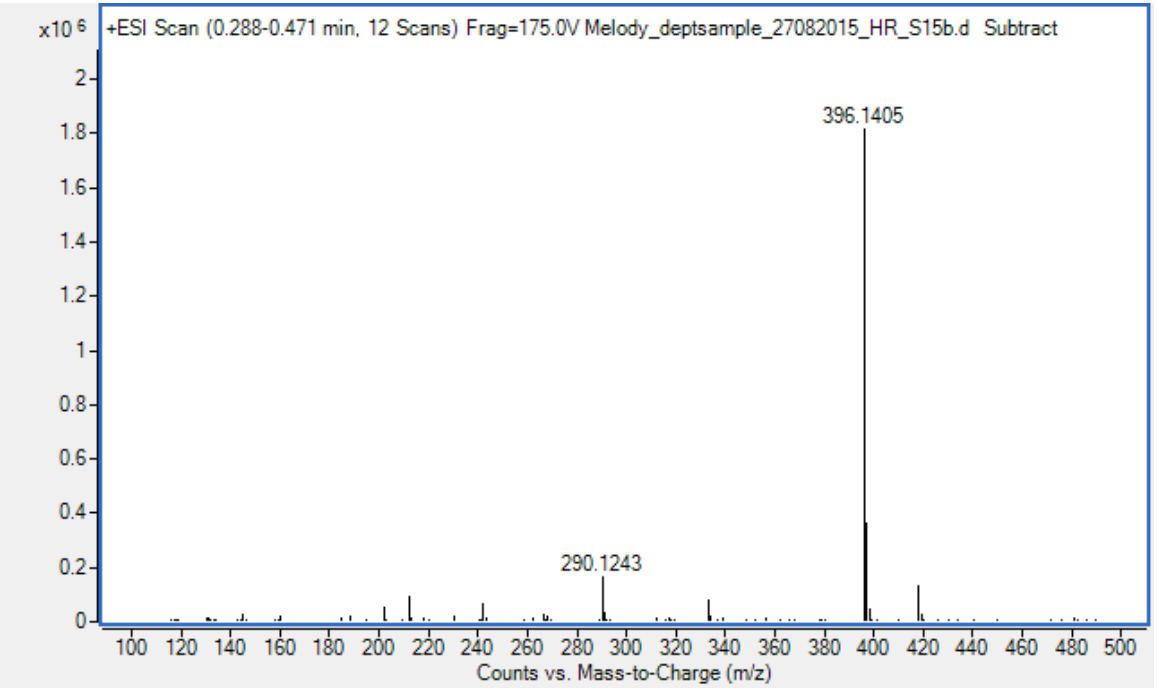
x10 6
+ESI Scan (0.288-0.471 min, 12 Scans) Frag=175.0V Melody_deptsample_27082015_HR_S15b.d Subtract
396.1405
290.1243
Counts vs. Mass-to-Charge (m/z)

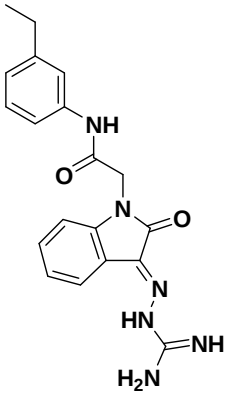
NH
O
N
O
N
HN
NH
H2N

10-31

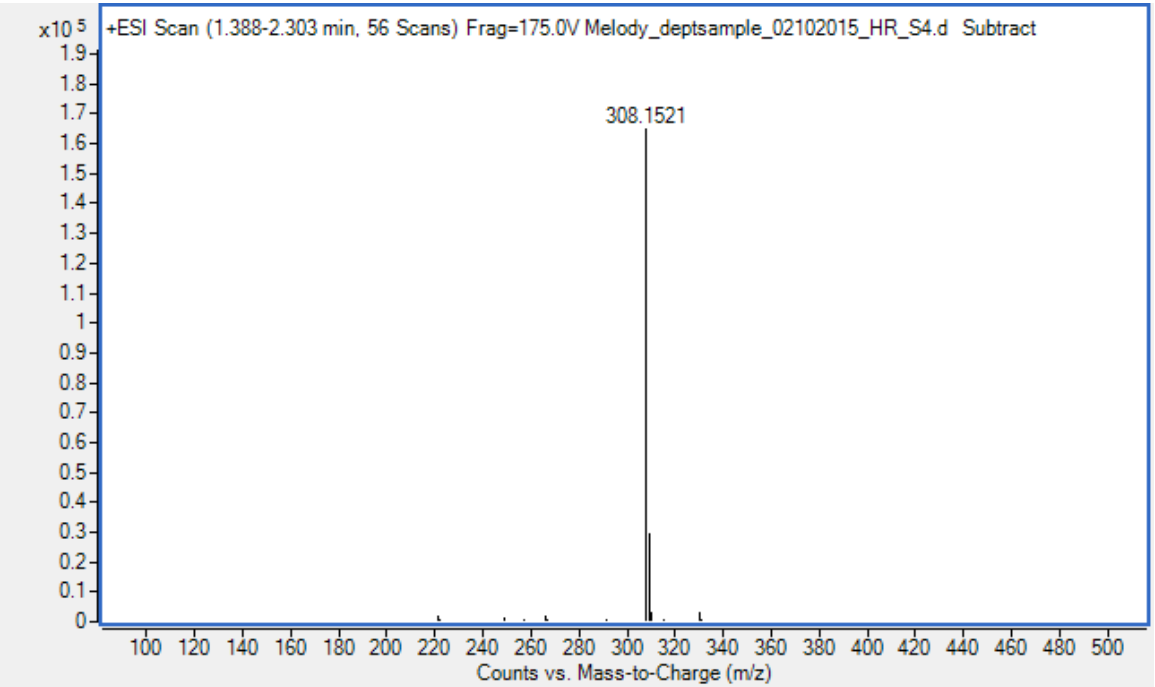
x10 5
+ESI Scan (1.388-2.303 min, 56 Scans) Frag=175.0V Melody_deptsample_02102015_HR_S4.d Subtract
308.1521
1.9
1.8
1.7
1.6
1.5
1.4
1.3
1.2
1.1
1
0.9
0.8
0.7
0.6
0.5
0.4
0.3
0.2
0.1
0
100 120 140 160 180 200 220 240 260 280 300 320 340 360 380 400 420 440 460 480 500
Counts vs. Mass-to-Charge (m/z)

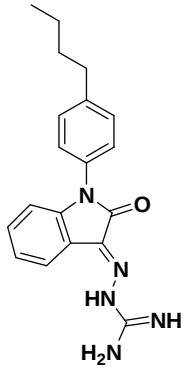
N
O
N
HN
NH
H2N

10-32

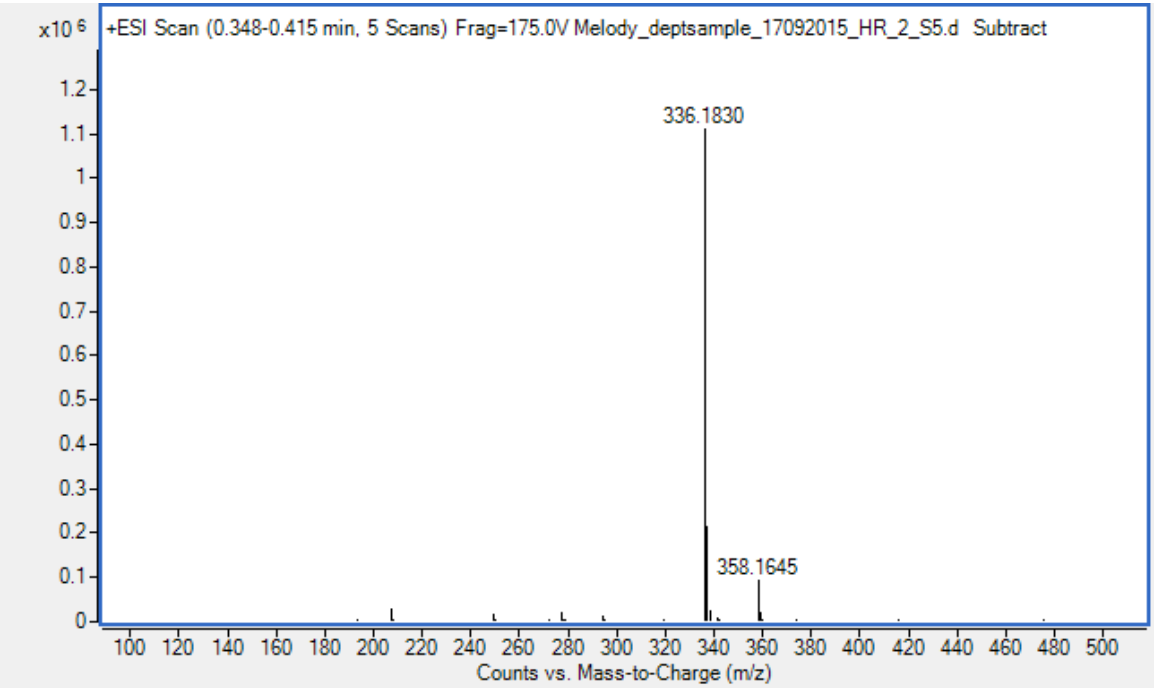
x10 6
+ESI Scan (0.348-0.415 min, 5 Scans) Frag=175.0V Melody_deptsample_17092015_HR_2_S5.d Subtract
336.1830
358.1645
Counts vs. Mass-to-Charge (m/z)

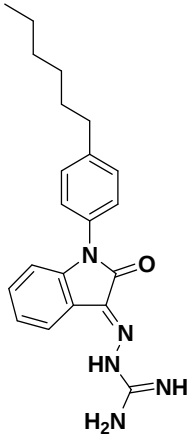
N
O
N
HN
NH
H2N

10-33

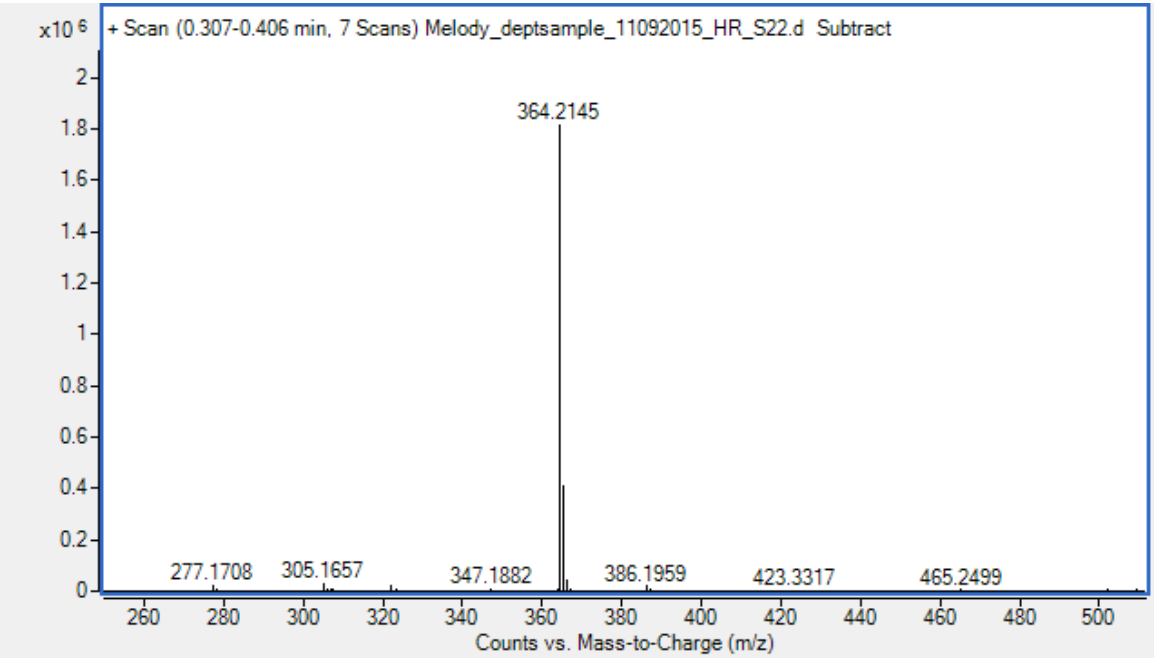
x10 6
+ Scan (0.307-0.406 min, 7 Scans) Melody_deptsample_11092015_HR_S22.d Subtract
364.2145
277.1708
305.1657
347.1882
386.1959
423.3317
465.2499
Counts vs. Mass-to-Charge (m/z)

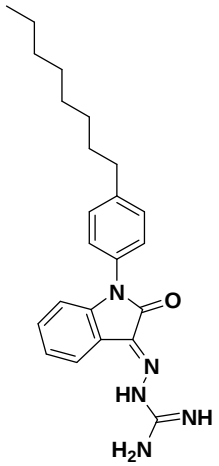
N
O
N
HN
NH
H2N

10-34

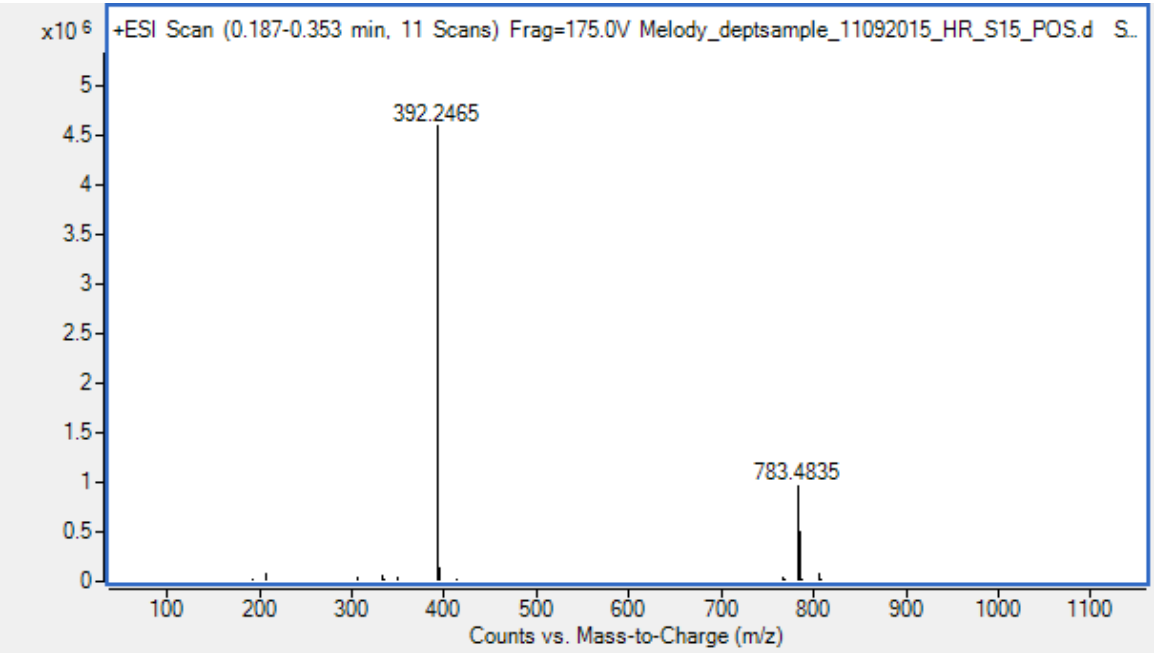
x10 6
+ESI Scan (0.187-0.353 min, 11 Scans) Frag=175.0V Melody_deptsample_11092015_HR_S15_POS.d S..
392.2465
783.4835
5
4.5
4
3.5
3
2.5
2
1.5
1
0.5
0
100
200
300
400
500
600
700
800
900
1000
1100
Counts vs. Mass-to-Charge (m/z)

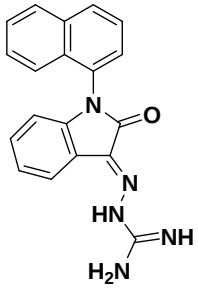
N
O
N
HN
NH
H2N

10-35

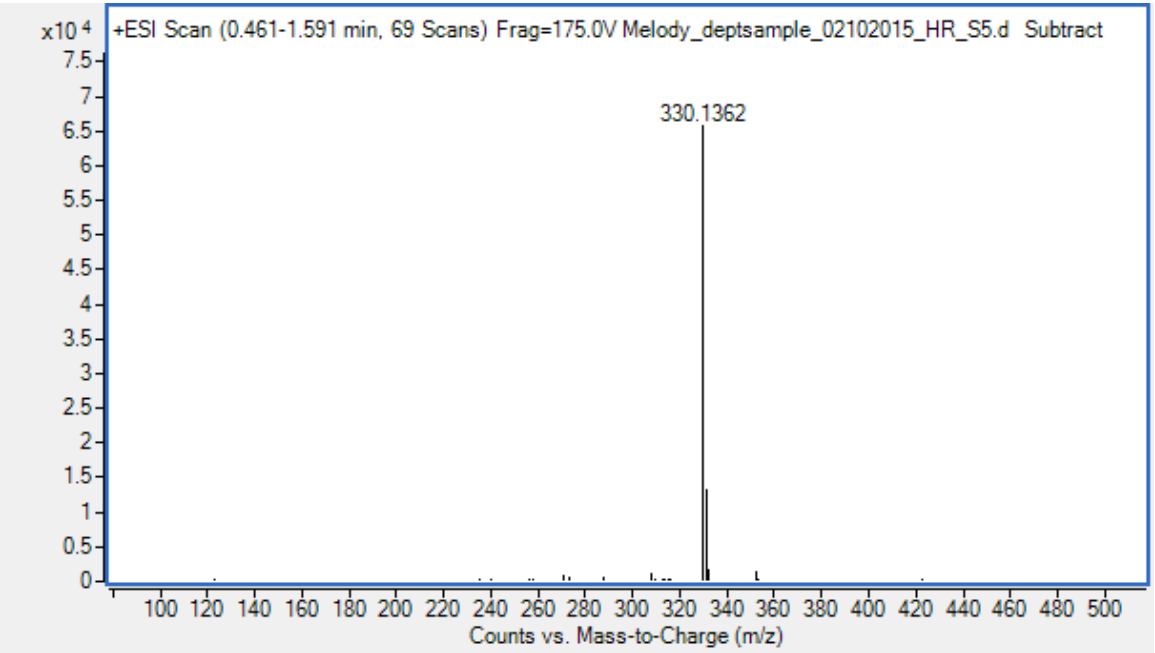
x10 4
+ESI Scan (0.461-1.591 min, 69 Scans) Frag=175.0V Melody_deptsample_02102015_HR_S5.d Subtract
330.1362
7.5
7
6.5
6
5.5
5
4.5
4
3.5
3
2.5
2
1.5
1
0.5
0
100 120 140 160 180 200 220 240 260 280 300 320 340 360 380 400 420 440 460 480 500
Counts vs. Mass-to-Charge (m/z)

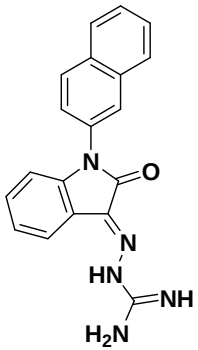
N
O
N
HN
NH
H2N

10-36

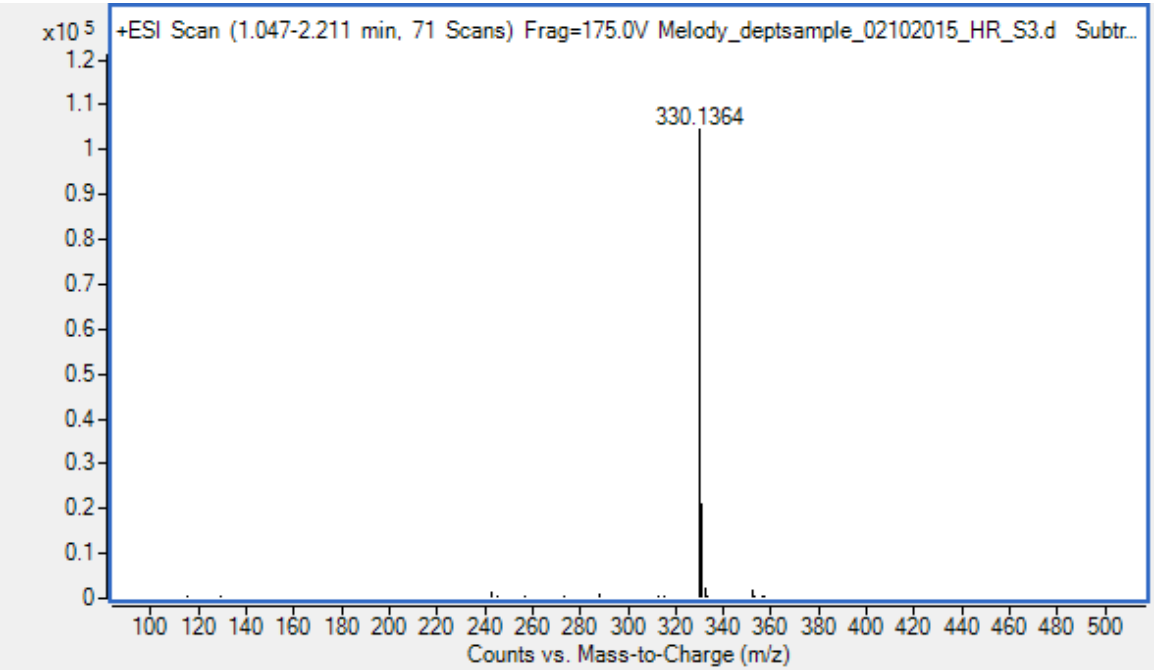
x10 5
+ESI Scan (1.047-2.211 min, 71 Scans) Frag=175.0V Melody_deptsample_02102015_HR_S3.d Subtr...
330.1364
1.2
1.1
1
0.9
0.8
0.7
0.6
0.5
0.4
0.3
0.2
0.1
0
100 120 140 160 180 200 220 240 260 280 300 320 340 360 380 400 420 440 460 480 500
Counts vs. Mass-to-Charge (m/z)

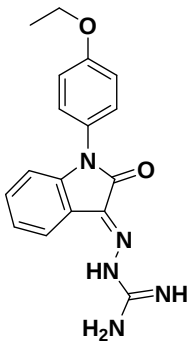
O
N
O
N
HN
NH
H2N

10-37

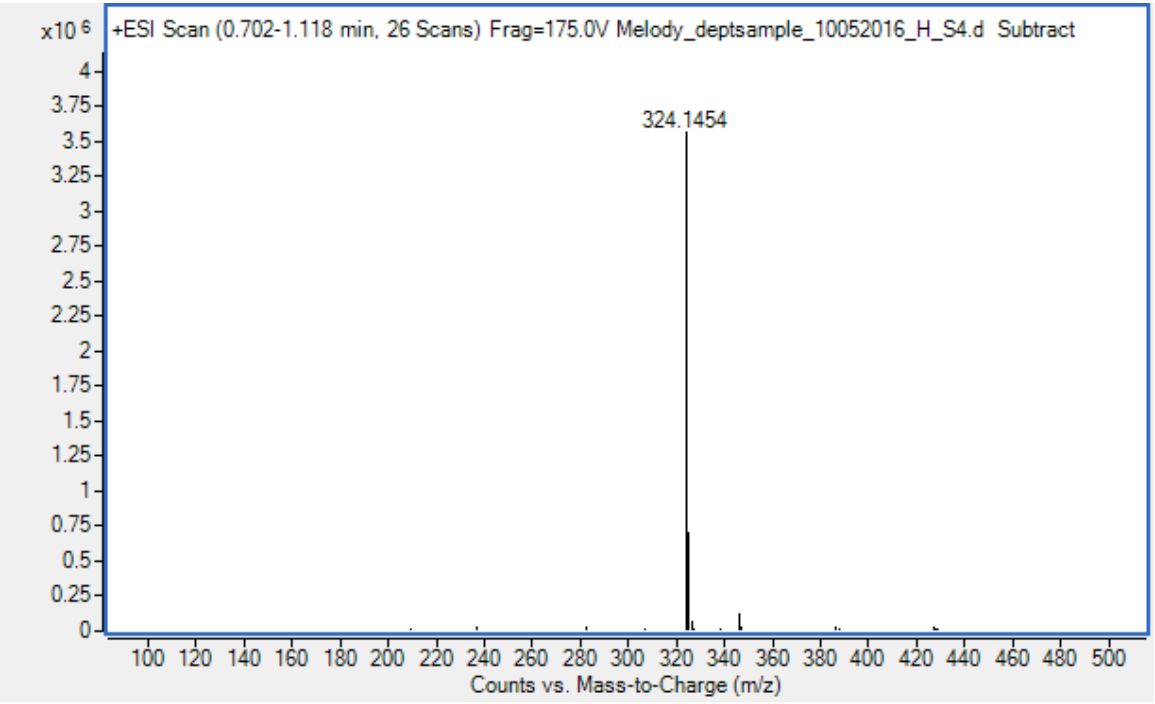
x10 6
+ESI Scan (0.702-1.118 min, 26 Scans) Frag=175.0V Melody_deptsample_10052016_H_S4.d Subtract
324.1454
4
3.75
3.5
3.25
3
2.75
2.5
2.25
2
1.75
1.5
1.25
1
0.75
0.5
0.25
0
100 120 140 160 180 200 220 240 260 280 300 320 340 360 380 400 420 440 460 480 500
Counts vs. Mass-to-Charge (m/z)

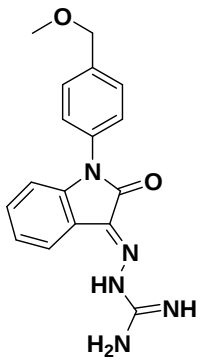
O
N
O
N
HN
NH
H2N

10-38

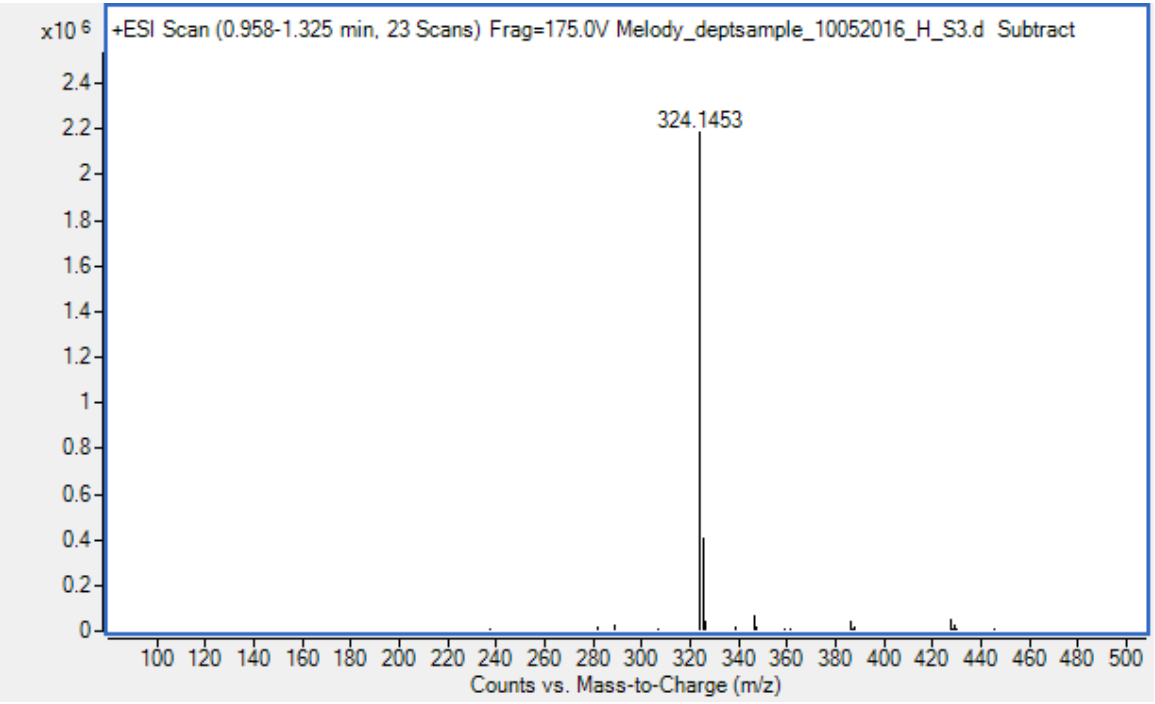
x10 6
+ESI Scan (0.958-1.325 min, 23 Scans) Frag=175.0V Melody_deptsample_10052016_H_S3.d Subtract
324.1453
2.4
2.2
2
1.8
1.6
1.4
1.2
1
0.8
0.6
0.4
0.2
0
100 120 140 160 180 200 220 240 260 280 300 320 340 360 380 400 420 440 460 480 500
Counts vs. Mass-to-Charge (m/z)

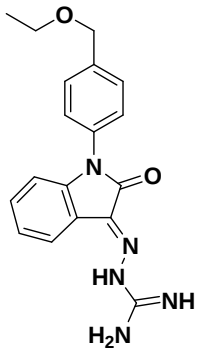
O
N
O
N
HN
NH
H2N

10-39

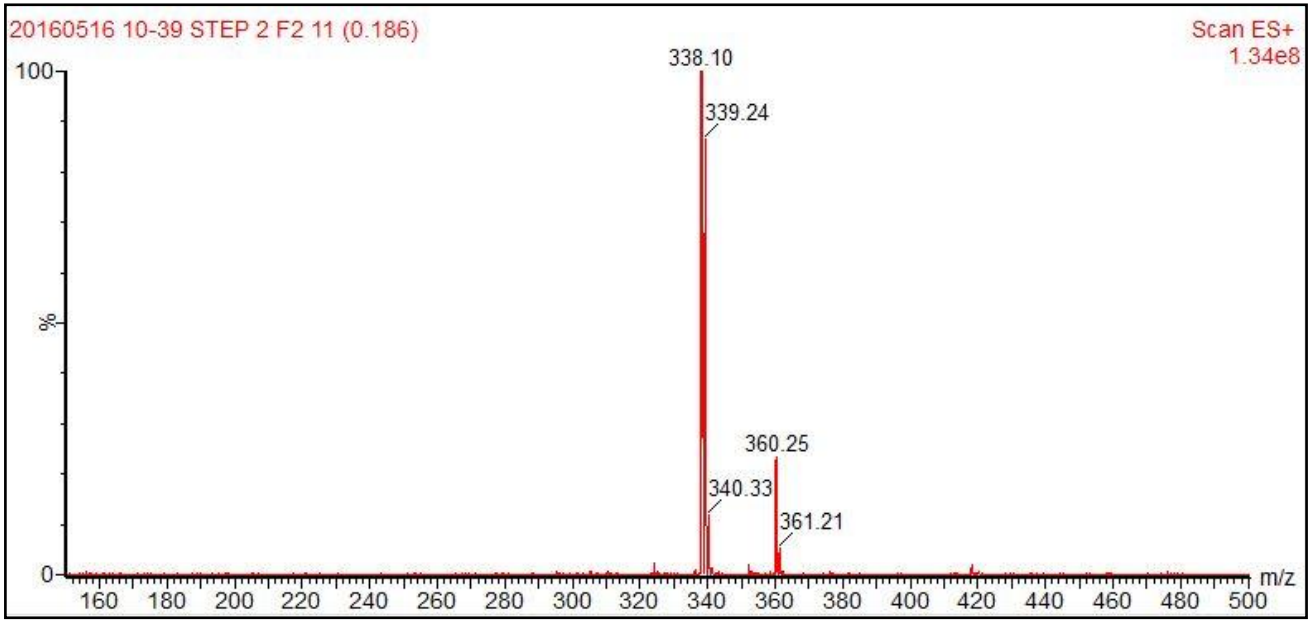
20160516 10-39 STEP 2 F2 11 (0.186)
Scan ES+
1.34e8
100
%
0
338.10
339.24
360.25
340.33
361.21
m/z
160 180 200 220 240 260 280 300 320 340 360 380 400 420 440 460 480 500

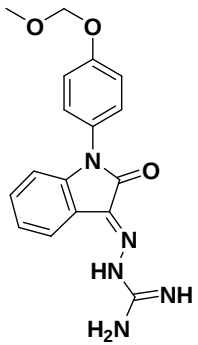
O
O
N
O
N
HN
NH
H2N

10-40

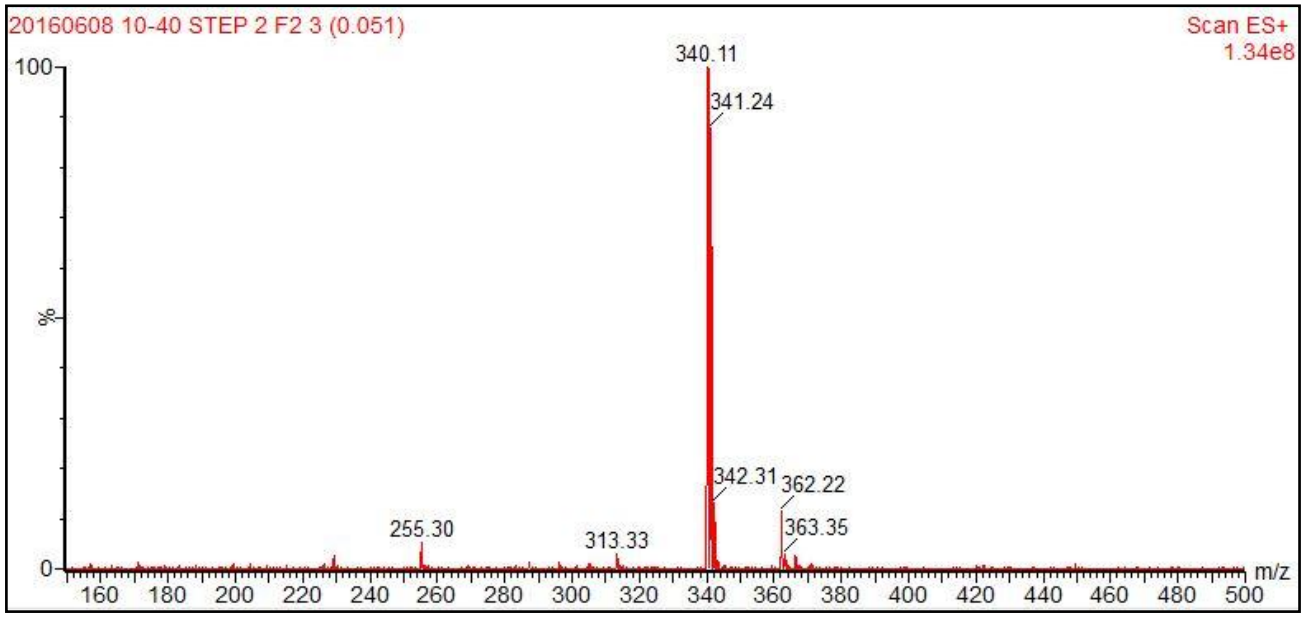
20160608 10-40 STEP 2 F2 3 (0.051)
Scan ES+
1.34e8
100
%
0
340.11
341.24
342.31
362.22
363.35
255.30
313.33
m/z
160 180 200 220 240 260 280 300 320 340 360 380 400 420 440 460 480 500

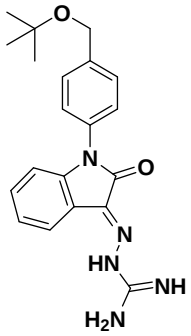
O
N
O
N
HN
NH
H2N

10-41

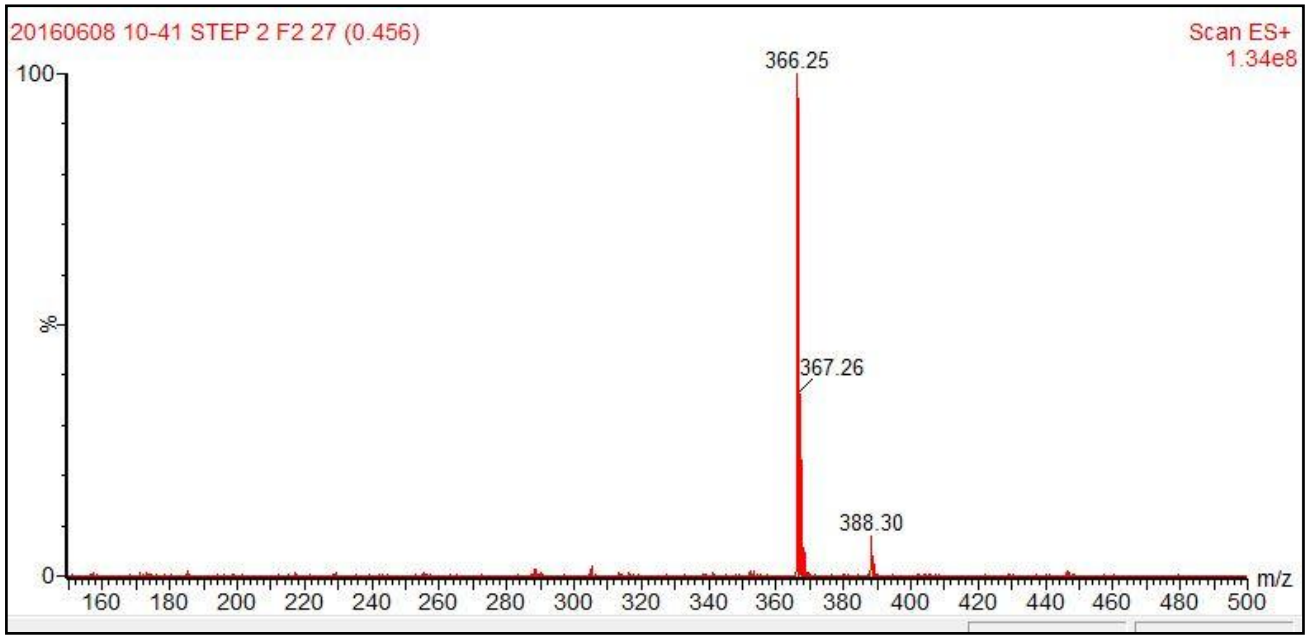
20160608 10-41 STEP 2 F2 27 (0.456)
Scan ES+
1.34e8
100
%
0
366.25
367.26
388.30
m/z
160 180 200 220 240 260 280 300 320 340 360 380 400 420 440 460 480 500

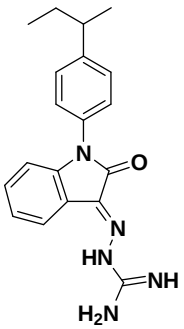
N
O
N
HN
NH
H2N

10-42

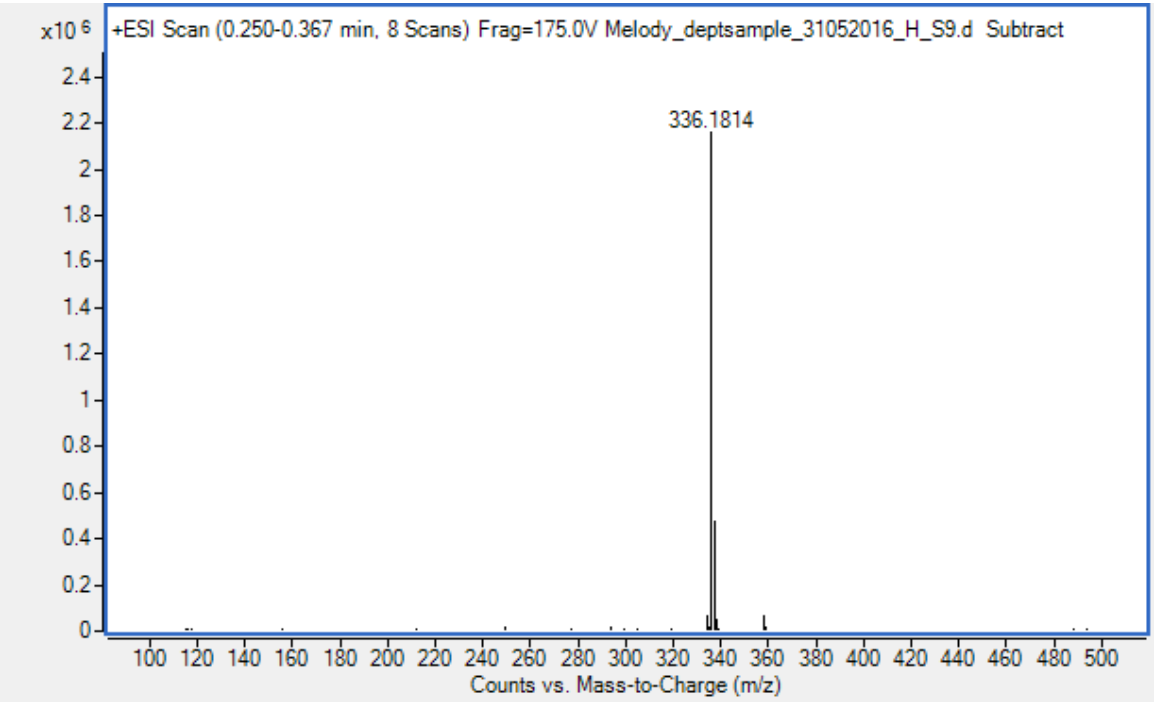
x10 6
+ESI Scan (0.250-0.367 min, 8 Scans) Frag=175.0V Melody_deptsample_31052016_H_S9.d Subtract
336.1814
2.4
2.2
2
1.8
1.6
1.4
1.2
1
0.8
0.6
0.4
0.2
0
100 120 140 160 180 200 220 240 260 280 300 320 340 360 380 400 420 440 460 480 500
Counts vs. Mass-to-Charge (m/z)

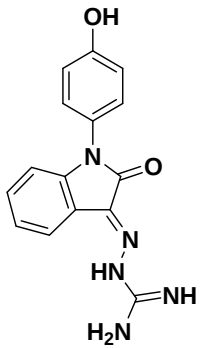
OH
N
O
N
HN
NH
H2N

10-43

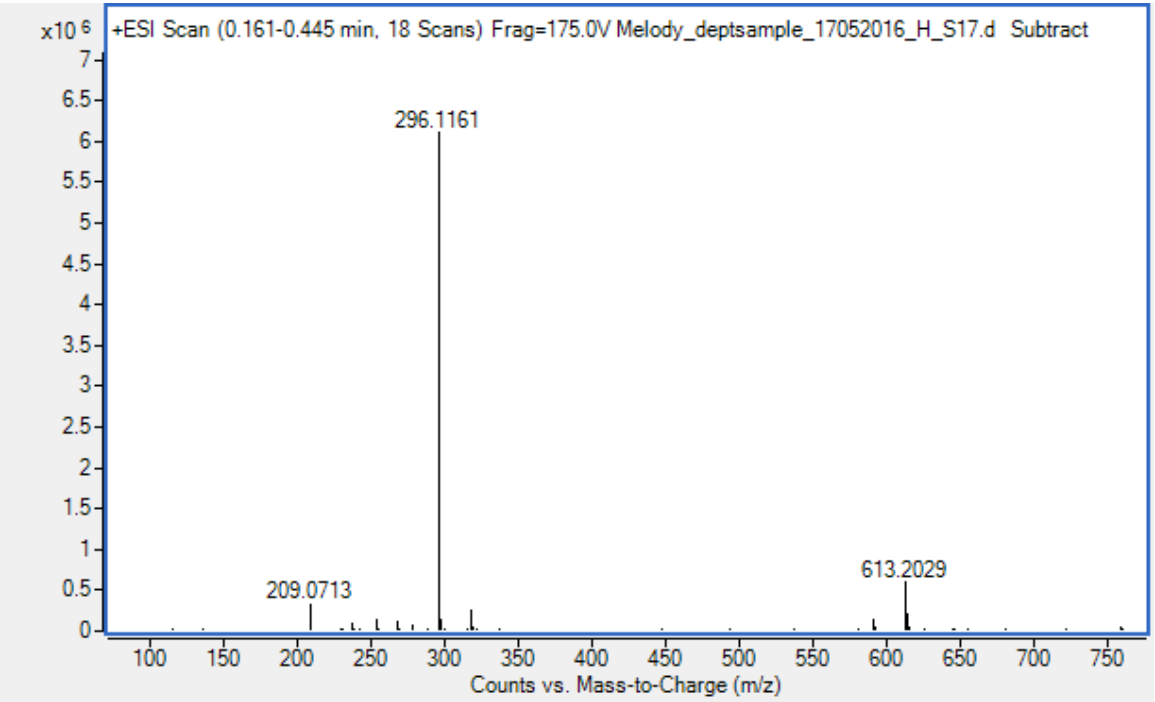
x10 6
+ESI Scan (0.161-0.445 min, 18 Scans) Frag=175.0V Melody_deptsample_17052016_H_S17.d Subtract
296.1161
209.0713
613.2029
Counts vs. Mass-to-Charge (m/z)

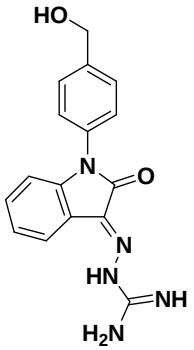
HO
N
O
N
HN
NH
H2N

10-44

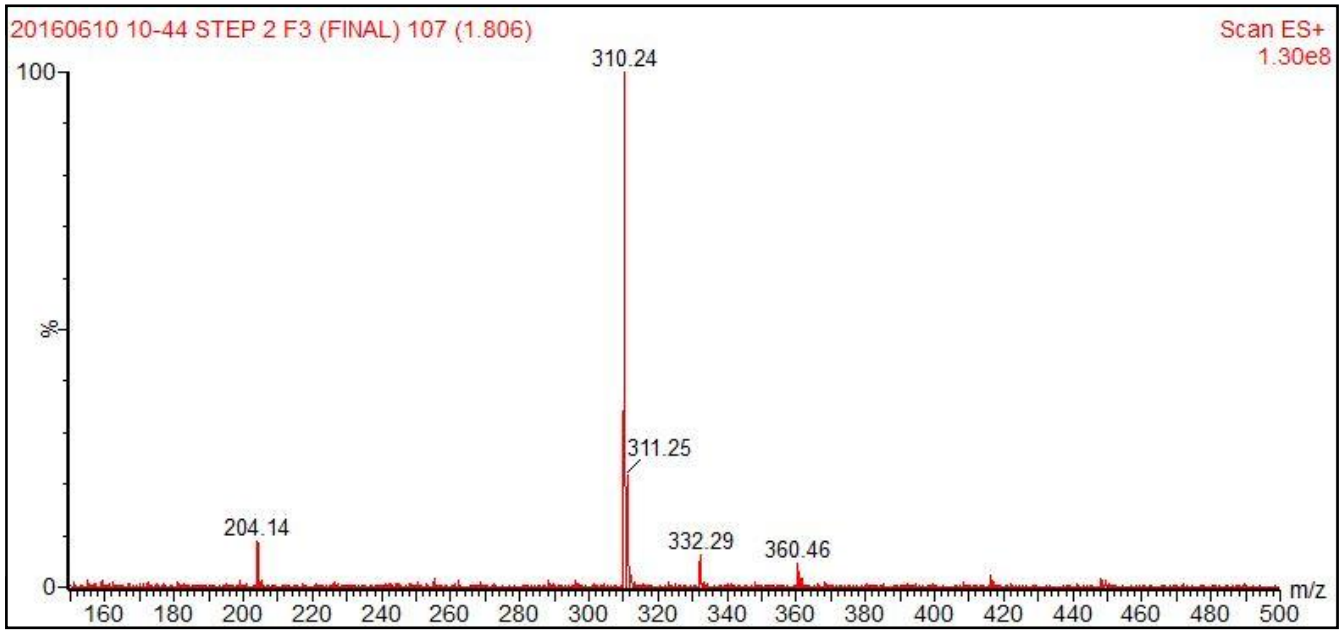
20160610 10-44 STEP 2 F3 (FINAL) 107 (1.806)
Scan ES+
1.30e8
100
%
0
310.24
311.25
204.14
332.29
360.46
m/z
160 180 200 220 240 260 280 300 320 340 360 380 400 420 440 460 480 500

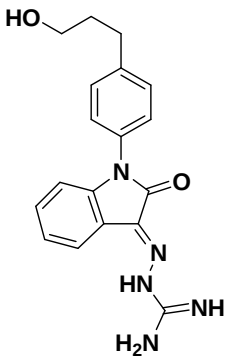
HO
N
O
N
HN
NH
H2N

10-45

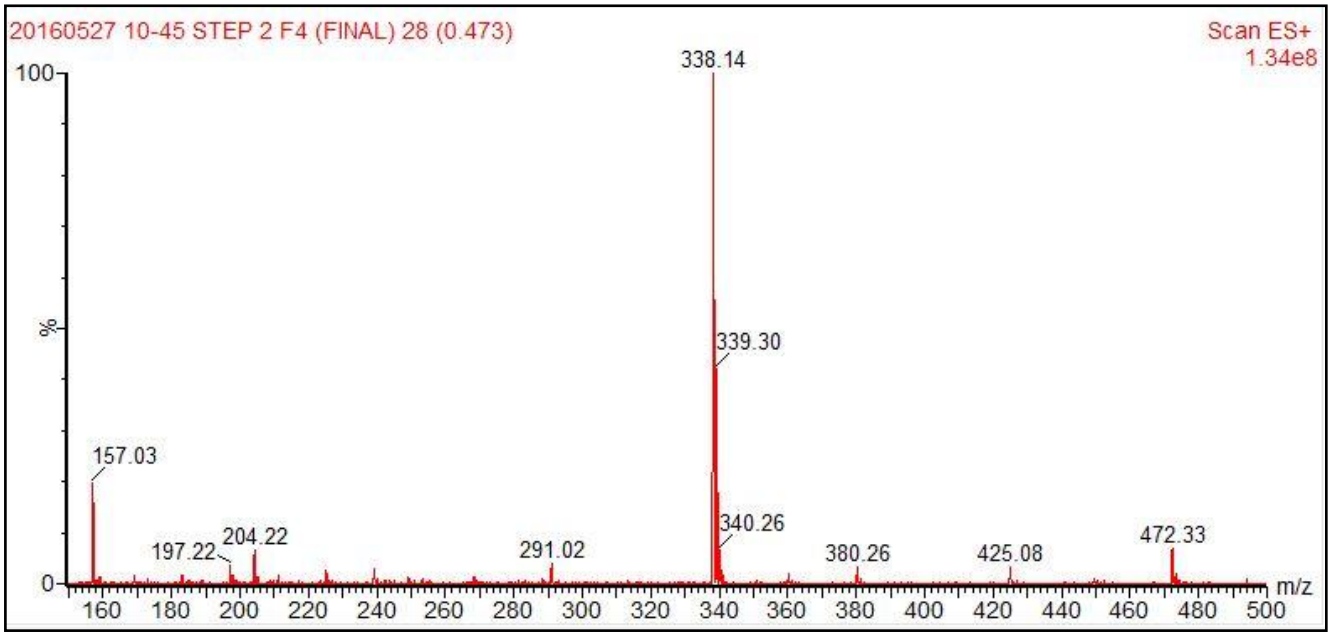
20160527 10-45 STEP 2 F4 (FINAL) 28 (0.473)
Scan ES+
1.34e8
100
%
0
338.14
339.30
157.03
340.26
197.22
204.22
291.02
380.26
425.08
472.33
m/z
160 180 200 220 240 260 280 300 320 340 360 380 400 420 440 460 480 500

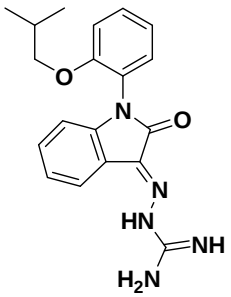
O
N
O
N
HN
NH
H2N

10-46

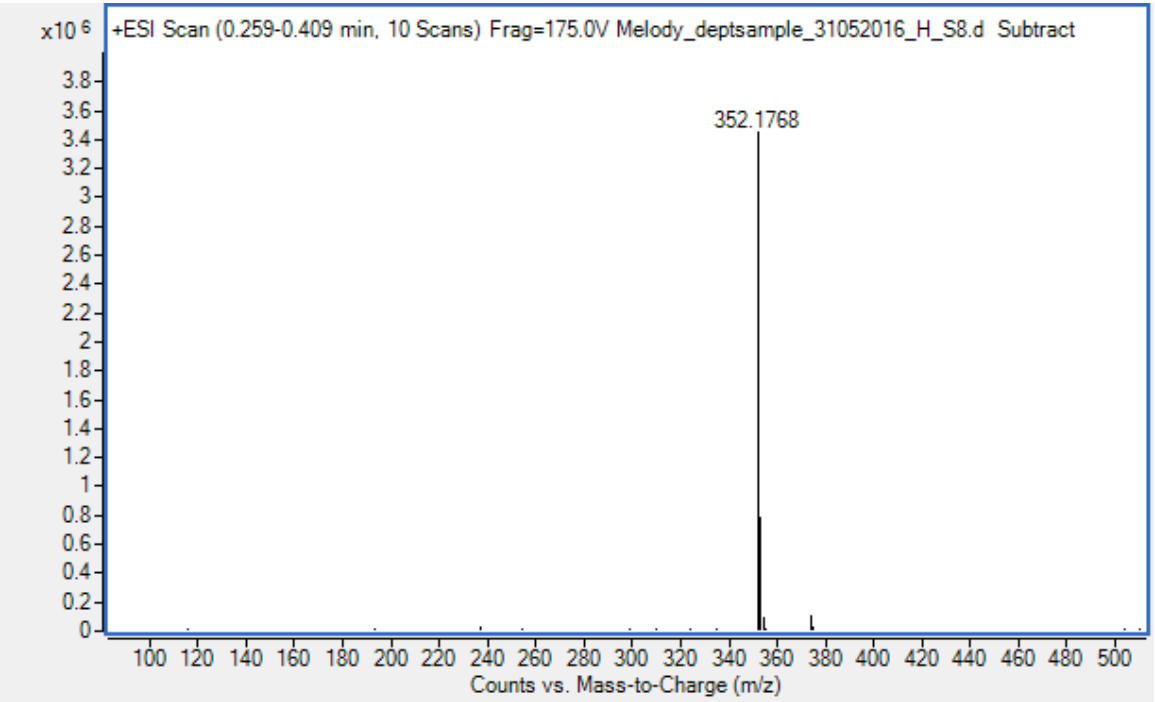
x10 6
+ESI Scan (0.259-0.409 min, 10 Scans) Frag=175.0V Melody_deptsample_31052016_H_S8.d Subtract
352.1768
3.8
3.6
3.4
3.2
3
2.8
2.6
2.4
2.2
2
1.8
1.6
1.4
1.2
1
0.8
0.6
0.4
0.2
0
100 120 140 160 180 200 220 240 260 280 300 320 340 360 380 400 420 440 460 480 500
Counts vs. Mass-to-Charge (m/z)

Appendix II

Ä KTA purification spectrum and corresponding SDS-PAGE gel of PBP2

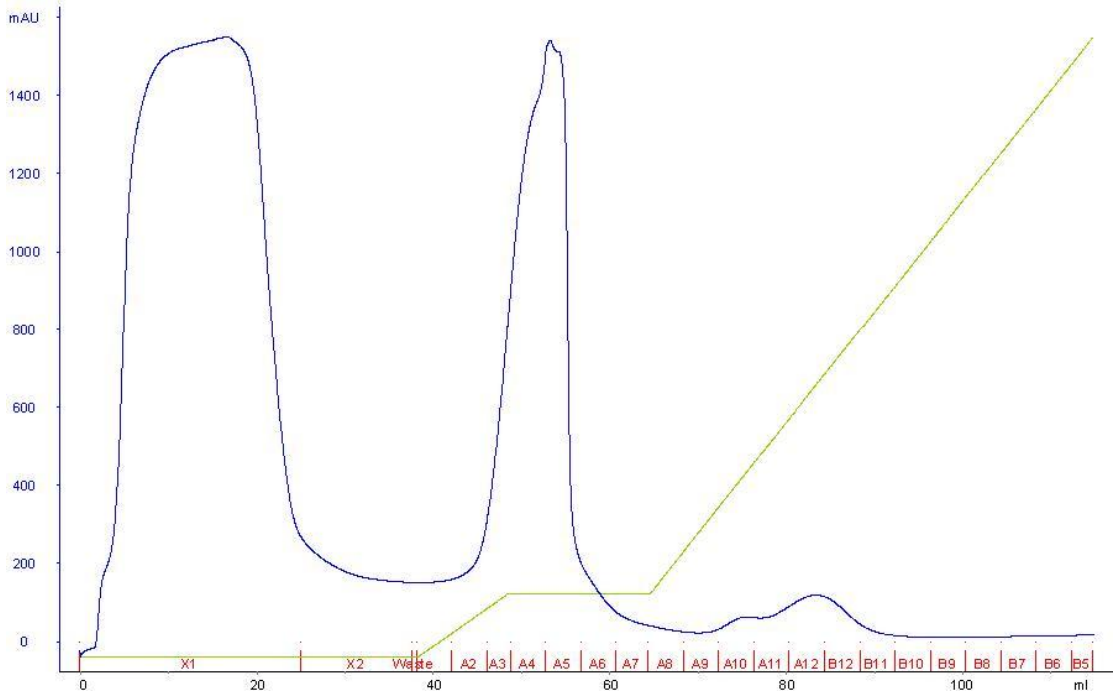

Fig. S2.1(a) ÄKTA purification spectrum of full-length PBP2 using 20 mM Fos-Choline-14 as membrane solubilizing detergent. PBP2 was eluted at A10 to B11.

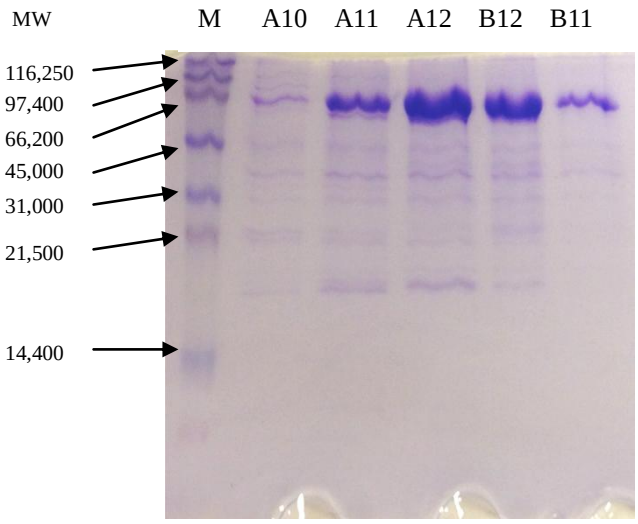

Fig. S2.1(b) SDS-PAGE gel of the full-length PBP2 using 20 mM Fos-Choline-14 as membrane solubilizing detergent. M refers to low range molecular markers. PBP2 was eluted at A10 to B11.

Appendix III

STD-NMR method validation spectrum

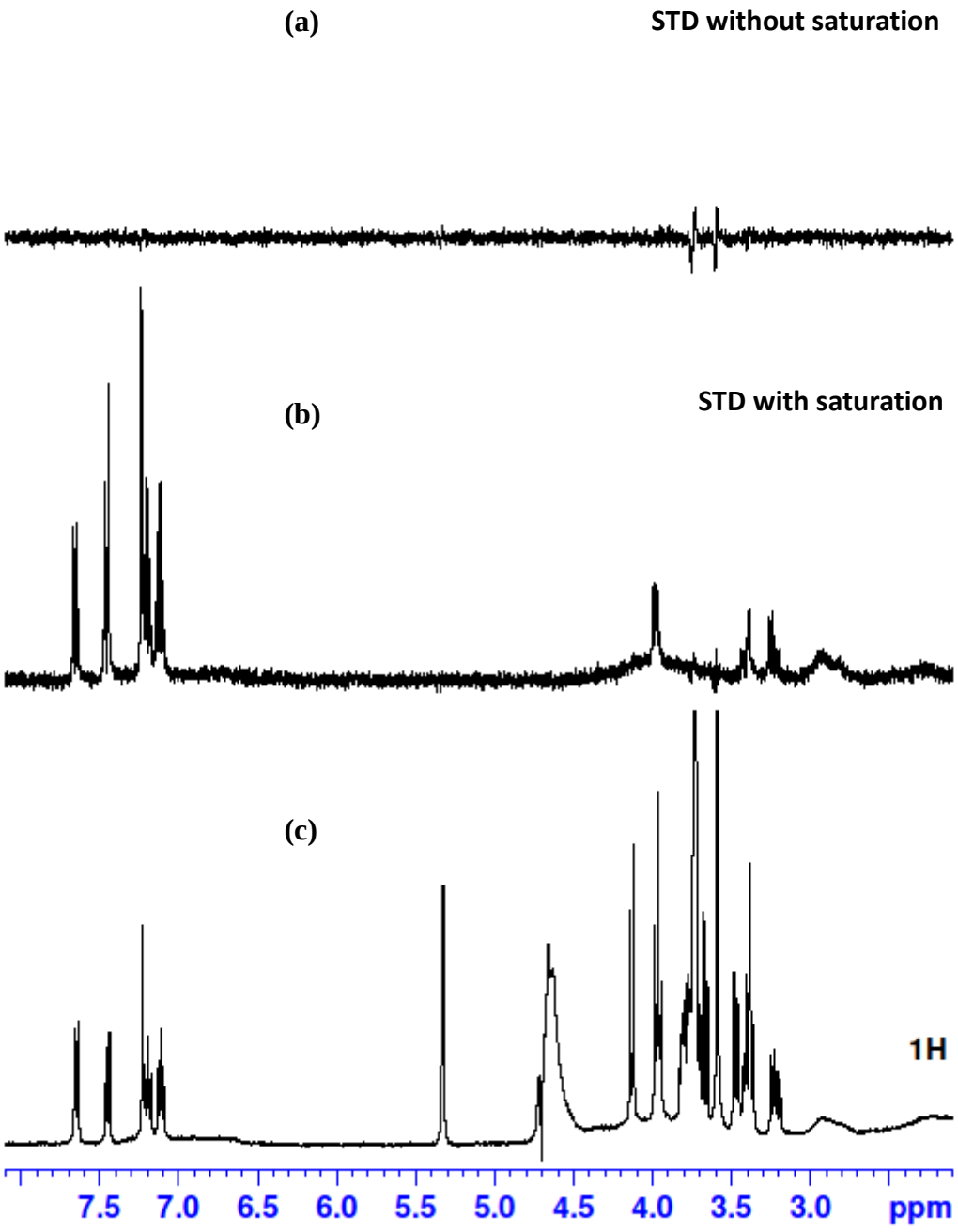

Fig. S3.1 STD-NMR method validation. Upper spectrum: STD signals without selective saturation; middle spectrum: STD signals with selective saturation; lower spectrum: reference ^{1}H NMR. The reaction mixture were: BSA (0.1 mM) + $_{L}$-tryptophan (5 mM) + sucrose (5 mM) in 40 % DMSO-d_6 / D_2O solution (550 μL).

References

1. W.H.O., *Antimicrobial resistance: global report on surveillance 2014*. World Health Organization, 2014.

2. Sosa, A. d. J., Byarugaba, D. K., Amábile-Cuevas, C. F., Hsueh, P.-R., Kariuki, S., and Okeke, I. N., ed. *Antimicrobial Resistance in Developing Countries*. Springer, 2010.

3. Smith, T. L., Pearson, M. L., Wilcox, K. R., Cruz, C., Lancaster, M. V., Robinson-Dunn, B., Tenover, F. C., Zervos, M. J., Band, J. D., White, E., Jarvis, W. R., and Staphylococ, G. I., *Emergence of vancomycin resistance in Staphylococcus aureus.* New England Journal of Medicine, 1999. **340**(7): 493-501.

4. Liu, Y. Y., Wang, Y., Walsh, T. R., Yi, L. X., Zhang, R., Spencer, J., Doi, Y., Tian, G. B., Dong, B. L., Huang, X. H., Yu, L. F., Gu, D. X., Ren, H. W., Chen, X. J., Lv, L. C., He, D. D., Zhou, H. W., Liang, Z. S., Liu, J. H., and Shen, J. Z., *Emergence of plasmid-mediated colistin resistance mechanism MCR-1 in animals and human beings in China: a microbiological and molecular biological study.* Lancet Infectious Diseases, 2016. **16**(2): 161-168.

5. Patrick, G. L., *An introduction to Medicinal Chemistry*. Oxford University Press, 1995.

6. Pasteur, L., *On the extension of the germ theory to the etiology of certain*

common diseases. Comptes Rendus de l'Académie des Sciences (Proceedings of the Academy of sciences), 1880: 1033-1044.

7. Johnson, B. A., Anker, H., and Meleney, F. L., *Bacitracin: A New Antibiotic Produced by a Member of the B. Subtilis Group.* Science, 1945. **102**(2650): 376-377.

8. Ehrlich, J., Bartz, Q. R., Smith, R. M., Joslyn, D. A., and Burkholder, P. R., *Chloromycetin, a New Antibiotic From a Soil Actinomycete.* Science, 1947. **106**(2757): 417.

9. Duggar, B. M., *Aureomycin; a product of the continuing search for new antibiotics.* Annals of the New York Academy of Sciences, 1948. **51**(2): 177-181.

10. Koyama, Y., Kurosasa, A., Tsuchiya, A., and Takakuta, K., *A new antibiotic "colistin" produced by spore-forming soil bacteria.* The Journal of antibiotics, 1950. **3**: 457-458.

11. Greenwood, D., Finch, R., Davey, P., and Wilcox, M., *Antimicrobial Chemotherapy* 5th ed. Oxford University Press, 2007.

12. Walsh, C., *Antibiotics Actions, Origins, Resistance*. ASM Press, 2003.

13. Abraham, E. P. and Chain, E., *An Enzyme from Bacteria Able to Destroy Penicillin.* Nature, 1940. **146**: 837.

14. Lim, D. and Strynadka, N. C., *Structural basis for the beta lactam resistance of PBP2a from methicillin-resistant Staphylococcus aureus.* Nature Structural Biology, 2002. **9**(11): 870-876.

15. Biswas, S., Mohammad, M. M., Patel, D. R., Movileanu, L., and van den Berg, B., *Structural insight into OprD substrate specificity.* Nature Structural & Molecular Biology, 2007. **14**(11): 1108-1109.

16. Ziervogel, B. K. and Roux, B., *The Binding of Antibiotics in OmpF Porin.* Structure, 2013. **21**(1): 76-87.

17. Bryskier, A., ed. *Antibacterial Agents Antibacterials and antifungals*. ASM Press, 2005.

18. Huang, L. Y., Huang, S. H., Chang, Y. C., Cheng, W. C., Cheng, T. J., and Wong, C. H., *Enzymatic synthesis of lipid II and analogues.* Angewandte Chemie International Edition, 2014. **53**(31): 8060-8065.

19. van Heijenoort, J., *Lipid intermediates in the biosynthesis of bacterial peptidoglycan.* Microbiology and Molecular Biology Reviews, 2007. **71**(4): 620-635.

20. Mohammadi, T., Sijbrandi, R., Lutters, M., Verheul, J., Martin, N. I., den Blaauwen, T., de Kruijff, B., and Breukink, E., *Specificity of the Transport of Lipid II by FtsW in Escherichia coli.* Journal of Biological Chemistry, 2014.

289(21): 14707-14718.

21. Sham, L. T., Butler, E. K., Lebar, M. D., Kahne, D., Bernhardt, T. G., and Ruiz, N., *MurJ is the flippase of lipid-linked precursors for peptidoglycan biogenesis.* Science, 2014. **345**(6193): 220-222.

22. Lovering, A. L., Safadi, S. S., and Strynadka, N. C. J., *Structural Perspective of Peptidoglycan Biosynthesis and Assembly.* Annual Review of Biochemistry, 2012. **81**: 451-478.

23. Fisher, J. F., Meroueh, S. O., and Mobashery, S., *Bacterial resistance to beta-lactam antibiotics: Compelling opportunism, compelling opportunity.* Chemical Reviews, 2005. **105**(2): 395-424.

24. Thakuria, B. and Lahon, K., *The Beta Lactam Antibiotics as an Empirical Therapy in a Developing Country: An Update on Their Current Status and Recommendations to Counter the Resistance against Them.* Journal of Clinical and Diagnostic Research, 2013. **7**(6): 1207-1214.

25. Kumarasamy, K. K., Toleman, M. A., Walsh, T. R., Bagaria, J., Butt, F., Balakrishnan, R., Chaudhary, U., Doumith, M., Giske, C. G., Irfan, S., Krishnan, P., Kumar, A. V., Maharjan, S., Mushtaq, S., Noorie, T., Paterson, D. L., Pearson, A., Perry, C., Pike, R., Rao, B., Ray, U., Sarma, J. B., Sharma, M., Sheridan, E., Thirunarayan, M. A., Turton, J., Upadhyay, S., Warner, M.,

Welfare, W., Livermore, D. M., and Woodford, N., *Emergence of a new antibiotic resistance mechanism in India, Pakistan, and the UK: a molecular, biological, and epidemiological study.* Lancet Infectious Diseases, 2010. **10**(9): 597-602.

26. Rahman, M., Shukla, S. K., Prasad, K. N., Ovejero, C. M., Pati, B. K., Tripathi, A., Singh, A., Srivastava, A. K., and Gonzalez-Zorn, B., *Prevalence and molecular characterisation of New Delhi metallo-beta-lactamases NDM-1, NDM-5, NDM-6 and NDM-7 in multidrug-resistant Enterobacteriaceae from India.* International Journal of Antimicrobial Agents, 2014. **44**(1): 30-37.

27. Enright, M. C., Robinson, D. A., Randle, G., Feil, E. J., Grundmann, H., and Spratt, B. G., *The evolutionary history of methicillin-resistant Staphylococcus aureus (MRSA).* Proceedings of the National Academy of Sciences (USA), 2002. **99**(11): 7687-7692.

28. Datta, N. and Kontomichalou, P., *Penicillinase synthesis controlled by infectious R factors in Enterobacteriaceae.* Nature, 1965. **208**(5007): 239-241.

29. Beceiro, A. and Bou, G., *Class C beta-lactamases: an increasing problem worldwide.* Reviews in Medical Microbiology, 2004. **15**(4): 141-152.

30. Reading, C. and Farmer, T., *The Inhibition of Beta-Lactamases from Gram-Negative Bacteria by Clavulanic Acid.* Biochemical Journal, 1981.

199(3): 779-787.

31. Chaibi, E. B., Sirot, D., Paul, G., and Labia, R., *Inhibitor-resistant TEM beta-lactamases: phenotypic, genetic and biochemical characteristics.* Journal of Antimicrobial Chemotherapy, 1999. **43**(4): 447-458.

32. Bonnet, R., Sampaio, J. L. M., Labia, R., De Champs, C., Sirot, D., Chanal, C., and Sirot, J., *A novel CTX-M beta-lactamase (CTX-M-8) in cefotaxime-resistant Enterobacteriaceae isolated in Brazil.* Antimicrobial Agents and Chemotherapy, 2000. **44**(7): 1936-1942.

33. Chopra, I., *Glycylcyclines: third-generation tetracycline antibiotics.* Current Opinion in Pharmacology, 2001. **1**(5): 464-469.

34. Karageorgopoulos, D. E., Kelesidis, T., Kelesidis, I., and Falagas, M. E., *Tigecycline for the treatment of multidrug-resistant (including carbapenem-resistant) Acinetobacter infections: a review of the scientific evidence.* Journal of Antimicrobial Chemotherapy, 2008. **62**(1): 45-55.

35. Rose, W. E. and Rybak, M. J., *Tigecycline: first of a new class of antimicrobial agents.* Pharmacotherapy, 2006. **26**(8): 1099-1110.

36. Wenzel, R., Bate, G., and Kirkpatrick, P., *Tigecycline.* Nature Reviews Drug Discovery, 2005. **4**(10): 809-810.

37. Sun, Y., Cai, Y., Liu, X., Bai, N., Liang, B., and Wang, R., *The emergence of*

clinical resistance to tigecycline. International Journal of Antimicrobial Agents, 2013. **41**(2): 110-116.

38. Derouaux, A., Sauvage, E., and Terrak, M., *Peptidoglycan glycosyltransferase substrate mimics as templates for the design of new antibacterial drugs.* Frontiers in Immunology, 2013. **4**: 1-6.

39. Schuman, B., Evans, S. V., and Fyles, T. M., *Geometric attributes of retaining glycosyltransferase enzymes favor an orthogonal mechanism.* Plos One, 2013. **8**(8): e71077.

40. Lovering, A. L., de Castro, L. H., Lim, D., and Strynadka, N. C. J., *Structural insight into the transglycosylation step of bacterial cell-wall biosynthesis.* Science, 2007. **315**(5817): 1402-1405.

41. Taylor, J. G., Li, X. C., Oberthur, M., Zhu, W. J., and Kahne, D. E., *The total synthesis of moenomycin A.* Journal of the American Chemical Society, 2006. **128**(47): 15084-15085.

42. Ostash, B. and Walker, S., *Moenomycin family antibiotics: chemical synthesis, biosynthesis, and biological activity.* Natural Product Reports, 2010. **27**(11): 1594-1617.

43. de Kruijff, B., van Dam, V., and Breukink, E., *Lipid II: A central component in bacterial cell wall synthesis and a target for antibiotics.* Prostaglandins,

Leukotrienes and Essential Fatty Acids, 2008. **79**(3-5): 117-121.

44. Breukink, E. and de Kruijff, B., *Lipid II as a target for antibiotics.* Nature Reviews Drug Discovery, 2006. **5**(4): 321-332.

45. Sheldrick, G. M., Jones, P. G., Kennard, O., Williams, D. H., and Smith, G. A., *Structure of Vancomycin and Its Complex with Acetyl-D-Alanyl-D-Alanine.* Nature, 1978. **271**(5642): 223-225.

46. Williamson, M. P. and Williams, D. H., *Structure Revision of the Antibiotic Vancomycin - the Use of Nuclear Overhauser Effect Difference Spectroscopy.* Journal of the American Chemical Society, 1981. **103**(22): 6580-6585.

47. Gardete, S. and Tomasz, A., *Mechanisms of vancomycin resistance in Staphylococcus aureus.* Journal of Clinical Investigation, 2014. **124**(7): 2836-2840.

48. Bierbaum, G. and Sahl, H. G., *Lantibiotics: Mode of Action, Biosynthesis and Bioengineering.* Current Pharmaceutical Biotechnology, 2009. **10**(1): 2-18.

49. Chatterjee, C., Paul, M., Xie, L. L., and van der Donk, W. A., *Biosynthesis and mode of action of lantibiotics.* Chemical Reviews, 2005. **105**(2): 633-683.

50. Hsu, S. T. D., Breukink, E., Tischenko, E., Lutters, M. A. G., de Kruijff, B., Kaptein, R., Bonvin, A. M. J. J., and van Nuland, N. A. J., *The nisin-lipid II complex reveals a pyrophosphate cage that provides a blueprint for novel*

antibiotics. Nature Structural & Molecular Biology, 2004. **11**(10): 963-967.

51. Ling, L. L., Schneider, T., Peoples, A. J., Spoering, A. L., Engels, I., Conlon, B. P., Mueller, A., Schaberle, T. F., Hughes, D. E., Epstein, S., Jones, M., Lazarides, L., Steadman, V. A., Cohen, D. R., Felix, C. R., Fetterman, K. A., Millett, W. P., Nitti, A. G., Zullo, A. M., Chen, C., and Lewis, K., *A new antibiotic kills pathogens without detectable resistance.* Nature, 2015. **517**(7535): 455-459.

52. Fukase, K., Kitazawa, M., Sano, A., Shimbo, K., Fujita, H., Horimoto, S., Wakamiya, T., and Shiba, T., *Total Synthesis of Peptide Antibiotic Nisin.* Tetrahedron Letters, 1988. **29**(7): 795-798.

53. Jin, K., Sam, I. H., Po, K. H. L., Lin, D., Zadeh, E. H. G., Chen, S., Yuan, Y., and Li, X. C., *Total synthesis of teixobactin.* Nature Communications, 2016. **7**: 12394.

54. Giltrap, A. M., Dowrnan, L. J., Nagalingam, G., Ochoa, J. L., Linington, R. G., Britton, W. J., and Payne, R. J., *Total Synthesis of Teixobactin.* Organic Letters, 2016. **18**(11): 2788-2791.

55. Gampe, C. M., Tsukamoto, H., Doud, E. H., Walker, S., and Kahne, D., *Tuning the Moenomycin Pharmacophore To Enable Discovery of Bacterial Cell Wall Synthesis Inhibitors.* Journal of the American Chemical Society,

2013. **135**(10): 3776-3779.

56. Cheng, T. J. R., Wu, Y. T., Yang, S. T., Lo, K. H., Chen, S. K., Chen, Y. H., Huang, W. I., Yuan, C. H., Guo, C. W., Huang, L. Y., Chen, K. T., Shih, H. W., Cheng, Y. S. E., Cheng, W. C., and Wong, C. H., *High-throughput identification of antibacterials against methicillin-resistant Staphylococcus aureus (MRSA) and the transglycosylase.* Bioorganic & Medicinal Chemistry, 2010. **18**(24): 8512-8529.

57. Schwartz, B., Markwalder, J. A., and Wang, Y., *Lipid II: Total synthesis of the bacterial cell wall precursor and utilization as a substrate for glycosyltransfer and transpeptidation by penicillin binding protein (PBP) 1b of Eschericia coli.* Journal of the American Chemical Society, 2001. **123**(47): 11638-11643.

58. Galley, N. F., O'Reilly, A. M., and Roper, D. I., *Prospects for novel inhibitors of peptidoglycan transglycosylases.* Bioorganic Chemistry, 2014. **55**: 16-26.

59. Blanchaert, B., Adams, E., and Van Schepdael, A., *An overview of analytical methods for monitoring bacterial transglycosylation.* Analytical Methods, 2014. **6**(19): 7590-7596.

60. Sauvage, E. and Terrak, M., *Glycosyltransferases and Transpeptidases/Penicillin-Binding Proteins: Valuable Targets for New Antibacterials.* Antibiotics, 2016. **5**(1): 12.

61. Kitchen, D. B., Decornez, H., Furr, J. R., and Bajorath, J., *Docking and scoring in virtual screening for drug discovery: Methods and applications.* Nature Reviews Drug Discovery, 2004. **3**(11): 935-949.

62. Pham, T. A. and Jain, A. N., *Parameter estimation for scoring protein-ligand interactions using negative training data.* Journal of Medicinal Chemistry, 2006. **49**(20): 5856-5868.

63. Hindle, S. A., Rarey, M., Buning, C., and Lengauer, T., *Flexible docking under pharmacophore type constraints.* Journal of Computer-Aided Molecular Design, 2002. **16**(2): 129-149.

64. Wishart, D. S., Knox, C., Guo, A. C., Shrivastava, S., Hassanali, M., Stothard, P., Chang, Z., and Woolsey, J., *DrugBank: a comprehensive resource for in silico drug discovery and exploration.* Nucleic Acids Research, 2006. **34**(Database issue): D668-672.

65. Yang, M., Zhou, L., Zuo, Z. L., Tang, X. Y., Liu, J., and Ma, X., *Structure-based virtual screening for glycosyltransferase(51).* Molecular Simulation, 2008. **34**(9): 849-856.

66. Zsoldos, Z., Reid, D., Simon, A., Sadjad, S. B., and Johnson, A. P., *eHiTS: A new fast, exhaustive flexible ligand docking system.* Journal of Molecular Graphics & Modelling, 2007. **26**(1): 198-212.

67. Derouaux, A., Turk, S., Olrichs, N. K., Gobec, S., Breukink, E., Amoroso, A., Offant, J., Bostock, J., Mariner, K., Chopra, I., Vernet, T., Zervosen, A., Joris, B., Frere, J. M., Nguyen-Disteche, M., and Terrak, M., *Small molecule inhibitors of peptidoglycan synthesis targeting the lipid II precursor.* Biochemical Pharmacology, 2011. **81**(9): 1098-1105.

68. Wang, Y., Chan, F. Y., Sun, N., Lui, H. K., So, P. K., Yan, S. C., Chan, K. F., Chiou, J., Chen, S., Abagyan, R., Leung, Y. C., and Wong, K. Y., *Structure-based Design, Synthesis, and Biological Evaluation of Isatin Derivatives as Potential Glycosyltransferase Inhibitors.* Chemical Biology & Drug Design, 2014. **84**(6): 685-696.

69. Tang, Y. J., Zeng, X. Q., and Liang, J., *Surface Plasmon Resonance: An Introduction to a Surface Spectroscopy Technique.* Journal of Chemical Education, 2010. **87**(7): 742-746.

70. Stembera, K., Vogel, S., Buchynskyy, A., Ayala, J. A., and Welzel, P., *A surface plasmon resonance analysis of the interaction between the antibiotic moenomycin A and penicillin-binding protein 1b.* Chembiochem, 2002. **3**(6): 559-565.

71. Bury, D., Dahmane, I., Derouaux, A., Dumbre, S., Herdewijn, P., Matagne, A., Breukink, E., Mueller-Seitz, E., Petz, M., and Terrak, M., *Positive*

cooperativity between acceptor and donor sites of the peptidoglycan glycosyltransferase. Biochemical Pharmacology, 2015. **93**(2): 141-150.

72. Cheng, T. J. R., Sung, M. T., Liao, H. Y., Chang, Y. F., Chen, C. W., Huang, C. Y., Chou, L. Y., Wu, Y. D., Chen, Y., Cheng, Y. S. E., Wong, C. H., Ma, C., and Cheng, W. C., *Domain requirement of moenomycin binding to bifunctional transglycosylases and development of high-throughput discovery of antibiotics.* Proceedings of the National Academy of Sciences (USA), 2008. **105**(2): 431-436.

73. Lakowicz, J. R., *Principles of Fluorescence Spectroscopy*. 3rd ed. Springer, 2006.

74. Viegas, A., Manso, J., Nobrega, F. L., and Cabrita, E. J., *Saturation-Transfer Difference (STD) NMR: A Simple and Fast Method for Ligand Screening and Characterization of Protein Binding.* Journal of Chemical Education, 2011. **88**(7): 990-994.

75. Rühl, T., Daghish, M., Buchynskyy, A., Barche, K., Volke, D., Stembera, K., Kempin, U., Knoll, D., Hennig, L., Findeisen, M., Oehme, R., Giesa, S., Ayala, J., and Welzel, P., *Studies on the interaction of the antibiotic moenomycin A with the enzyme penicillin-binding protein 1b.* Bioorganic & Medicinal Chemistry, 2003. **11**(13): 2965-2981.

76. da Silva, J. F. M., Garden, S. J., and Pinto, A. C., *The chemistry of isatins: a review from 1975 to 1999.* Journal of the Brazilian Chemical Society, 2001. **12**(3): 273-324.

77. Vine, K. L., Matesic, L., Locke, J. M., and Skropeta, D., *Recent Highlights in the Development of Isatin-Based Anticancer Agents.* Advances in Anticancer Agents in Medicinal Chemistry, 2013. **2**: 254-312.

78. Pandeya, S. N., Smitha, S., Jyoti, M., and Sridhar, S. K., *Biological activities of isatin and its derivatives.* Acta Pharmaceutica, 2005. **55**(1): 27-46.

79. Medvedev, A., Buneeva, O., and Glover, V., *Biological targets for isatin and its analogues: Implications for therapy.* Biologics: Targets and Therapy, 2007. **1**(2): 151-162.

80. Wang, Y., *Development of new inhibitors for the bacterial glycosyltransferase: computational docking, synthesis and bioassays*. in Department of Applied Biology and Chemical Technology, Ph.D. Thesis, The Hong Kong Polytechnic University, 2014.

81. Lam, P. Y. S., Clark, C. G., Saubern, S., Adams, J., Winters, M. P., Chan, D. M. T., and Combs, A., *New aryl/heteroaryl C-N bond cross-coupling reactions via arylboronic acid cupric acetate arylation.* Tetrahedron Letters, 1998. **39**(19): 2941-2944.

82. Chan, D. M. T., Monaco, K. L., Wang, R. P., and Winters, M. P., *New N- and O-arylations with phenylboronic acids and cupric acetate.* Tetrahedron Letters, 1998. **39**(19): 2933-2936.

83. Evans, D. A., Katz, J. L., and West, T. R., *Synthesis of diaryl ethers through the copper-promoted arylation of phenols with arylboronic acids. An expedient synthesis of thyroxine.* Tetrahedron Letters, 1998. **39**(19): 2937-2940.

84. Wolfe, J. P., Wagaw, S., Marcoux, J. F., and Buchwald, S. L., *Rational development of practical catalysts for aromatic carbon-nitrogen bond formation.* Accounts of Chemical Research, 1998. **31**(12): 805-818.

85. Hartwig, J. F., *Transition metal catalyzed synthesis of arylamines and aryl ethers from aryl halides and triflates: Scope and mechanism.* Angewandte Chemie International Edition, 1998. **37**(15): 2046-2067.

86. Hartwig, J. F., *Evolution of a Fourth Generation Catalyst for the Amination and Thioetherification of Aryl Halides.* Accounts of Chemical Research, 2008. **41**(11): 1534-1544.

87. Craig, P. N., *Interdependence between Physical Parameters and Selection of Substituent Groups for Correlation Studies.* Journal of Medicinal Chemistry, 1971. **14**(8): 680-684.

88. Topliss, J. G., *Utilization of Operational Schemes for Analog Synthesis in Drug Design.* Journal of Medicinal Chemistry, 1972. **15**(10): 1006-1010.

89. Adachi, M., Zhang, Y., Leimkuhler, C., Sun, B. Y., LaTour, J. V., and Kahne, D. E., *Degradation and reconstruction of moenomycin A and derivatives: Dissecting the function of the isoprenoid chain.* Journal of the American Chemical Society, 2006. **128**(43): 14012-14013.

90. Clinical and Laboratory Standards Institute. *Methods for Dilution Antimicrobial Susceptibility Tests for Bacteria That Grow Aerobically; Approved Standard—Seventh Edition.* Clinical and Laboratory Standards Institute. 2006.

91. Tripathi, K. D., *Essentials of Medical Pharmacology*. Jaypee Brothers Medical Publishers (P) Ltd, 2008.

92. Fujita, T., Iwasa, J., and Hansch, C., *A New Substituent Constant, Pi, Derived from Partition-Coefficients.* Journal of the American Chemical Society, 1964. **86**: 5175-5180.

93. Hammett, L. P., *The effect of structure upon the reactions of organic compounds benzene derivatives.* Journal of the American Chemical Society, 1937. **59**: 96-103.

94. Trott, O. and Olson, A. J., *AutoDock Vina: improving the speed and accuracy*

of docking with a new scoring function, efficient optimization, and multithreading. Journal of Computational Chemistry, 2010. **31**(2): 455-461.

95. Grunwald, J. E. and Leffler, E., *Rates and Equilibria of Organic Reactions*. Wiley, 1963.

96. Bernardez, L. A., *Dissolution of polycyclic aromatic hydrocarbons from a non-aqueous phase liquid into a surfactant solution using a rotating disk apparatus.* Colloids and Surfaces A: Physicochemical and Engineering Aspects, 2008. **320**(1-3): 175-182.

97. Venkitakrishnan, R. P., Benard, O., Max, M., Markley, J. L., and Assadi-Porter, F. M., *Use of NMR saturation transfer difference spectroscopy to study ligand binding to membrane proteins.* Methods in Molecular Biology, 2012. **914**: 47-63.

98. Stockman, B. J. and Dalvit, C., *NMR screening techniques in drug discovery and drug design.* Progress in Nuclear Magnetic Resonance Spectroscopy, 2002. **41**(3-4): 187-231.

99. Gossert, A. and Jahnke, W., *NMR in drug discovery: A practical guide to identification and validation of ligands interacting with biological macromolecules.* Progress in Nuclear Magnetic Resonance Spectroscopy, 2016. **97**: 82-125.

100. Krishna, N. R. and Jayalakshmi, V., *Complete relaxation and conformational exchange matrix analysis of STD-NMR spectra of ligand-receptor complexes.* Progress in Nuclear Magnetic Resonance Spectroscopy, 2006. **49**(1): 1-25.

101. Krishnan, V. V., *Ligand screening by saturation-transfer difference (STD) NMR spectroscopy.* Current Analytical Chemistry, 2005. **1**(3): 307-320.

102. Shuker, S. B., Hajduk, P. J., Meadows, R. P., and Fesik, S. W., *Discovering high-affinity ligands for proteins: SAR by NMR.* Science, 1996. **274**(5292): 1531-1534.

103. Pellecchia, M., Bertini, I., Cowburn, D., Dalvit, C., Giralt, E., Jahnke, W., James, T. L., Homans, S. W., Kessler, H., Luchinat, C., Meyer, B., Oschkinat, H., Peng, J., Schwalbe, H., and Siegal, G., *Perspectives on NMR in drug discovery: a technique comes of age.* Nature Reviews Drug Discovery, 2008. **7**(9): 738-745.

104. Pellecchia, M., Sem, D. S., and Wuthrich, K., *NMR in drug discovery.* Nature Reviews Drug Discovery, 2002. **1**(3): 211-219.

105. Claridge, T. D. W., *High-Resolution NMR Techniques in Organic Chemistry*. 3rd ed. Elsevier, 2016.

106. Mayer, M. and Meyer, B., *Characterization of ligand binding by saturation transfer difference NMR spectroscopy.* Angewandte Chemie International

Edition, 1999. **38**(12): 1784-1788.

107. Klein, J., Meinecke, R., Mayer, M., and Meyer, B., *Detecting binding affinity to immobilized receptor proteins in compound libraries by HR-MAS STD NMR.* Journal of the American Chemical Society, 1999. **121**(22): 5336-5337.

108. Gottlieb, H. E., Kotlyar, V., and Nudelman, A., *NMR chemical shifts of common laboratory solvents as trace impurities.* Journal of Organic Chemistry, 1997. **62**(21): 7512-7515.

109. Sauvage, E., Kerff, F., Terrak, M., Ayala, J. A., and Charlier, P., *The penicillin-binding proteins: structure and role in peptidoglycan biosynthesis.* FEMS Microbiology Reviews, 2008. **32**(2): 234-258.

110. Helassa, N., Vollmer, W., Breukink, E., Vernet, T., and Zapun, A., *The membrane anchor of penicillin-binding protein PBP2a from Streptococcus pneumoniae influences peptidoglycan chain length.* The FEBS Journal, 2012. **279**(11): 2071-2081.

111. Wang, Y. S., Liu, D. J., and Wyss, D. F., *Competition STD NMR for the detection of high-affinity ligands and NMR-based screening.* Magnetic Resonance in Chemistry, 2004. **42**(6): 485-489.

112. Dalvit, C., Fasolini, M., Flocco, M., Knapp, S., Pevarello, P., and Veronesi, M., *NMR-based screening with competition water-ligand observed via*

gradient spectroscopy experiments: Detection of high-affinity ligands. Journal of Medicinal Chemistry, 2002. **45**(12): 2610-2614.

113. McMenamy, R. H. and Oncley, J. L., *The specific binding of L-tryptophan to serum albumin.* Journal of Biological Chemistry, 1958. **233**(6): 1436-1447.

114. Halliday, J., McKeveney, D., Muldoon, C., Rajaratnam, P., and Meutermans, W., *Targeting the forgotten transglycosylases.* Biochemical Pharmacology, 2006. **71**(7): 957-967.

115. Dumbre, S., Derouaux, A., Lescrinier, E., Piette, A., Joris, B., Terrak, M., and Herdewijn, P., *Synthesis of modified peptidoglycan precursor analogues for the inhibition of glycosyltransferase.* Journal of the American Chemical Society, 2012. **134**(22): 9343-9351.

116. Zuegg, J., Muldoon, C., Adamson, G., McKeveney, D., Le Thanh, G., Premraj, R., Becker, B., Cheng, M., Elliott, A. G., Huang, J. X., Butler, M. S., Bajaj, M., Seifert, J., Singh, L., Galley, N. F., Roper, D. I., Lloyd, A. J., Dowson, C. G., Cheng, T. J., Cheng, W. C., Demon, D., Meyer, E., Meutermans, W., and Cooper, M. A., *Carbohydrate scaffolds as glycosyltransferase inhibitors with in vivo antibacterial activity.* Nature Communications, 2015. **6**: 7719.

117. Garneau, S., Qiao, L., Chen, L., Walker, S., and Vederas, J. C., *Synthesis of mono- and disaccharide analogs of moenomycin and lipid II for inhibition of*

transglycosylase activity of penicillin-binding protein 1b. Bioorganic & Medicinal Chemistry, 2004. **12**(24): 6473-6494.

118. Sams-Dodd, F., *Target-based drug discovery: is something wrong?* Drug Discovery Today, 2005. **10**(2): 139-147.

119. Cheng, T., Li, Q., Zhou, Z., Wang, Y., and Bryant, S. H., *Structure-based virtual screening for drug discovery: a problem-centric review.* The AAPS Journal, 2012. **14**(1): 133-141.

120. Sung, M. T., Lai, Y. T., Huang, C. Y., Chou, L. Y., Shih, H. W., Cheng, W. C., Wong, C. H., and Ma, C., *Crystal structure of the membrane-bound bifunctional transglycosylase PBP1b from Escherichia coli.* Proceedings of the National Academy of Sciences (USA), 2009. **106**(22): 8824-8829.

121. Huang, C. Y., Shih, H. W., Lin, L. Y., Tien, Y. W., Cheng, T. J., Cheng, W. C., Wong, C. H., and Ma, C., *Crystal structure of Staphylococcus aureus transglycosylase in complex with a lipid II analog and elucidation of peptidoglycan synthesis mechanism.* Proceedings of the National Academy of Sciences (USA), 2012. **109**(17): 6496-6501.

122. Barrett, D., Leimkuhler, C., Chen, L., Walker, D., Kahne, D., and Walker, S., *Kinetic characterization of the glycosyltransferase module of Staphylococcus aureus PBP2.* Journal of Bacteriology, 2005. **187**(6): 2215-2217.

123. Schwartz, B., Markwalder, J. A., Seitz, S. P., Wang, Y., and Stein, R. L., *A kinetic characterization of the glycosyltransferase activity of Eschericia coli PBP1b and development of a continuous fluorescence assay.* Biochemistry, 2002. **41**(41): 12552-12561.

124. Liu, C. Y., Guo, C. W., Chang, Y. F., Wang, J. T., Shih, H. W., Hsu, Y. F., Chen, C. W., Chen, S. K., Wang, Y. C., Cheng, T. J. R., Ma, C., Wong, C. H., Fang, J. M., and Cheng, W. C., *Synthesis and Evaluation of a New Fluorescent Transglycosylase Substrate: Lipid II-Based Molecule Possessing a Dansyl-C20 Polyprenyl Moiety.* Organic Letters, 2010. **12**(7): 1608-1611.

125. Huang, S. H., Wu, W. S., Huang, L. Y., Huang, W. F., Fu, W. C., Chen, P. T., Fang, J. M., Cheng, W. C., Cheng, T. J. R., and Wong, C. H., *New Continuous Fluorometric Assay for Bacterial Transglycosylase Using Forster Resonance Energy Transfer.* Journal of the American Chemical Society, 2013. **135**(45): 17078-17089.

126. Breukink, E., van Heusden, H. E., Vollmerhaus, P. J., Swiezewska, E., Brunner, L., Walker, S., Heck, A. J. R., and de Kruijff, B., *Lipid II is an intrinsic component of the pore induced by nisin in bacterial membranes.* Journal of Biological Chemistry, 2003. **278**(22): 19898-19903.

127. Kohlrausch, U. and Holtje, J. V., *One-Step Purification Procedure for*

UDP-N-Acetylmuramyl-Peptide Murein Precursors from Bacillus-Cereus. FEMS Microbiology Letters, 1991. **78**(2-3): 253-258.